The Preparation and Characterization of Stannous Fluoride Materials Containing Strontium

Alena Kolarikova Peroutka

A Thesis

in

The Department

of

Chemistry

Presented in Partial Fulfilment of the Requirements

for the Degree of Master of Science at

Concordia University

Montreal, Quebec, Canada

April 1998

ABSTRACT

The Preparation and Characterization of Stannous Fluoride Materials Containing Strontium

Alena Kolarikova Peroutka

The reaction of aqueous solutions of strontium nitrate and stannous fluoride results in the formation of a precipitate which is $SrSn_2F_6.H_2O$, or $Sr_2Sn_2NO_3F_7.2H_2O$, or a mixture of both, depending on the conditions. The reaction has been studied as a function of various reaction parameters, such as molar ratio, order of addition of reagents, mixing speed, time and temperature. The preparation of these materials is described here.

The nature of the products was investigated by various analytical techniques, such as atomic absorption spectrophotometry, fluoride ion electrode analysis, infrared spectroscopy, X-ray diffraction, thermal analyses and Mössbauer spectroscopy.

Recrystallization of $SrSn_2F_6.H_2O$ and $Sr_2Sn_2NO_3F_7.2H_2O$ from nitric acid was performed in primarily an effort to obtain single crystals that could be used for crystal structure determination by X-ray single crystal diffraction. In addition, it was also used to investigate if any new materials are formed by this method, since it is known to happen if $PbSnF_4$ is recrystallized in nitric acid. Furthermore, highly oriented samples and higher purity of both materials are obtained by recrystallization.

Reactions between strontium chloride and stannous fluoride in aqueous solutions were also investigated under similar conditions.

ACKNOWLEDGEMENTS

I would like to thank Dr. Georges Dénès, my research thesis supervisor for the guidance, advice, motivation and encouragement he gave me throughout my graduate studies.

Also, I would like to extend my thanks to the members of my Research Committee, Drs. Marcus. F. Lawrence, Raymond Le Van Mao and David B. Jack for their interest and valuable advice.

Many thanks to the Technical Staff at Concordia University for the support, to Rozenn Thoraval and Sonia Le Noc from the I.U.T. de Lannion, France, for their contribution to the research during their training period at Concordia university and to my fellow colleagues for their input, friendship and encouragement during my research.

Finally, I would like to thank my husband Miro for his support, confidence and belief in me.

TABLE OF CONTENTS

LIST OF FIGURES

LIST OF TABLES

CHAPTER 1. INTRODUCTION

1.1 Earlier Work on the MF_2 / SnF_2 Systems

The interest in the MF_2 / SnF_2 materials (M = divalent main group elements) originates from the fact that they possess unusual structural and physical properties.

The structure of many of them derives from the fluorite - type structure (CaF_2), however, the presence of a steroactive non - bonding electron pair, also called lone pair of electrons, on tin(II), prevents it from taking the eight-fold cubic coordination of the divalent metal. This results in various structural distortions that can be ordered as in $PbSnF_4$ [1-6] or disordered as in $PbSn_4F_{10}$[7-8] and in the $M_{1-x}Sn_xF_2$ solid solutions (M=Ca and Pb) [8-12].

When tin(II) and the metal(II) are ordered, highly anisotropic structures are obtained. This can be well observed in $PbSnF_4$, which has very high anisotropic properties, such as texture (high preferred orientations) and crystal shapes (very thin large platelets) [13-14].

Changes in the type of order between tin(II) and the metal(II), also between inequivalent fluorine atoms, and changes in the type of site distortions, as temperature is varied, gives rise to a variety of complex solid state phase transitions, particularly in $PbSnF_4$ [5,15-18].

Phase transitions are also observed in PbF_2 and $PbSnF_4$ upon applying mechanical energy [19-21] and when the conditions of preparation are varied [6,14-17, 22].

These materials are among the best fluoride ion conductors known. At the present time, $PbSnF_4$ is the best fluoride ion conductor [9-10,15,22-29]. Such conductors have potentials for a wide range of applications although none has reached the commercial stage yet. This includes their possible use as chemical sensors (fluoride ion electrodes) and applications as solid electrolytes in solid state batteries, fuel - cell electrolytes or pressure sensors [30-31].

Fluoride ions are predicted to be the best anionic conductors because they are light, univalent and have a small ionic size.

The high fluoride ion mobility in the fluorite type MF_2 arises from the presence of a large number of Frenkel defects (combinations of interstitials and vacancies of the same species) in the fluorite type structure. In MF_2/SnF_2 materials, the structure of which is derived from the fluorite type, it is due to the presence of a large rate of disorder on the fluoride sites and from the high polarizability of the tin(II) atom. In the fluorite (CaF_2 type) structure, the high rate of Frenkel defects is due to the fact that half of the F_8 cubes (one in each unit cell) are vacant (no metal in their center), and therefore these vacant sites can be used as F^- interstitial sites (fig.1). In α-$PbSnF_4$, these sites are no longer vacant since they are occupied by a fluorine atom which is axially bonded to tin. Partial occupancy of this site in not possible since this Sn-F bond has a very strong covalent character and thus is very difficult to break (Sn-F≈2.00Å, compared to the sum of the ionic radii of Sn^{2+} and F^- which is 2.28 Å). Therefore, this fluorine is not mobile and cannot be a charge carrier.

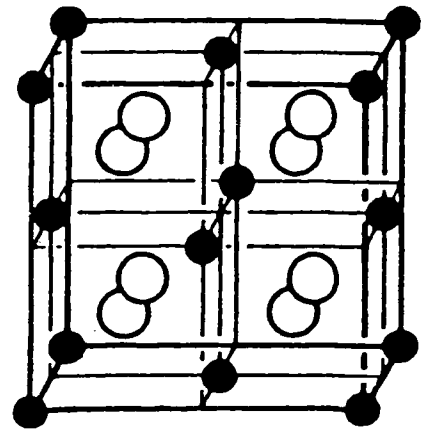

(a)

(O: F, •: Ca)

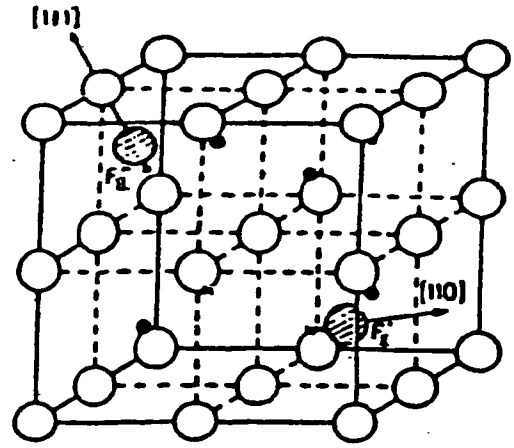

(b)

(O: F_I, •: Ca, x: V_{FI})

Figure 1: a) Fluorite (CaF_2) Structure

b) Frenkel Defects in the Fluorite (CaF_2) Structure

Despite of this, the conductivity of $PbSnF_4$ is three orders of magnitude as high as that of β-PbF_2. This has been attributed to the combination of ionic and covalent bonds within the same structure, which is a distortion of the typically ionic fluorite structure [27]. This results in the underpopulation of some fluorine sites and the presence of interstitials in the lone pairs layers. The population of the interstitial sites has been shown by neutron diffraction to increase with temperature [5].

The non - transition metal(II) derivatives of the complex tin(ii) fluoride ions were first prepared and studied by J.D.Donaldson and B.J.Senior in the course of their general investigation of derivatives of SnF_2 [32].

In this pioneering work, Donaldson and Senior prepared $SrSn_2F_6$ and $SrSn_4F_{10}$ from cooled melts of the appropriate mixtures of SnF_2 and SrF_2. They also found that $SrSn_2F_6$ could be prepared upon addition of a hot saturated solution of strontium nitrate to an aqueous solution of tin(II) fluoride (30% W/V) at 90°C, however, $SrSn_4F_{10}$ could not be prepared from aqueous solutions. $SrSn_2F_6$ prepared by the two methods is reported to be identical, as shown by X-ray powder diffraction. In addition they found that if a hot solution of tin(II) fluoride was added to a solution of strontium nitrate under the same conditions as described above, the precipitate obtained is $Sr_2Sn_2NO_3F_7.2H_20$, instead of $SrSn_2F_6$. By using transition point data to plot the freezing point of SnF_2 / SrF_2 melts, Donaldson and Senior found two maxima in the SnF_2 - SrF_2 phase diagram, at 67% and 80% SnF_2 in SrF_2, which indicate the presence of two congruently melting compounds, $SrSn_2F_6$ and $SrSn_4F_{10}$, respectively. They

did not observe any melting maximum at 50%, like in the case of the SnF_2 / PbF_2 system, and therefore they concluded that probably no $SrSnF_4$ compound existed, in contrast with $PbSnF_4$, which they predicted and isolated in the same work. However, in a subsequent work, Dénès et al. were successful in isolating $SrSnF_4$ and studying it's properties [1, 16].

Dénès also prepared $SrSn_2F_6$ by the reaction of strontium carbonate with a hot aqueous HF solution of SnF_2 [33]. The product obtained was characterized by X-ray diffraction and was found to be the same as $SrSn_2F_6$ reported by Donaldson and Senior.

Donaldson and Senior characterized $SrSn_2F_6$ and $Sr_2Sn_2NO_3F_7.2H_20$ by X-ray powder diffraction, infrared spectroscopy and Mössbauer spectroscopy. Using their infrared spectra, they suggested that the SnF_3^- ion was present in both compounds, with tin (II) in sp^3 hybridization, therefore in a triangular pyramidal environment (fig. 2).

The infrared assignment was based on their assumption (also from infrared and Mössbauer spectroscopies) of a similar, although distorted, coordination of tin in $PbSnF_4$ and the presence of PbF^+ in the same material. However, this has since been proven to be wrong [2-5]. Neutron diffraction has shown that in $PbSnF_4$, Sn(II) is in a SnF_5E (E = lone pair) pseudooctahedral environment with one short axial and four longer equatorial bonds; in addition, Pb(II) is in a $PbF_4F_4'F_4''$ pseudocube with four shorter (Pb-F) and four longer (Pb-F') bonds, and in addition another 4 Pb·····F" longer interactions (F" forms the short Sn-F" axial bonds), (fig. 3). This casts serious

sp^3 hybridization

pyramidal structure

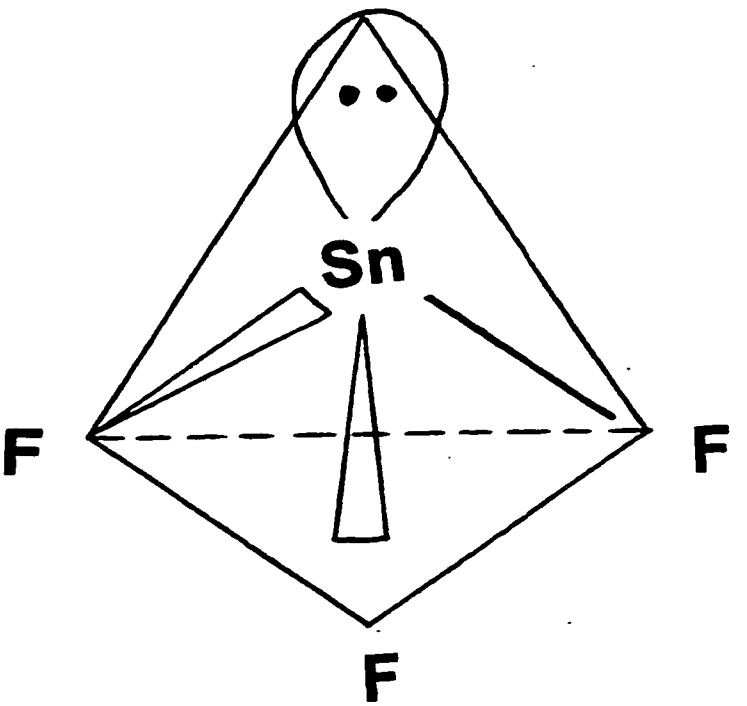

Figure 2 : Environment of Tin(II) in SnF_3^- ion

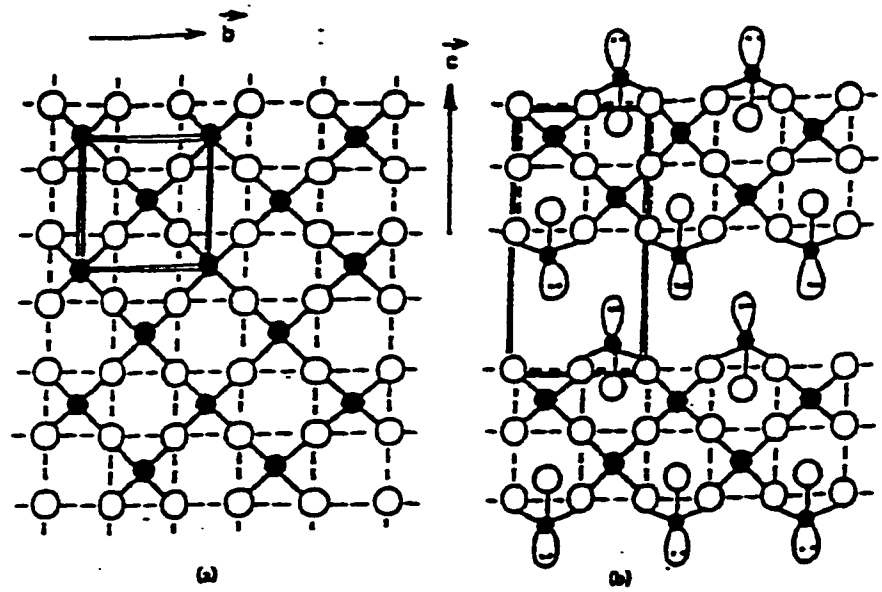

Projection of the structures of : (a) β-PbF_2, (b) α-$PbSnF_4$

Coordination of : (c) lead in β-PbF_2, (d) tin in α-$PbSnF_4$

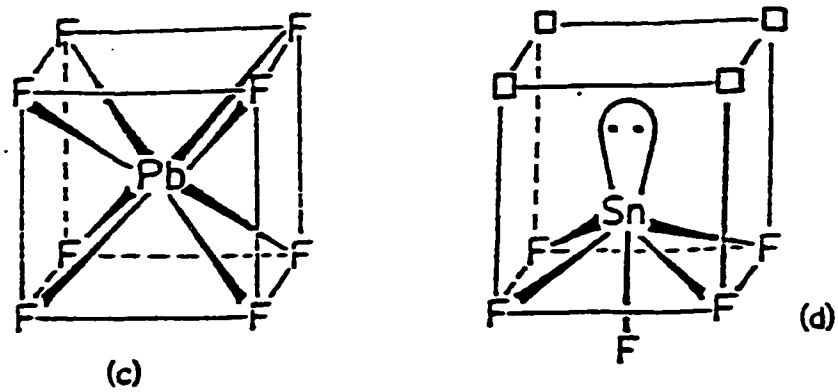

Figure 3: Structure of β-PbF_2 and α-$PbSnF_4$

doubts on the structural conclusions about these species from their infrared spectra alone, and requires a closer examination. Obviously, only X-ray or neutron diffraction of a single crystal or of a powdered sample (Rietveld profile analysis) can give a reliable crystal structure.

The structures and properties of the materials obtained from aqueous solutions of SnF_2 and $Pb(NO_3)_2$ and of SnF_2 and $Ca(NO_3)_2.4H_2O$ have shown that the composition and properties of the materials obtained is often extremely sensitive to variations in the method of preparation [6,11,14,19,21,34-38]. This was not reported by Donaldson and Senior, with the exception of the order of addition of reagents (i.e. whether the metal(II) nitrate solution is added to the SnF_2 solution or vice versa), which plays an important role in the stoichiometry of the product. However, the influence of the molar ratio X on the composition of the product as well as other important parameters were not investigated.

A few years ago, Dénès and Greedan attempted the resolution of the crystal structure of $SrSn_2F_6$ by neutron powder diffraction [39]. X-ray single crystal diffraction could not be used since no sufficiently large single crystal could be obtained. The sample used was prepared by Dénès from a slurry of $SrCO_3$ in a hot aqueous HF solution of SnF_2 [33]. When the neutron powder pattern was recorded, the background count was very high and therefore the peak / background ratio was too poor to make the data usable for a structure resolution. This could be attributed only to incoherent scattering by ^1H, and it was an indicator that the sample was hydrated. A TGA (thermogravimetric

analysis) experiment showed that the sample loses weight very slowly when held overnight at 250°C under nitrogen. The weight loss was consistent with the loss of one molecule of water for one unit formula of $SrSn_2F_6$, indicating that the formula of the product is $SrSn_2F_6.H_2O$, and not the anhydrous compound reported by Donaldson and Senior. In addition the weight loss was reversible, i.e. anhydrous $SrSn_2F_6$ picks up H_2O from air spontaneously to give back the monohydrate. This explains why Donaldson obtained the same product from aqueous solutions and cooled melts, since the latter spontaneously rehydrates in air.

The previous research of the materials formed by the reaction between strontium salts and tin fluoride was rather incomplete. Special attention was never paid to the various important reaction parameters, some of which can greatly influence the reaction outcome. Therefore, the major part of this work is concerned with a detailed investigation of the formation and the behavior of the materials formed in the strontium nitrate / tin fluoride system. The objectives of this study was to establish the conditions of preparation of $SrSn_2F_6.H_2O$ and $Sr_2Sn_2NO_3F_7.2H_2O$ using well defined reaction parameters, to characterize the products obtained, to further investigate the influence of the order of addition of the reagents and the molar ratio on the stoichiometry of the products. Also, parameters such as temperature, time, mixing speed, were varied and their influence on the compounds observed. The effect of recrystallization of $SrSn_2F_6.H_2O$ and $Sr_2Sn_2NO_3F_7.2H_2O$ from nitric acid was also investigated.

1.2 Earlier Work on the $BaCl_2$ / SnF_2 System

Donaldson and Senior were also the first to investigate reactions in the SnF_2 / BaF_2 system by reactions of aqueous solutions of SnF_2 and barium nitrate [32]. New compounds $BaSn_2F_6$ and $BaSn_4F_{10}$ were isolated. This research was continued by Dénès, who prepared $BaSnF_4$ by direct reaction at high temperature and characterized its structural and conducting properties [1,3,16,25,26,27,40].

Muntasar further studied reactions of SnF_2 and $BaCl_2.2H_20$ in aqueous solutions and reactions of ground SnF_2 + $BaCl_2$ + BaF_2 in various proportions at 350^0C, 500^0C and 600^0C in copper tubes under nitrogen [11, 41-48]. During this investigation was proven that in addition to the mixed fluorides already known, chlorofluorides can also be obtained. Reactions were carried out for X=Ba/Sn ratios of 0.06 to 18.0. At low Ba/Sn ration (X<0.5), $BaSn_2F_6$ and $BaSn_4F_{10}$ were obtained.

Reaction mixtures with X=0.52 to 5.00 yielded several new chlorofluorides of Ba and Sn with covalently bonded tin. Two of these materials, $BaSn_2Cl_2F_4$ and $Ba_3Sn_3Cl_4F_8.2.6H_20$ were characterized. The Mössbauer spectrum of these materials shows a large quadrupole doublet, which indicates that tin(II) is covalently bonded and has a stereoactive lone pair on a hybrid orbital.

In addition, for X>5, a solid solution $Ba_{1-x}Sn_xCl_{1+y}F_{1-y}$, non-stoichiometric in both metals and anions, with ionically bonded tin , was obtained. This material was characterized as pure BaClF type solid solution

with a very wide range of compositions ($0<x<0.23$; $-0.30<y<0.20$). The X-ray diffraction pattern shows only the Bragg peaks characteristic of BaClF, with some shift due to minor changes of the unit-cell parameters when some Ba^{2+} is replaced by Sn(II) and when come Cl^- is replaced by F^- or vice versa. No order between the two metals or between the substitutional anions is observed. The two anionic sites remain ordered, like in unsubstituted BaClF. A moderate increase of the linewidth upon metal and/or anion substitution is observed. This is most likely due to the presence of some stress, which the structure is subjected to, when it accomodates the ions substitutions.

^{119}Sn Mössbauer spectroscopy shows a single tin(II) line at about 4mm/s, that is characteristic of ionic tin(II) with a non-stereoactive lone pair. This situation was unexpected for tin(II) bonded to fluorine and chlorine, and is similar to $SnCl_2$, which was before the only known case when Sn-Cl bonds are present [46]. The reason might be that Sn^{2+} is incorporated in the typical ionic lattice of BaClF. The strong tin(II) signal shows that the lattice is strong, in agreement with the presence of strong ionic bonds.

The crystal structure of BaClF (fig. 4) is isotypic to PbClF and is derived from the MF_2 fluorite type by a tetragonal distortion due to order between the two types of anions [47]. In the fluorite type, the metal ions are squeezed between two layers of fluoride ions (MF_8 cubes). In BaClF, each metal ion is squeezed between a layer of fluoride ions (as in MF_2) and a layer of chloride ions. The chloride ions are bulkier and as a result the Cl sheets are

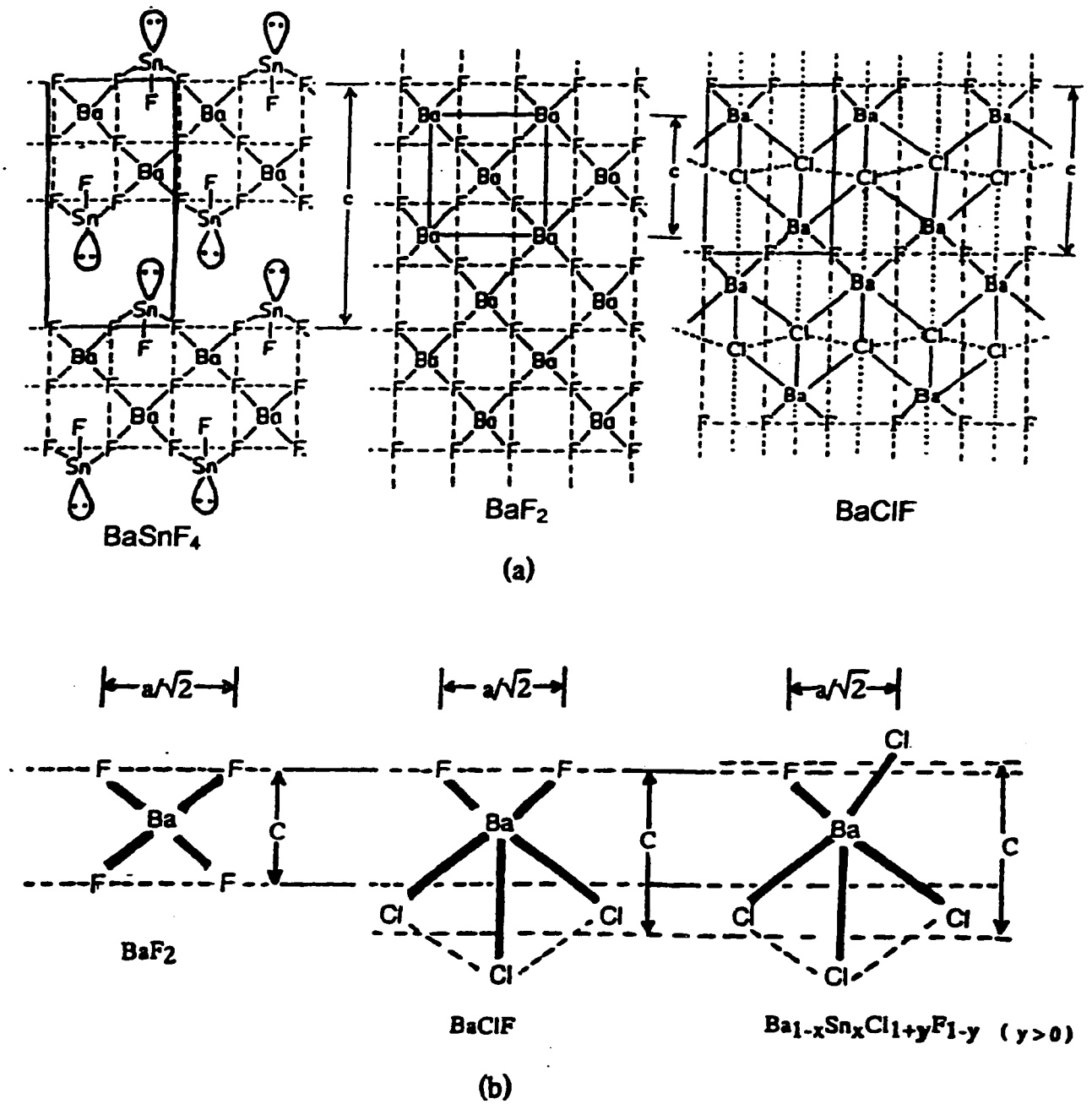

Figure 4: a) Structures of $BaSnF_4$, BaF_2 and BaClF

b) Increase of c in $Ba_{1-x}Sn_xCl_{1+y}F_{1-y}$ with y>0

corrugated and shifted to an axial position relative to Ba. This results in a $MF_4ClCl'_4Cl''$ coordination of the metal ion. The M-Cl" interaction is very weak. This ionic structure is found for highly electropositive divalent metals and for lead(II), which, in this case, carries a $6s^0$ non-stereoctive lone pair. Tin(II), due to its lower electropositivity, favors covalent bonding, with tin being hybridized and the and the stereoactive lone pair occupying one of the hybrid orbitals.

1.3 Objectives of This Work

The aims of the first part of this work are to gain a better understanding of the two materials already known to precipitate by reactions of SnF_2 and $Sr(NO_3)_2$.

In the second part of this work, reactions in the $SrCl_2$ / SnF_2 / H_20 system were studied in an attempt to prepare new chloride fluoride materials and maybe stabilize ionic tin(II) like in the case of the $BaCl_2$ / SnF_2 system. The influence of the order of addition of the reagents and the molar ratio on the stoichiometry of the products was investigated.

CHAPTER 2. EXPERIMENTAL

2.1. INSTRUMENTAL

2.1.1. X - RAY POWDER DIFFRACTION

2.1.1.1. PRINCIPLES

The X-ray powder diffraction method is based on the interactions between X-rays and crystals. It gives us valuable information about the structural arrangement of crystals. X-rays are electromagnetic radiations of short wavelength and therefore high frequency and high energy. Crystals are capable to diffract a radiation that has a wavelength similar to the interatomic separation. When a beam of X-rays strikes a crystal, wave interference occurs between beams scattered by families of planes (equidistant parallel planes) in the crystal and a diffraction pattern is created. The characteristics of this pattern are related to the structure of the crystal. The diffraction angle (Bragg angle) is a function of the distance between two adjacent planes of a family and the intensity of the diffracted beams depends on the nature of the atoms (number of electrons) present in the crystal and their position relative to one another.

The distance between the planes of a given family is called "d-spacing" and it can be determined from the position of the diffracted beams using Bragg equation:

$$2d \sin \theta = n \lambda \qquad (1)$$

where "d" is the "d spacing", "θ" is the diffraction angle (i.e. half of the 2θ angle between the incident beam and the diffracted beam), "n" is the order of diffraction (integer number >0) and "λ" the wavelength of the radiation. The difference between the path lengths of the two waves is "$2d \sin \theta$" (fig. 5).

If the crystal is molecular, the diffraction pattern is often used to map the electron density of the molecules. Each crystalline material has a different set of families of planes, spaced differently and the distribution of atoms in the crystal will be different, therefore, they will give a set of diffracted beams (called diffraction pattern) which are different both in line position and in intensity. Therefore, the diffraction pattern of a crystalline phase is usually unique and as a result it can be used for fingerprinting , i.e. for phase identification. From the diffraction powder pattern obtained on a crystalline sample, one can also extract the unit cell parameters (a,b,c edges and α, β, γ angles), provided the (hkl) indexation of the Bragg peaks is known (fig. 6). The unit cell is the smallest unit volume that contains at least one whole molecule and all the symmetry elements of the crystals.

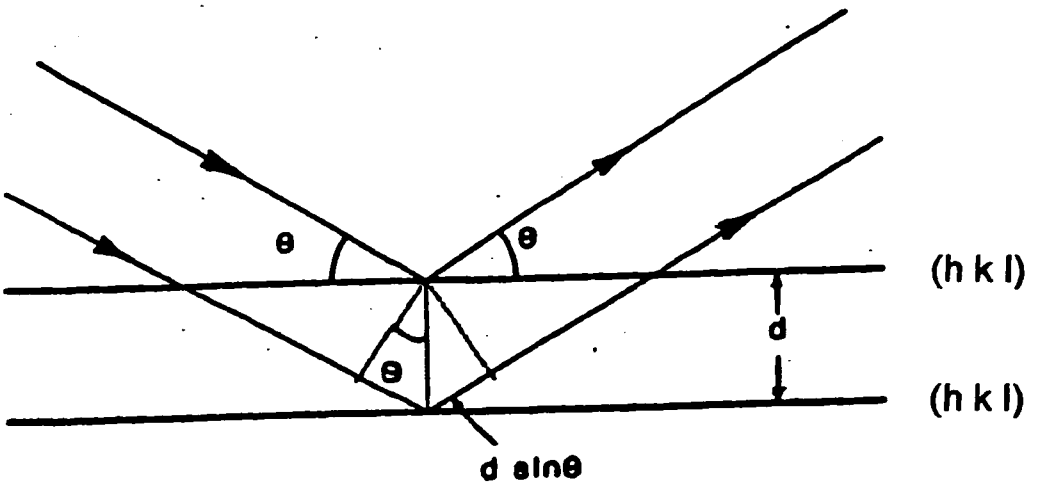

Figure 5: Diffraction of a Monochromatic Radiation by a Crystal Lattice (Bragg law)

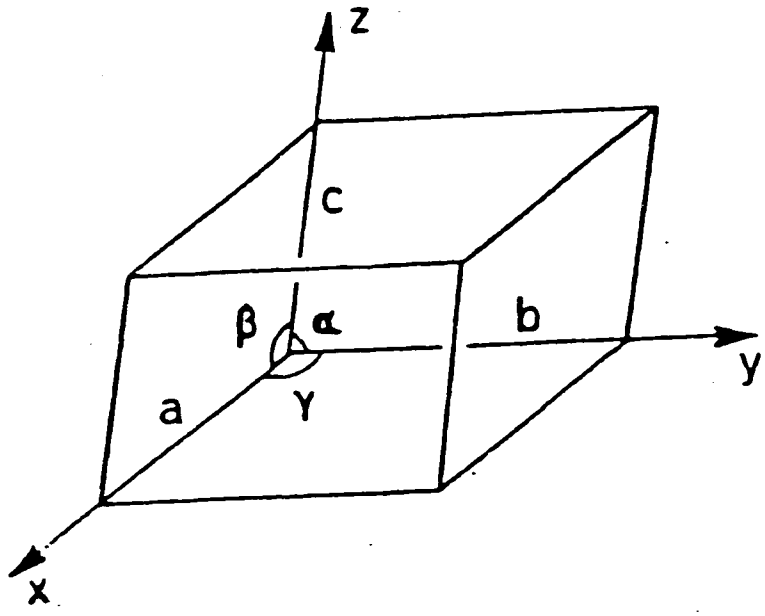

Figure 6: Unit Cell Nomenclature

The following important facts have to be mentioned:

1) Non crystalline materials such as glass, amorphous materials, liquids and gases give no diffraction pattern and will not be detected easily.

2) Microcrystalline materials (particle diameters smaller than ca. 1000 Å, using our X-ray diffractometer) give broadened lines and no pattern is recorded if the particles are smaller than ca.30 Å. Within the range ca.30 - 1000 Å, the average particle diameter can be calculated from the line broadening.

3) The relative intensity of the lines of a powder pattern can vary widely due to texture effect, if the crystallites (small crystals in a powder) are not randomly oriented. This effect is particularly frequent in divalent tin compounds because of the anisotropy of bonding generated by the tin lone pair, which often results in sheet - like or needle - shaped crystallites with a tendency to stack parallel to each other, and therefore are not randomized [48].

2.1.1.2. INSTRUMENTATION

X-ray powder diffraction was carried out on a Philips PW 1050-25 diffractometer, using the Ni - filtered Kα radiation of copper (λ = 1.54178 Å for Kα). The X-ray tube was powered at 800 W (40 kV and 20 mA). Figure 7 shows the geometry of diffraction for the Philips line focusing diffractometer. The radiation diffracted in the plane of the page at a given 2θ angle is brought

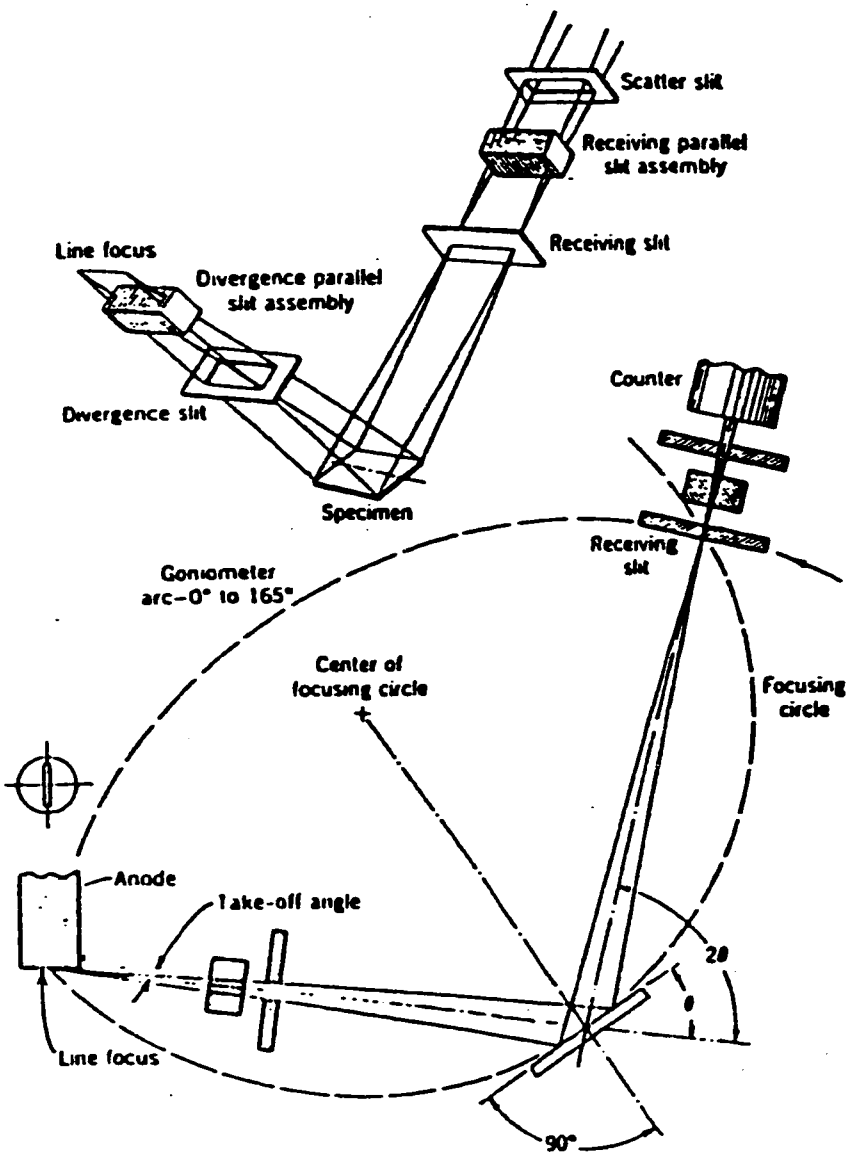

Figure 7: A Schematic Arrangement of the Line Focusing X-ray Powder Diffractometer

to an approximate focus on the circumference of a circle - the focusing circle - by positioning on the focusing circle, the sample surface tangent to the circle, the X-ray tube target and the receiving slit. The sample surface bisects the diffraction angle 2θ in this case. The X-ray beam diffracted from the surface of the sample is focused into the receiving slit before entering the detector or counter. This assures strong and narrow Bragg peaks and a weak background.

The angular range required to obtain the desired diffraction pattern is scanned by rotating the counter at a constant speed (0.5° (θ) per minute). In order to maintain the geometry of the focusing circle, the sample is geared to rotate about the same axis at half the speed of the counter. The detector is a Xe/CO_2 scintillation counter. After detection, the signal is amplified and analyzed in a pulse height analyzer, then sent to the computer, as a measurement of intensity versus diffraction angle θ. The diffractometer is automated with the Sietronics Sie112 system. The recorded pattern is analyzed and compared to the patterns stored in the Powder Diffraction Files (PDF) of the JCPDS database (JCPDS=Joint Committee for Powder Diffraction Standards). The patterns were recorded in the step scanning mode, at an angular speed of 0.5° (θ) per minute, in the angular range 5 to 60° (2θ).

2.1.1.3. SAMPLE PREPARATION

In the X-ray powder method, the sample to be examined must be a flat surface fine powder and placed in a beam of monochromatic X-rays. Each crystallite, i.e. each particle of the powder, is a small single crystal oriented at random with respect to the incident beam and with respect to other crystallites (unless preferred orientation is present), otherwise, the line intensity will be greatly modified.

Each sample was manually ground to a fine powder by using a mortar and pestle and placed in a plexiglass sample holder, whose window area is 2 cm^2, by pressing the powder with a glass slide to form a flat smooth surface which is placed on the focusing circle at the center of the diffractometer. Preferred orientation is usually enhanced by the pressure applied to the powder to form a smooth flat surface. Preferred particle orientation is often difficult to control, and it strongly affects relative peak intensities, therefore, it must always be kept in mind when assessing peak intensities. As mentioned previously, the size of the particles in the powder is also an important parameter since broadening will occur if the sample is microcrystalline. Surface roughness may also have a significant effect on relative peak intensity and their position since a part of the sample is shifted from the focusing circle when the surface is not smooth.

2.1.2. MÖSSBAUER SPECTROSCOPY

2.1.2.1. PRINCIPLES

The phenomenon of emission and reabsorption of a γ-ray photon without loss of energy due to recoil of the nucleus and without thermal broadening is known as the Mössbauer effect [46]. Its unique feature is in the production of monochromatic γ-radiation with a very narrowly defined energy spectrum, so it can be used to resolve minute energy differences. The direct application of the Mössbauer effect to chemistry arises from it's ability to detect the slight variations in the energy of interaction between the nucleus and the extra-nuclear electrons, variations which had previously been considered negligible.

Mössbauer spectroscopy is a very powerful technique for probing specific atom sites in various compounds containing an element that has a Mössbauer nuclide (such as ^{119}Sn). This technique provides the valence state of tin and gives useful information on the nature of the chemical bond and the site distortion through two parameters - the isomer shift and the quadrupole splitting.

The isomer shift is due to the difference in "s" electron density at the nucleus between the absorber (sample) and the γ-ray source; it gives information about the valence state, degree of ionicity and the nature of ligands.

The quadrupole splitting is due to the interaction between the electric field gradient (e.f.g.) at tin and the quadrupole moment of the nucleus (in the excited state only for ^{119}Sn, since the nuclear spins in the ground state and in the excited state of ^{119}Sn are $I_g=\frac{1}{2}$ and $I_e=\frac{3}{2}$) (fig.8). The e.f.g. arises from an

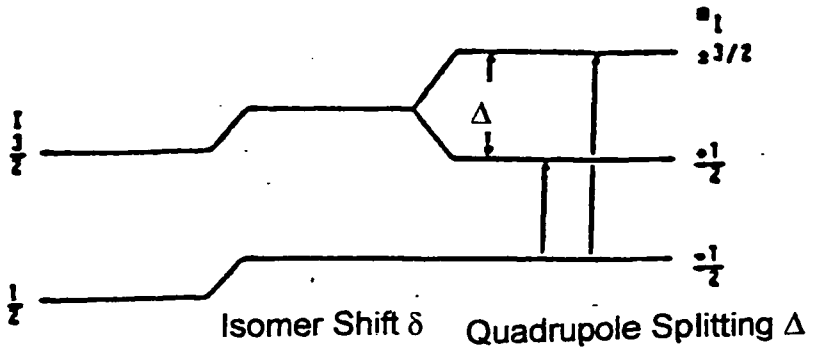

(a) Absorber energy levels.

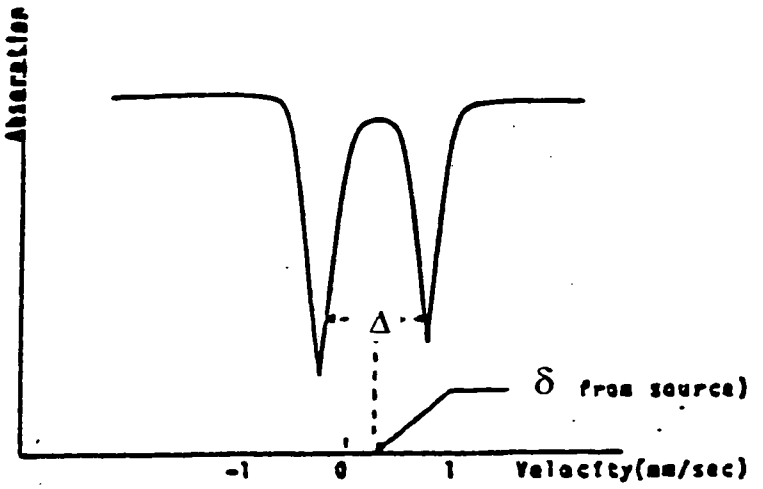

(b) Resultant Mössbauer spectrum.

Figure 8: Nuclear Energy Levels, Isomer Shift and Quadrupole Splitting

aspherical distribution of electric charges around tin. There are two contributions to the electric field gradient : $(e.f.g.)_{val}$ is the valence contribution caused by non - spherical orbitals (p,d or f) in partly filled subshells; $(e.f.g.)_{lat}$ is the lattice contribution caused by a non - regular atomic coordination (not regular cubic, octahedral or tetrahedral), and its effect is weaker because the ligands are further away from the nucleus than the valence electrons. The two contributions to the e.f.g. can be partly shielded by core electrons, and they can add up or partly cancel one another depending on their signs. Calculation of the e.f.g. is usually not possible, except in pure metals and in purely ionic compounds. The quadrupole splitting provides information on the site symmetry and hybridization of the orbitals [46].

2.1.2.2. INSTRUMENTATION

The Mössbauer absorption spectrum is a record of the transmission of resonant γ-rays through an absorber as a function of the Doppler velocity, with respect to the source. The measurement of a Mössbauer spectrum is carried out by repetitively scanning the whole velocity range required. It means accumulating the whole spectrum simultaneously, and allowing continuous monitoring of the resolution.

A schematic illustration of a Mössbauer spectrometer is presented on figure 9 [46]. The main component is the multichannel analyzer. It can store an accumulated total of γ-counts (using binary memory storage like a

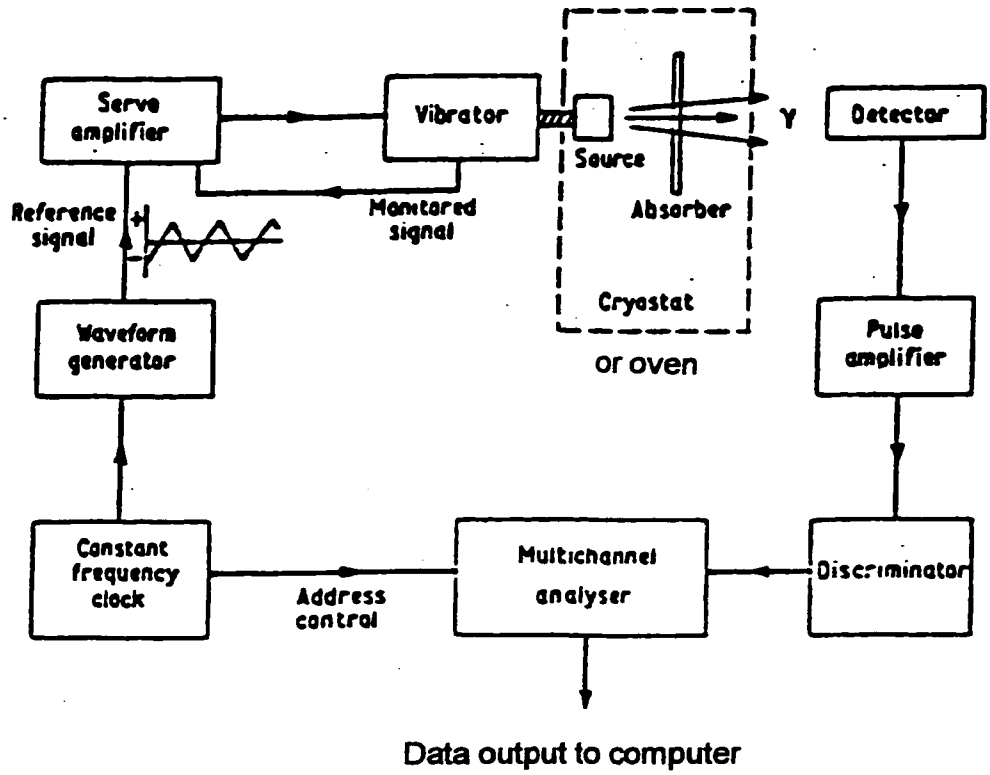

Figure 9: Schematic Arrangement for a Mössbauer Spectrometer

computer) in one of several hundred individual registers called channels. Each channel is kept open in turn for short fixed length period of time controlled by a very precise constant frequency clock device. Any γ-counts registered by the detection system during that time interval are added to the accumulated total already stored in the open channel. The timing pulses from the clock are used to synchronise a voltage waveform, that serves as a command signal to the servo-amplifier controlling an electromechanical vibrator called transducer. The latter moves the source relative to the absorber. A waveform, with a voltage increasing linearly with time, imparts a motion with a constant acceleration in which the drive shaft and the source spend equal time intervals at each velocity increment. The multichannel analyzer and the drive are synchronized so that the velocity changes linearly from -v to +v with increasing channel number. In this way, the source is always moving at the same velocity when a given channel is open and the counts registered into any given channel always corresponds to the same velocity of the source.

The geometric arrangement of the source, absorber and detector are important since the angle θ between emitted γ-rays and the axis of the motion of the source creates the cosine effect, which causes a spread in the apparent Doppler energy, therefore resulting in line broadening. The way of reducing this effect is adequate separation between source and detector.

The velocity range required to completely encompass the energy differences for all spectra acquired was fixed at $\pm$8mm/sec.

For ^{119}Sn Mössbauer spectroscopy, a Harshaw (Tl)NaI scintillation detector was used. The pulses are passed through a discriminator (single channel analyzer), which rejects most of the nonresonant background radiation, and are finally fed to the open channel address in the multichannel analyzer.

2.1.2.3. SAMPLE PREPARATION

All spectra were recorded at room temperature using a nominally 10mCi $Ca^{119m}SnO_3$ γ-ray source. The isomer shifts were referenced to a standard $CaSnO_3$ absorber at room temperature as zero isomer shift.

The samples were ground and weighed, then placed in a teflon holder and pressed into a thin layer by the teflon cap which was screwed into the base. In the cases when preferred orientation was investigated, the sample was not ground since we wanted to study the effect of crystal orientation on the Mössbauer spectrum. All samples were then placed into the γ-ray beam. The γ-ray source was covered with a thin palladium foil to absorb the X-ray lines due to nuclear conversion, and data were acquired over a period of several days.

2.1.3. ATOMIC ABSORPTION SPECTROPHOTOMETRY

2.1.3.1. PRINCIPLES

When heated to a sufficiently high temperature, most compounds break apart into atoms in the gaseous phase. Unlike the optical spectra of condensed phases, the spectra of these atoms consist of very sharp lines. Each element has its own characteristic spectrum. Because the lines are so sharp, there is usually little overlap between the spectra of different elements in the same sample.

In atomic spectrophotometry, samples are vaporized at very high temperatures and the concentrations of selected atoms are determined by measuring absorption or emission at their characteristic wavelengths. It is a highly sensitive quantitative technique; analyte concentrations in the parts-per-million are routine.

In atomic absorption spectrophotometry the absorption of light by free gaseous atoms in a flame is used to measure the concentration of atoms [49].

2.1.3.2. INSTRUMENTATION

The apparatus for atomic absorption spectrophotometry is shown on figure 10. The liquid sample is aspired into a flame the temperature of which is 2000 to 3000 K. The sample is atomized in the flame, which takes the place of the cuvet in conventional spectrophotometry. The pathlength of the flame is typically 10 cm. To measure the light absorbance of specific atoms in the flame the light source uses a cathode made of the same element. This source emits light with the characteristic frequencies of those atoms [49].

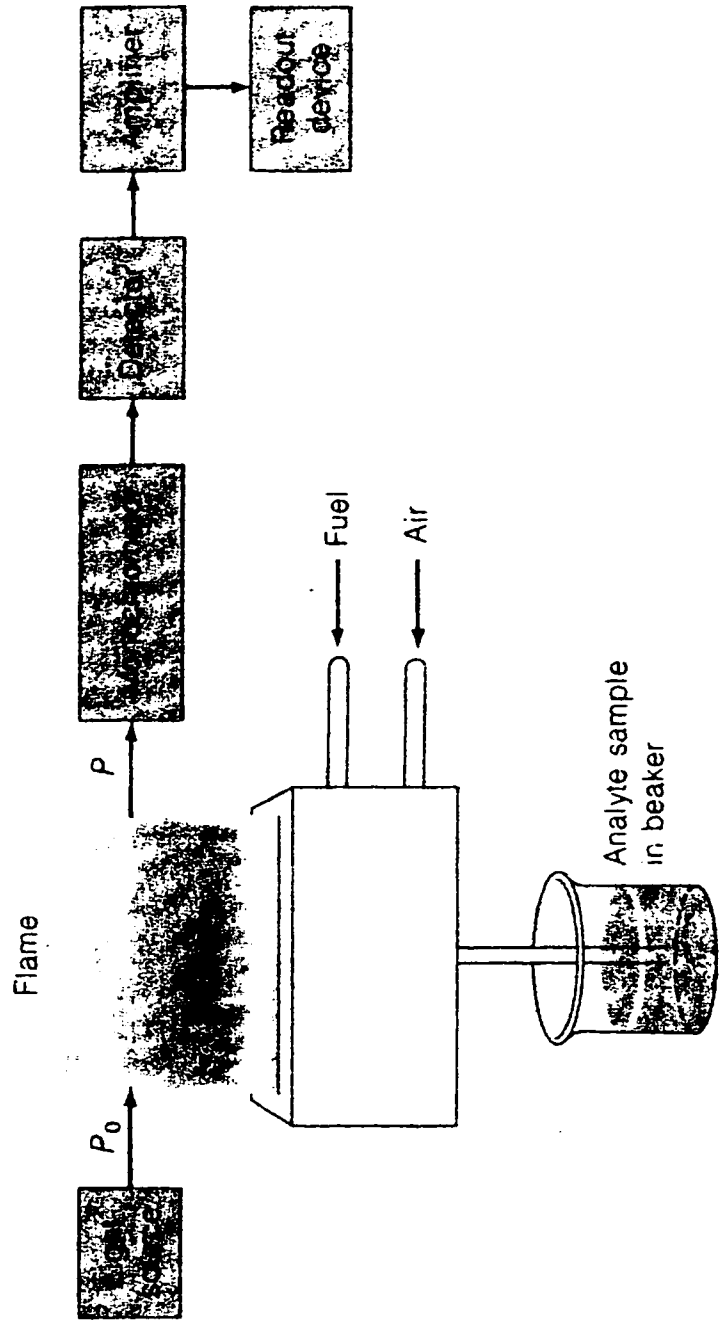

Figure 10: Outline of an Atomic Absorption Spectrometer

All measurements were performed on Perkin Elmer Atomic Absorption Spectrometer Model 503. The source beam was alternately directed through the flame and around the flame by a chopper. After recombination, the two beams passed through a monochromator to a detector and readout system. The difference between the two beams was integrated over three seconds and displayed.

The source used is a hollow cathode lamp. Fuel and support gas are mixed in a premix chamber burner, then they enter in the burner head where the combustion occurs.

2.1.3.3. SAMPLE PREPARATION

Atomic absorption spectrophotometry was used to determine the amount of strontium and tin in the samples. A set of standards was prepared for both elements. Samples of known mass were dissolved in concentrated HCl which was then diluted with water to 10% HCl and then they were diluted with a 10% HCl solution below the maximal detection limit. Their absorbance was measured, calibration lines were constructed and the amount of tin and strontium in the samples was determined using the calibration curves and the measured absorbance of the samples. Table I. below gives the characteristic wavelengths and regions of linear response for both elements.

Table I. Characteristic wavelengths and regions of linear response of Strontium and Tin in Atomic Absorption Spectrophotometry

ELEMENT	CHARACTERISTIC WAVELENGTH (nm)	MAXIMAL DETECTION LIMIT (ppm)
Strontium	231.1 (visible)	5
Tin	286.3	300

2.1.4. FLUORIDE ION ELECTRODE

The fluoride electrode is a solid-state ion-selective electrode employing a crystal of inorganic salt as the ion-sensitive membrane. It consists of a crystal of LaF_3 doped with Eu(II) and 0.1M NaF and 0.1M NaCl filling solutions.

Fluoride ions from solution are absorbed on the surface of the crystal and can migrate through the crystal because there are anion vacancies created in the crystal by doping of LaF_3 by Eu(II), i.e. this crystal acts as a fluoride ion conductor.

Eu(II) has one positive charge less than La(III) and therefore one anion vacancy is created for every La(III) substituted by Eu(II) in order to preserve

the electrical neutrality of the crystal. Fluoride ions can migrate and create a potential across the crystal. This is depicted on figure 11.

The response of the electrode can be described by the following equation:

$$E = \text{constant} - 0.05916 \log [A_{F^-} (\text{outside})] \qquad (2)$$

where A_{F^-} is activity of fluoride ions.

It gives a Nernst-type response over a concentration range from about 10^{-6} M to 1 M. This electrode gives 1000 times higher response to fluoride ion than to other ions. The only interfering species is the OH^- ion [49].

The fluoride sensitive electrode was used for the determination of fluoride ions present in the samples. A set standards of known concentration was prepared using NaF (1, 10, 100 ppm), their potentials were measured and plotted on semilog paper versus concentration. A calibration curve was constructed. Samples of unknown concentration were diluted to the required concentration range, their potentials were measured and the corresponding concentration was obtained from the graph. The total amount of fluoride ions in the sample could then be calculated.

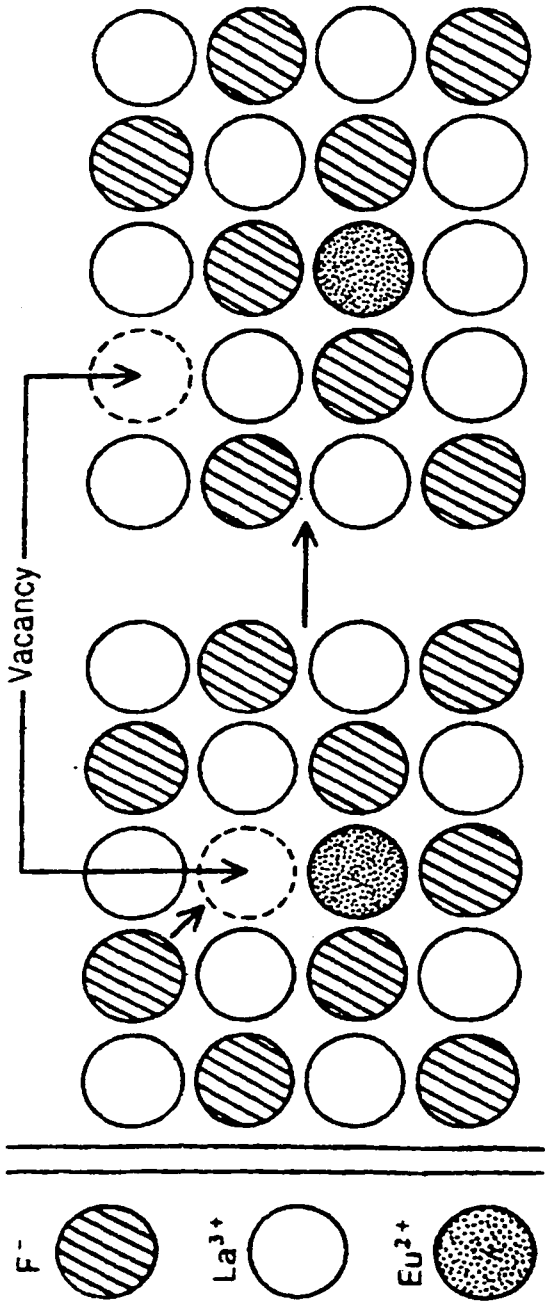

Migration of F^- through LaF_3 doped with EuF_2. Since Eu^{2+} has less charge than La^{3+}, an anion vacancy occurs for every Eu^{2+}. A neighboring F^- can jump into the vacancy, moving the vacancy to another site. Repetition of this process moves F^- through the lattice.

Figure 11: Migration of F^- through LaF_3 doped with EuF_2.

2.1.5. INFRARED SPECTROPHOTOMETRY

Compounds are able to absorb electromagnetic radiations of various wavelenghts. Absorption of radiations in the infrared region leads to vibrational excitations of bonds. Different types of bonds require different values of energy for those excitations and therefore they can be identified according to the frequency of radiation absorbed. In an infrared spectrum the main region of interest useful for the determination of organic functional groups is the region of 1400 - 4000cm^{-1}. The region above is called the "fingerprint region". Infrared spectrophotometry is a very accurate qualitative technique for the determination of various functional groups in organic compounds.

In this work, infrared spectrophotometry was employed in order to check whether the materials are hydrated or not. In the case of hydrated compounds, it is usually possible to observe a broad peak in the region around 3 330cm^{-1} which is caused by increased stretching vibrations of the O - H bond [50].

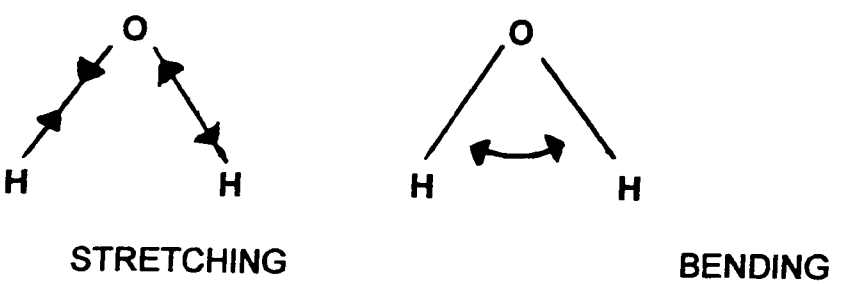

Figure 12: Stretching and Bending Vibrations in the Water Molecule

2.1.6. THERMAL ANALYSES

Thermal analysis can be defined as a measurement of physical or chemical properties of materials as a function of a temperature. The specific properties that can be studied by thermal analysis are for example enthalpy, heat capacity, coefficient of thermal expansion, sample mass. Uses of thermal analysis in solid state science are numerous and they include the study of solid state reactions, thermal decomposition, phase transitions and the determination of phase diagrams.

The two main analytical techniques used in this work are thermogravimetric analysis (TGA) and differential thermal analysis (DTA).

Thermogravimetric analysis is a technique in which the mass of a substance is measured as the temperature of the substance is varied. Changes in the mass reflect a decomposition or reaction of a substance with ambient atmosphere, giving often well defined products.

Differential thermal analysis detects changes between the temperature of the sample and that of a compound that does not undergo any transformation in the temperature range of study. All transformations involving an exchange of energy (with $\Delta H \neq 0$), e.g. chemical changes or first order phase transitions, are detected.

DTA and TGA can be recorded simultaneously. The PL-STA 1500 instrument was used for thermal analysis experiments. A sample weighing

between 5 and 15 mg was placed in a platinum holder inside the furnace. As the temperature inside the furnace increased, the mass was recorded versus temperature. Any loss of water, decomposition or reaction involving a loss or a gain of mass (i.e. involving a gas) can be observed on both the TGA curve and the DTA curve. The DTA curve will show any transformation, even not involving a mass change, provided there is a measurable enthalpy change ($\Delta H \neq 0$), i.e. for all first order transformations. The temperature of the oven was raised linearly versus time. However, at a temperature that is specific for each substance (e.g. first order phase transition or chemical change) the sample either releases or absorbs a certain amount of heat. On the curve, this will be recorded as an exothermic peak (heat release) or as an endothermic peak (heat absorption). Exothermic phenomena taking place on heating are always irreversible, whereas endothermic events are reversible, although they can be very sluggish due to kinetic factors (a high activation energy) [51]. This is the case of the $\alpha \rightarrow \beta$ allotropic transformation of $PbSnF_4$ [8,16,18,40].

Thermal analysis experiments were performed in order to determine the thermal stability and the degree of hydration of the materials and for evidencing any first order solid state phase transition (e.g. structual change) that may take place.

2.2. SYNTHESIS

2.2.1. COMPOUNDS IN THE STRONTIUM NITRATE - STANNOUS FLUORIDE SYSTEM

2.2.1.1. REAGENTS

$Sr(NO_3)_2$: BA Allied Chemical & Dye Corporation

SnF_2 : Ozark Mahoning, 99% purity

H_2O : distilled, deionized or double deionized

HNO_3 : HBD, 70%, assured ACS

2.2.1.2. REACTION CONDITIONS

All products were prepared by precipitation from aqueous solutions of strontium nitrate and stannous fluoride. A 1.5M stock solution of strontium nitrate was always prepared in advance.The solution of stannous fluoride was, however, prepared just prior to each use since it is prone to decomposition and it has been observed that the precipitate obtained in the reaction of lead(II) nitrate with tin(II) fluoride varies with aging of the SnF_2 solution [35].

One of the solutions was added to the other from a burette at a medium rate of 5 ml/min.The white precipitate was filtered out by suction. Regular filter paper and Buchner funnel were used for this purpose. All precipitates were repeatedly washed with water then transferred on a watch glass and allowed to dry at room temperature (about 3 days). The mass of the product was recorded, and then the sample was transferred into a properly labelled PVC vial for storage and use in further analyses.

All reactions were performed in air.

Some of the reactions were carried out above ambient temperature. A closed system consisting of a three necked, round bottomed flask fitted with a condenser, a thermometer and a burette was used. One of the reagents was placed in the flask, a stirring bar was added and cold water was circulated through the condenser to prevent evaporation. The round bottomed flask was placed inside a heater and the whole assembly was mounted on a stirring plate (fig. 13). The system was slowly heated to the desired temperature, allowed to equilibrate and then the reaction was performed by dropwise addition of the reagent from the burette to the reagent in the reaction flask resulting in immediate precipitation. The precipitate was allowed to cool down, filtered, washed and dried in the same conditions as for the ambient reactions.

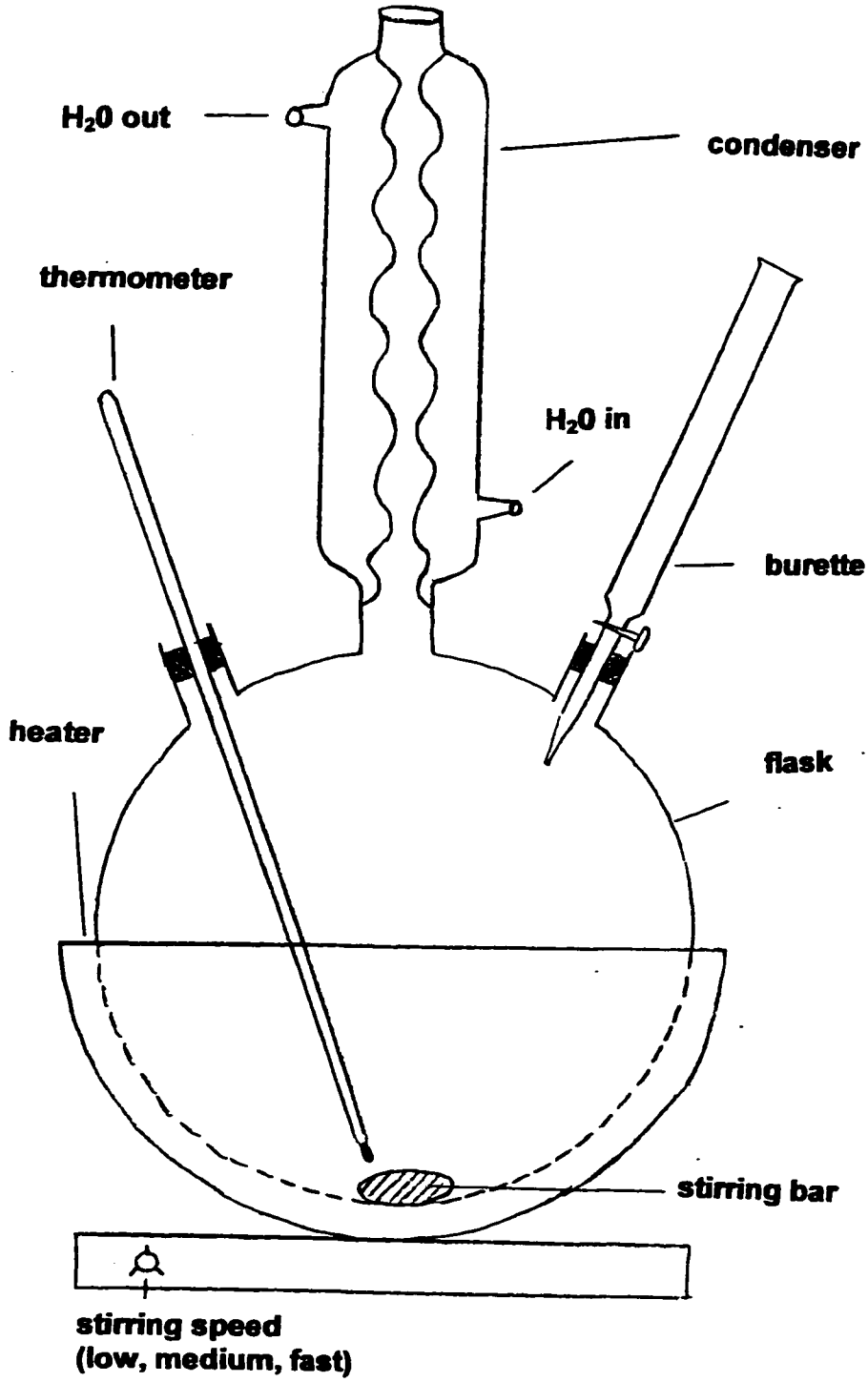

Figure 13: Assembly Used for the Reactions Carried out above Ambient Temperature

The following reaction parameters were kept constant all the time:

⇒ c [$Sr(NO_3)_2$] = 1.5M .....concentration of the $Sr(NO_3)_2$ solution

⇒ c [SnF_2] = 1.5M .....concentration of the SnF_2 solution

⇒ gas : air .....ambient gas

⇒ beaker : glass ..... nature of the beakers

⇒ rate of addition : medium (ca. 5ml/min)

In order to fully investigate the conditions of preparation, the following parameters were varied:

⇒ X = [$Sr(NO_3)_2$/ SnF_2] .....molar ratio

⇒ order of addition: Sr -> Sn .....the solution of strontium nitrate was added to the solution of tin fluoride

⇒ order of addition: Sn -> Sr .....the solution of tin fluoride was added to the solution of strontium nitrate

⇒ rate of stirring : low, medium or high

⇒ t (SnF_2).....time between the end of dissolution of SnF_2 and the beginning of the reaction

⇒ t (product)..... time between the end of reaction and the filtration of the product

⇒ V (H_20) .....volume of water used for washing of the precipitate

⇒ T (reaction).....temperature of the reaction

⇒ T (product).. ...temperature of heating of the products after precipitation

⇒ t (suspension).....suspension of dry products in H_2O for given periods of time

⇒ recrystallization of both products from 1N nitric acid:

a)V (HNO_3)..... volume of nitric acid used for recrystallization

b) t (heating rec.)..... heating time

c) t (product+HNO_3)..... time between the end of recrystallization and the filtration of the product

d) wet / dry..... recrystallization of wet versus dry products

2.2.2. COMPOUNDS IN THE STRONTIUM CHLORIDE - STANNOUS FLUORIDE SYSTEM

2.2.2.1 REAGENTS

$SrCl_2.6\ H_2O$: BA Allied Chemical & Dye Corporation

SnF_2 : Ozark Mahoning, 99% purity

H_2O : distilled, deionized or double deionized

2.2.2.2. REACTION CONDITIONS

In this second part of the work, samples were prepared the same way as in the strontium nitrate - stannous fluoride system with the exception of substitution 1.5M stock solution of strontium nitrate by 1.5M stock solution of strontium chloride.

The following reaction parameters were kept constant all the time:

⇒ c [$SrCl_2.6H_2O$] = 1.5M .....concentration of the $SrCl_2.6\ H_2O$ solution

⇒ c [SnF_2] = 1.5M .....concentration of the SnF_2 solution

⇒ gas : air .....ambient gas

⇒ beaker : glass .....nature fo beakers

⇒ t (SnF_2) = 0.....time between the end of dissolution of SnF_2 and the beginning of the reaction

⇒ T (reaction) ..... temperature of the reaction (room temperature)

⇒ rate of addition : medium (ca. 5ml/min)

The following parameters were varied:

⇒ X = [$SrCl_2.6H_2O$ / SnF_2] .....molar ratio

⇒ order of addition: Sr -> Sn .....the solution of strontium chloride was added to the solution of tin fluoride

⇒ order of addition: Sn -> Sr ..... the solution of tin fluoride was added to the solution of strontium chloride

⇒ rate of stirring : low, medium or high

⇒ t (product)..... time between the end of reaction and the filtration of the product

⇒ V (H_20) .....volume of water used for washing of the precipitate

⇒ T (product).. ...temperature of heating of the products after precipitation

Chapter 3.0. RESULTS AND DISCUSSION (1)

Chemical Analyses and Physical Characterization of the Materials Formed in the Strontium Nitrate - Stannous Fluoride System

3.1. YIELD

For the order of addition Sr -> Sn the yield relative to the limiting reagent is near 100% for X=0.1 and falls rapidly to stabilize between 60 and 65% at around the exact stoichiometry of the reaction, i.e. X = 0.33 :

$3SnF_{2\,(aq)} + Sr(NO_3)_{2\,(aq)} + H_2O \Rightarrow SrSn_2F_6.H_2O_{\,(s)} + Sn^{2+}_{(aq)} + 2NO_3^-{}_{(aq)}$

This indicates that the efficiency of the reaction is not perfect and increases for large excess of SnF_2. If the yield is expressed relative to the sum of the reagents, a maximum is obtained at X=0.3, it is close to the exact stoichiometry (X=0.33), as expected (fig. 14).

For the order of addition Sn -> Sr the interpretation of the yield relative to the sum of the reagents is more complicated because of the presence on more than one compound in the product (fig. 15). For molar ratios less or equal to 0.3, the curve is quasi identical to the case Sr -> Sn, with a maximum close to X=0.3. However, the decrease of yield is slower for X>0.3 and a second maximum is clearly visible as a shoulder on the curve. The presence of a mixture of products for $X \geqq 0.4$ makes the interpretation more difficult in that stoichiometry range.

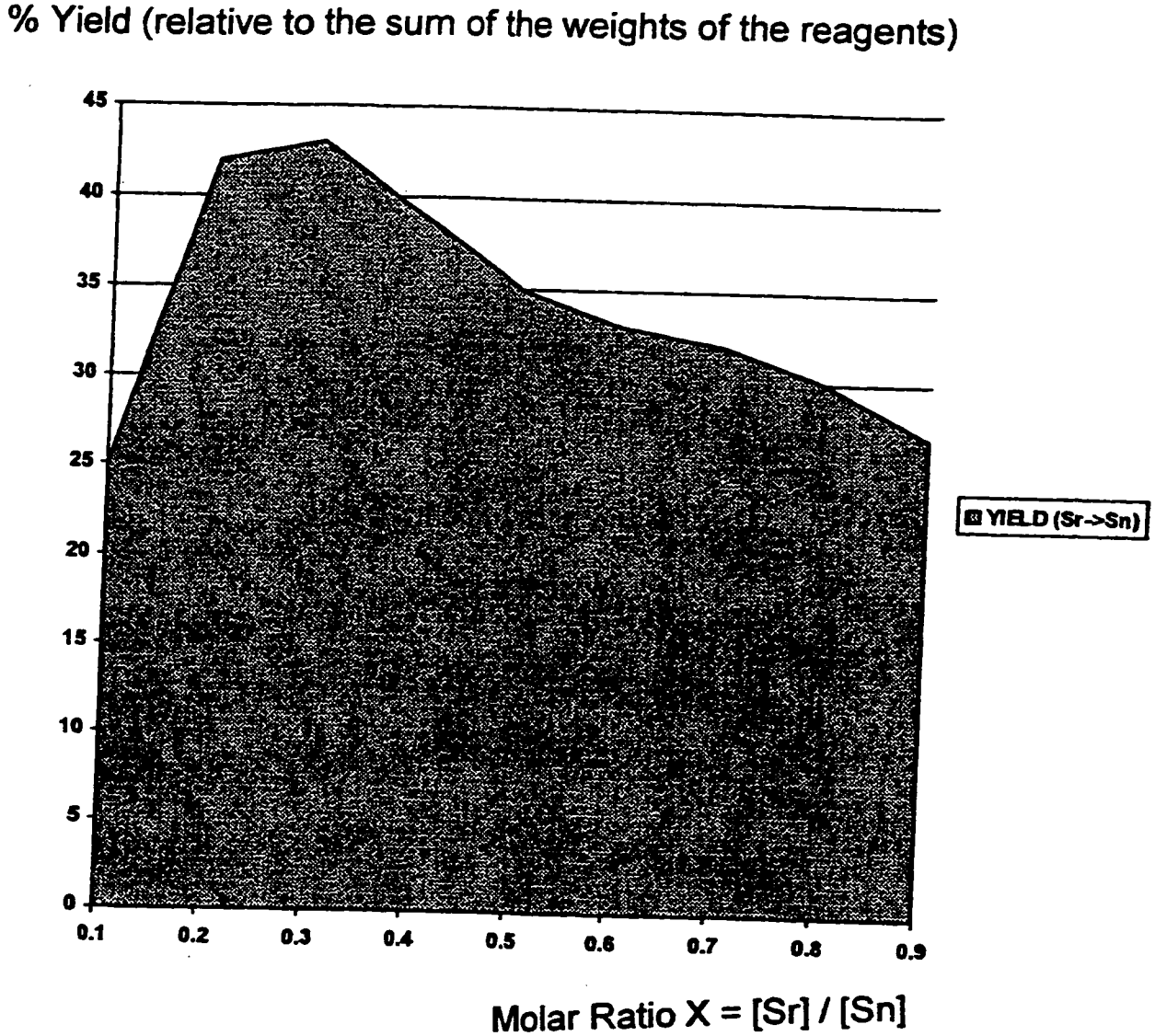

Figure 14: Yield of Precipitates for the Order of Addition Sr-->Sn

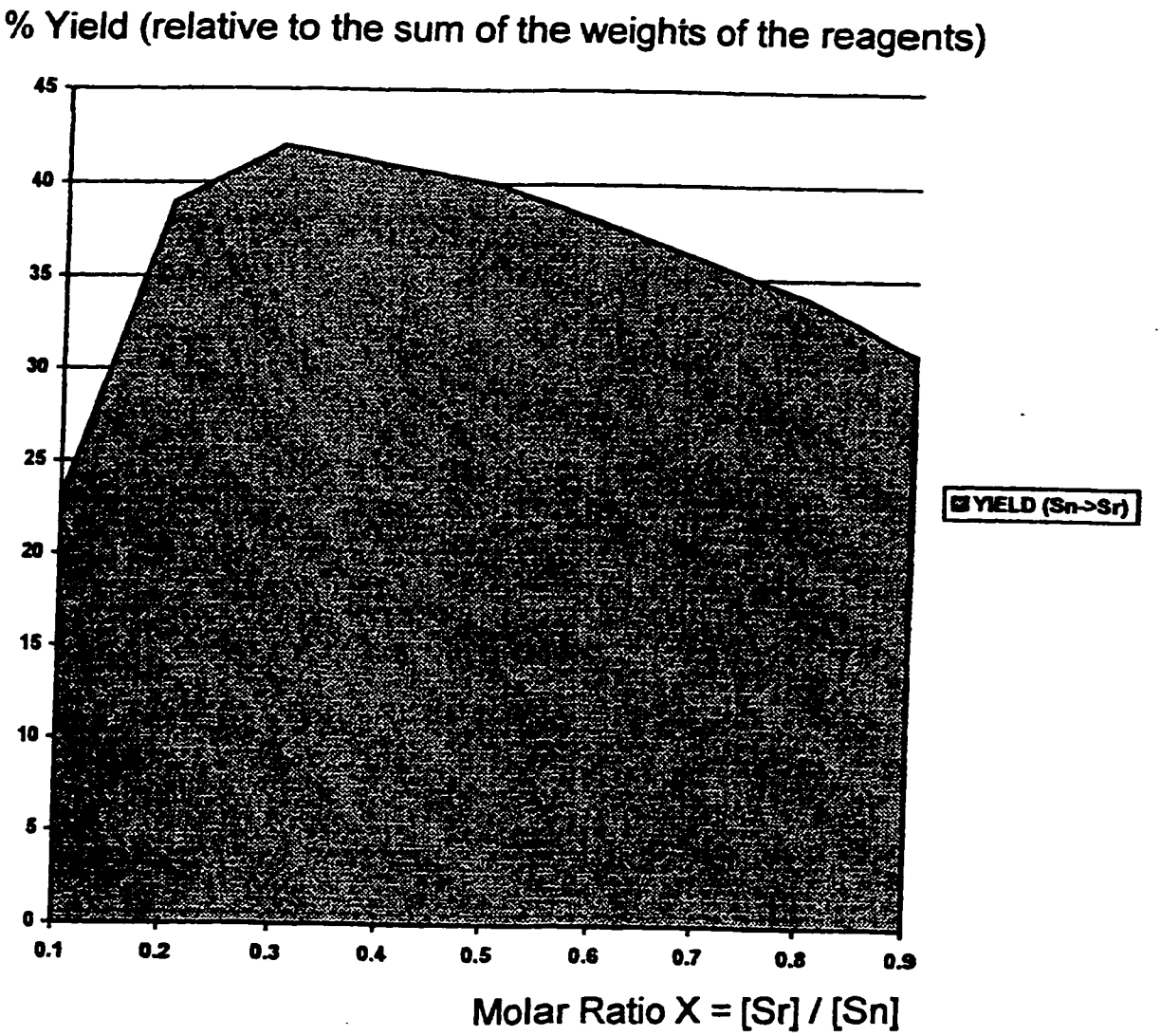

Figure 15: Yield of Precipitates for the Order of Addition Sn-->Sr

3.2. ELEMENTAL ANALYSIS

This work proved that there are two principal products obtained by various reactions between strontium nitrate and stannous fluoride. These crystalline white powders were identified as $SrSn_2F_6.H_2O$ and $Sr_2Sn_2NO_3F_7.2H_2O$. It was discovered that production of these materials is strongly sensitive to the reaction conditions. Changes in some of the investigated reaction parameters can greatly influence the product of the reaction and shift formation towards one or the other product or can result in a mixture of both.

All prepared samples are fine white powders. They were examined by X-ray powder diffraction in order to be identified. Several samples having an excellent search match (see section 3.6) were selected and analyzed further.

Atomic absorption spectrophotometry was used for quantitative analysis or tin and strontium and fluoride ion electrode analysis provided information about fluorine content. The results of elemental analysis of both principal compounds are presented in table II.

The data obtained are compared to the theoretical values and also to the results reported by Donaldson and Senior. All the results compare very well. Minor differences among the results can be attributed to the experimental error. In is important to mention that even though Donaldson and Senior did not report that $SrSn_2F_6$ is hydrated, no major discrepancies are apparent from the results of the elemental analysis, because the mass of one H_2O is small

ANALYSES OF THE PRODUCTS (WT %)				
ELEMENT OR GROUP	DONALDSON & SENIOR[32]	THEORETICAL		FOUND
		$SrSn_2F_6$	$SrSn_2F_6.H_2O$	
Sn	54.55	54.07	51.94	54.62
Sr	20.00	19.96	19.17	18.56
F	26.10	25.97	24.94	26.05
		$Sr_2Sn_2NO_3F_7.2H_2O$		
Sn	36.55	36.80		40.57
Sr	27.05	27.20		26.68
F	20.45	20.70		20.36
NO_3	9.55	9.60		
H_2O	5.70	5.60		

Table II: Results of Elemental Analysis of $SrSn_2F_6.H_2O$ and $Sr_2Sn_2NO_3F_7.2H_2O$

compared to the mass of $SrSn_2F_6$. The theoretical values for the two formulas are so close that one cannot distinquish between them based on the chemical analysis.This is due to the fact that their molar mass differs only by 3.94%. Therefore, elemental analysis does not allow to differentiate between the anhydrous and monohydrate formulas.

3.3. MÖSSBAUER SPECTROSCOPY

Selected samples of both compound were studied by Mössbauer spectroscopy in order to investigate the behaviour of tin in different environments. The Mössbauer parameters of non-oriented $SrSn_2F_6.H_2O$ and $Sr_2Sn_2NO_3F_7.2H_2O$ are reported in table III. The Mössbauer spectrum of each compound is shown on figures 16 and 17.

Table III: Mössbauer Spectroscopic Results

$SrSn_2F_6.H_2O$		This Work	Donaldson and Senior [32]
Sn (II)	δ (mm/s)	3.29	3.19
	Δ (mm/s)	1.75	1.75
	g_{11}	1.17	—
	% signal	96.0	—
Sn (IV)	δ (mm/s)	- 0.44	—
	Δ (mm/s)	ca.0	—
	% signal	4.0	—
$Sr_2Sn_2NO_3F_7.2H_2O$			
Sn (II)	δ (mm/s)	3.65	3.35
	Δ (mm/s)	1.24	1.30
	g_{11}	1.12	—
	% signal	95.5	—
Sn (IV)	δ (mm/s)	-0.14	—
	Δ (mm/s)	ca.0	—
	% signal	4.5	—

Note: All isomer shifts are given relative to $CaSnO_3$ at room temperature

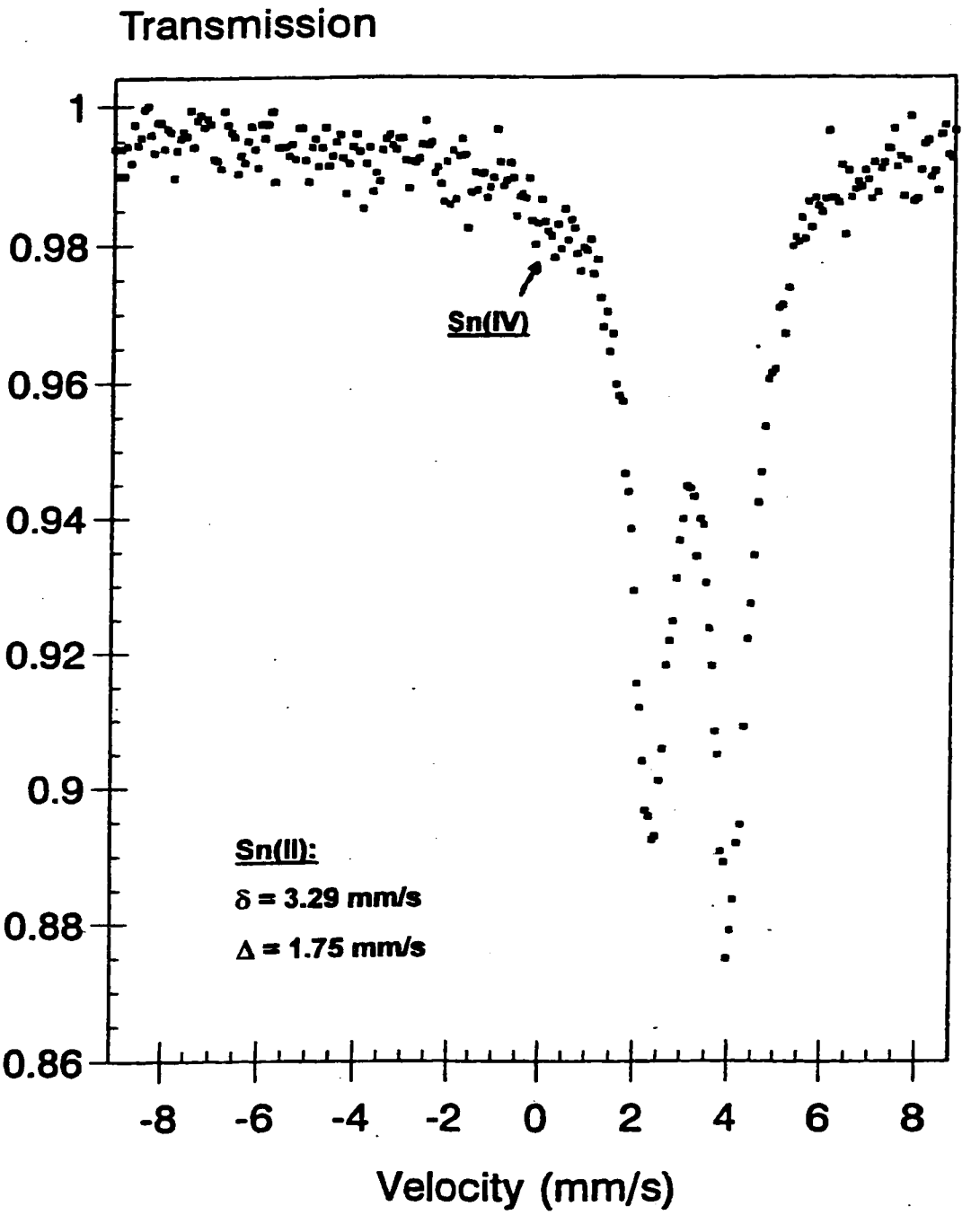

Figure 16: Mössbauer spectrum of $SrSn_2F_6.H_2O$

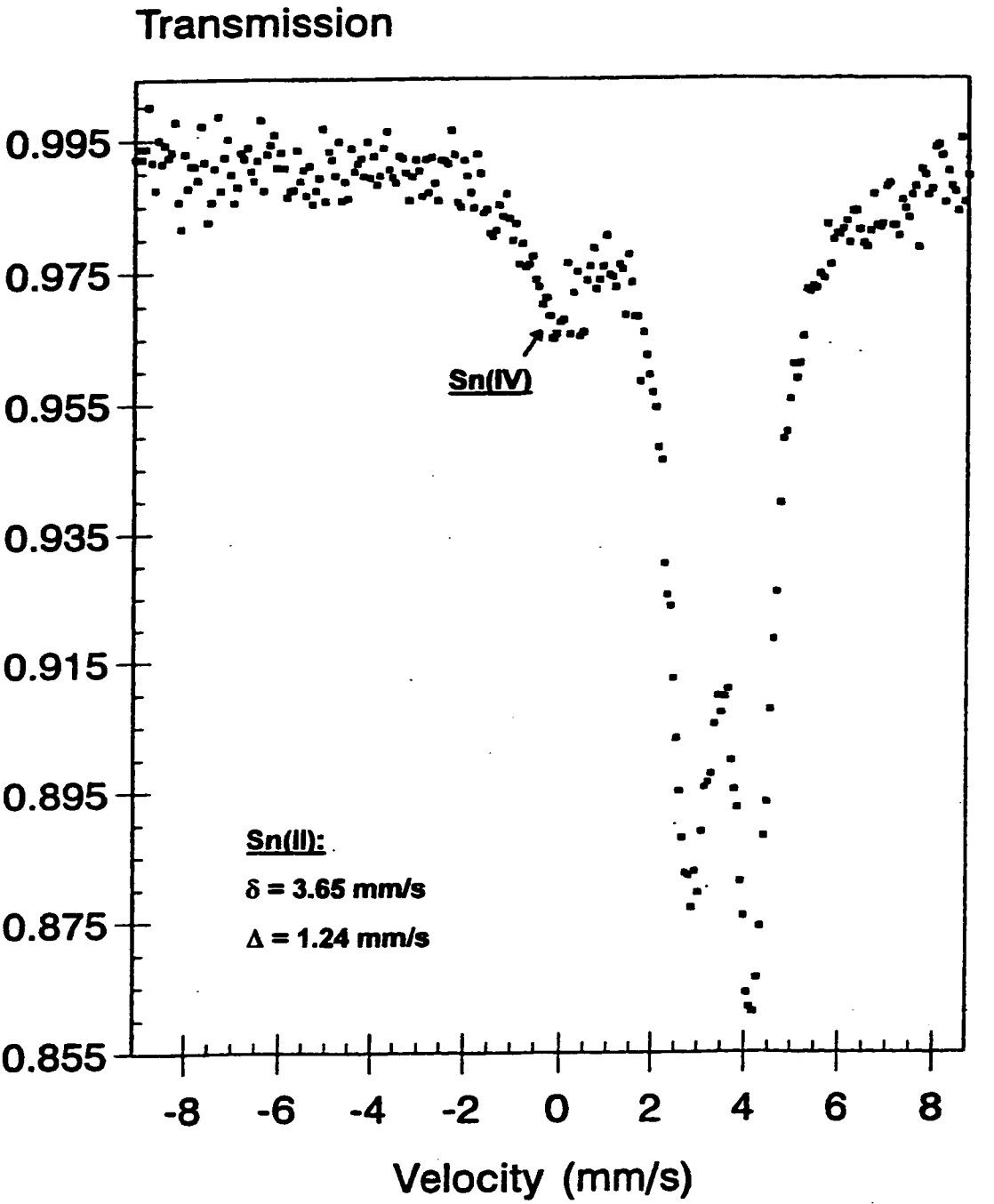

Figure 17: Mössbauer spectrum of $Sr_2Sn_2NO_3F_7.2H_2O$

The isomer shift and quadrupole splitting are characteristic of the values found commonly for divalent tin coordinated by fluorine and having a stereoactive lone pair of electrons [40]. For comparison, the values for α - SnF_2 are the following : δ = 3.40mm/s and Δ = 1.532mm/s. The hybridization in these compounds is $5s^{2-x}5p^x$ with x > 0 variable, and also most of the time, with a 5d contribution to hybridization (sp^3d or sp^3d^2), i.e. $5s^{2-x-y}5p^x5d^y$.

For $SrSn_2F_6.H_2O$, the isomer shift is smaller than for $Sr_2Sn_2NO_3F_7.2H_2O$. This means there is less "s" electron density in the lone pair and more "p" and "d" densities (i.e. x and y are larger); a smaller "s" density gives a smaller isomer shift. Since there is more "p" and "d" densities in the lone pair and the "p" and "d" orbitals are not spherical the electric field gradient (e.f.g.) at tin will be higher and it will give a larger splitting between the sublevels of the nuclear first excited state and it will result in a larger quadrupole splitting, in agreement with our observations.

The large quadrupole splitting in both compounds indicates that the tin lone pair is stereoactive (if it was not stereoactive, it would be fully "s" and thus spherical and this would give an isomer shift $\delta \approx 4.0$ mm/s and a zero or near zero quarupole splitting like in $SnCl_2$ and the $Ba_{1-x}Sn_xCl_{1+y}F_{1-y}$ solid solution[11, 41-45]). The stereoactivity of the lone pair results in the bonds to fluorine being all on the same side of the tin atom. This can create two effects:

- tin will vibrate anisotropically, and this results in a doublet asymmetry (Goldanskii - Karyagin effect)

- the crystallites will probably have strong cleavage directions (since lone pairs tend to cluster, often in planes) and it results in sheet or needle shaped crystallites, which favor texture effect (preferred orientation)

Both above effects give asymmetric doublets, which are observed in the case of both compounds, and cannot be separated easily. The Goldanskii - Karyagin parameter g_{11} is the ratio of the intensity of the two nuclear excited state sublevels:

$$g_{11} = \frac{I(\pm\frac{1}{2}, \pm\frac{3}{2})}{I(\pm\frac{1}{2}, \pm\frac{1}{2})} \qquad (3)$$

A symmetric doublet would have $g_{11} = 1$ (no Goldanskii - Karyagin effect).

In order to eliminate any possible preferred orientation from the samples of $SrSn_2F_6.H_2O$ and $Sr_2Sn_2NO_3F_7.2H_2O$, both samples were ground with crystalline sugar. Crystalline sugar was used for grinding for the following reasons: the sugar crystals are expected to grind the sample very effectively, since the sample particles are very soft; sugar contains only light atoms (H, C, O) and thus will not significantly reduce the intensity of the 23.8 keV gamma ray beam. The samples ground in sugar to break crystallites still show an asymmetric doublet, but the asymmetry is much smaller than on the oriented samples at $\theta = 0^\circ$. Since the asymmetry is the same way (although smaller) as on the oriented sample at $\theta = 0^\circ$, one could conclude that the asymmetry in the sample ground with sugar is due to residual preferred orientation, or on the other hand it could be due to recoil-free fraction

anisotropy (Goldanskii - Karyagin effect). Both reasons can be expected since both can be generated by the bonding anisotropy due to stereoactive lone pair. Rotating to $\theta = 45^{o}$, the sample ground in sugar produces no detectable change in doublet asymmetry. This shows that there is no residual preferred orientation in this sample, otherwise the spectrum would be more asymmetric when rotated by 45° (see below the experiments on highly oriented samples). This proves almost unambiguously that the spectrum asymmetry in the ground sample is due to the Goldanskii - Karyagin effect.

Further proof would be provided by variable temperature Mössbauer spectroscopy. At very low temperature (ca. 4.2 K), the amplitude of thermal vibrations is so small that the difference between the different directions is hard to see, and the spectrum should be symmetric, and the asymmetry should increase with increasing temperature.

The ultimate proof would be obtained by doing the following - on a good single crystal, the X-ray, or even better neutron, single crystal data should be collected versus temperature. Refinement of the crystal structure at several temperatures would give the Uij (anisotropic amplitude of thermal vibrations), which could be used to calculate the $(g11)_c$ Goldanskii - Karyagin parameter, which would be compared to the observed $(g11)_o$ obtained from the Mössbauer spectra recorded at the same temperatures on a non-oriented polycrystalline sample. Unfortunately, this cannot be done on this material unless a good quality crystal can be obtained, and this seems to be precluded by the sheet like crystal shape.

Several experiments were also performed on the highly oriented sample of $Sr_2Sn_2NO_3F_7.2H_2O$. For the highly oriented spectrum at $\theta = 0^o$ (gamma - ray beam perpendicular to the sample surface, and thus also to the sheet like crystallites, the doublet is very highly anisotropic with the lower velocity line being much weaker than the other. This indicates that θ is close to zero, i.e. that the lone pair (main contributor to Vzz) are about parallel to the direction of the gamma - ray beam, and thus perpendicular to the sheet-like crystallites, which explains the shape of crystallites (sheets). The same lone pair orientation is found in α -$PbSnF_4$ [2,3]. For the oriented sample, it was observed that, when θ increases, the asymmetry decreases, and is moderate at $\theta = 45^o$, as expected.

The small tin (IV) signal is due to surface oxidation of the crystallites and is found in all powdered tin (II) fluoride containing compounds. However, because the recoil-free fraction of SnO_2 [$f_a(SnO_2) = 0.44$] is much larger than that of Sn(II) - F compounds, e.g. 13 times as large as that of α - SnF_2 [f_a (α-SnF_2) = 0.034] at room temperature, the relative amount of tin(IV) in both samples is lower than 0.5% since tin(II) in both samples is likely to have a recoil-free fraction similar to that of α - SnF_2 [52].

3.4. INFRARED SPECTROPHOTOMETRY

The infrared spectra of $SrSn_2F_6.H_2O$ and $Sr_2Sn_2NO_3F_7.2H_2O$ are presented on figures 18 and 19. These spectra were recorded on FTIR Perkin Elmer 1600 (in KBr pellet). The main purpose of this experiment was to identify the water molecule in both compounds. We were looking for signs of stretching vibrations in the region around 3330 cm^{-1} and bending vibrations in the region of 1250 cm^{-1}. In the case of $SrSn_2F_6.H_2O$, the stretching vibrations of water are more apparent than the bending vibrations. However, the spectrum shows unambiguously that the sample is indeed hydrated. Care was taken to remove adsorbed water from the sample and KBr (drying).

On the other hand, the spectrum of $Sr_2Sn_2NO_3F_7.2H_2O$ shows unambiguously strong stretching as well as bending vibrations that are characteristic for the presence of water in the sample.

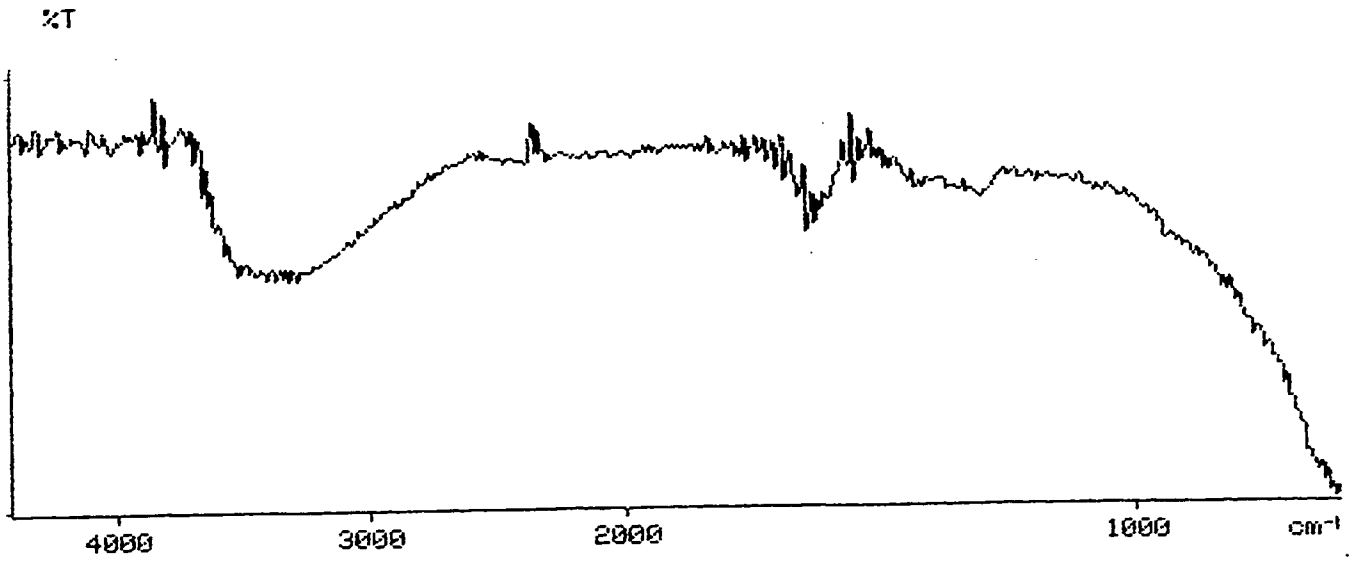

Figure 18: Infrared Spectrum of $SrSn_2F_6.H_2O$

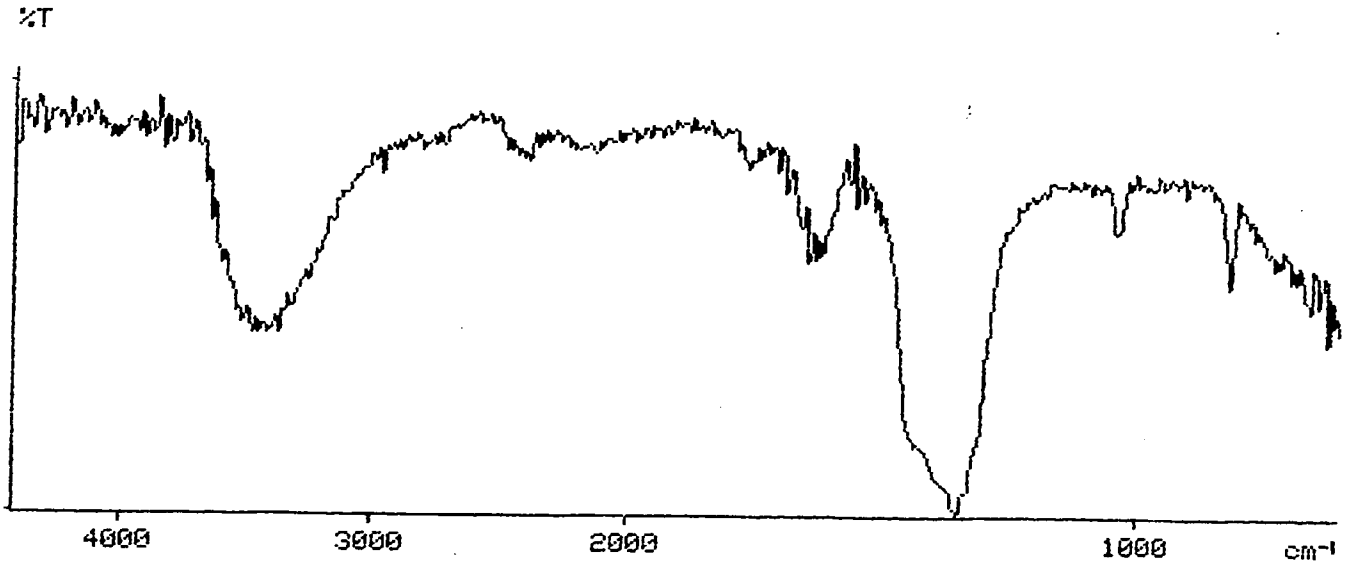

Figure 19: Infrared Spectrum of $Sr_2Sn_2NO_3F_7.2H_2O$

3.5. THERMAL ANALYSES

The main objective of this experiment was to investigate the thermal characteristics and behaviour of both compounds and more particularly $SrSn_2F_6 \cdot H_2O$ and study its dehydration.

Simultaneous DTA / TGA was performed in an attempt to observe the dehydration identified by Greedan, and also in order to measure the melting or decomposition temperature as well as check for the presence of any solid state phase transition.

The TGA curve (fig. 20) shows a slight weight loss (m= -0.4%) corresponding to ca. 10% of the total water contained in the material in the range 273 - 336°C, then at around 350 °C starts a slow but continuous further loss of weight, which accelerates very rapidly above ca. 500 °C. The experiment was stopped at ca. 675 °C after a 7% weight loss. From figure 20, it is apparent that there is no clear step for 3.94% loss of weight, which would correspond to the reaction of dehydration:

$$SrSn_2F_6.H_2O \xrightarrow[\Delta\, m = -3.94\%]{heat} SrSn_2F_6 + H_2O \qquad (4)$$

However, two small discontinuities can be seen on the TGA curve at 541°C and 555°C, the latter corresponding exactly to 3.94% weight loss. A repeat of the experiment showed that these discontinuities are not experimental artifacts, they are real (fig. 21). It is obvious that the water

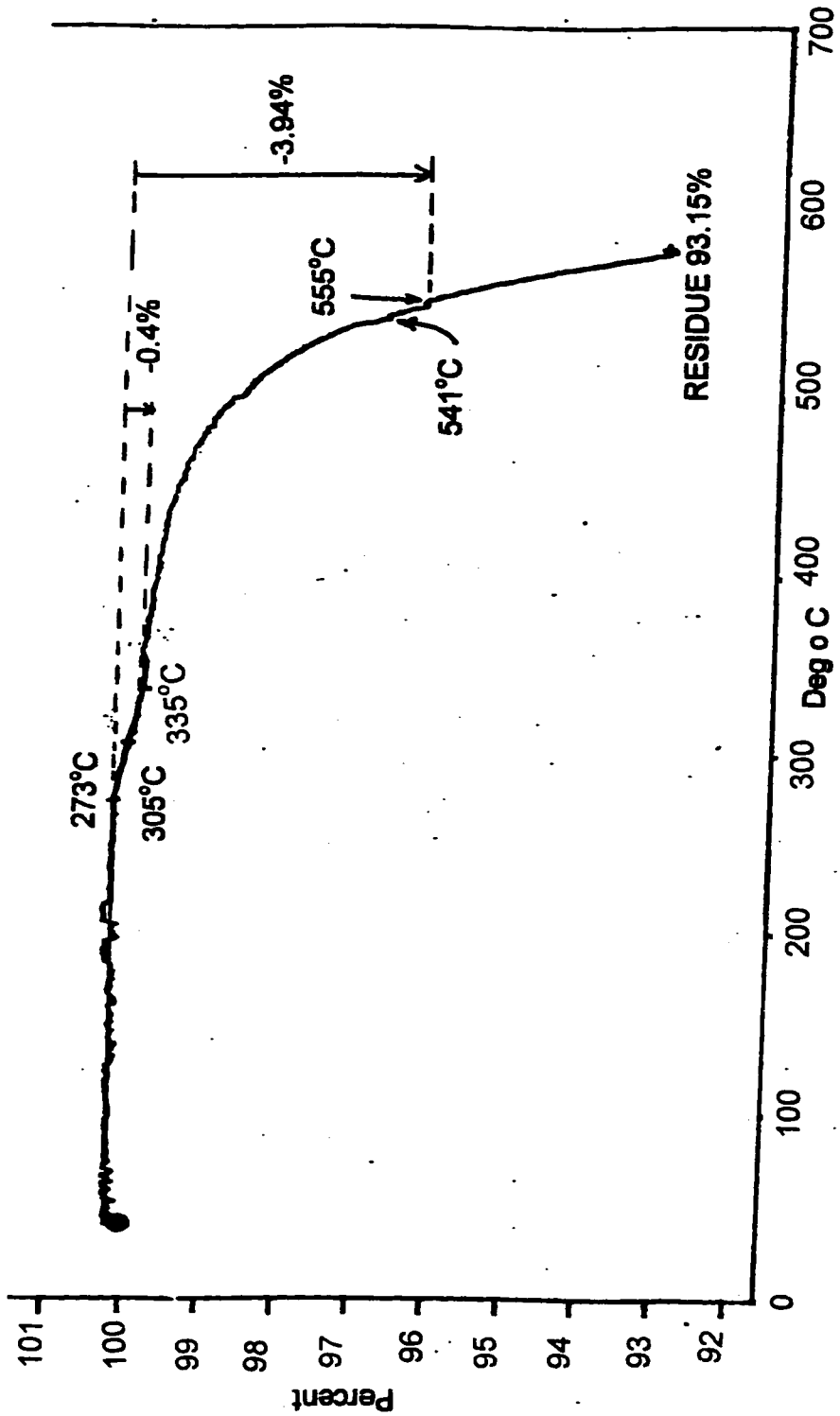

Figure 20: TGA Curve of $SrSn_2F_6.H_2O$

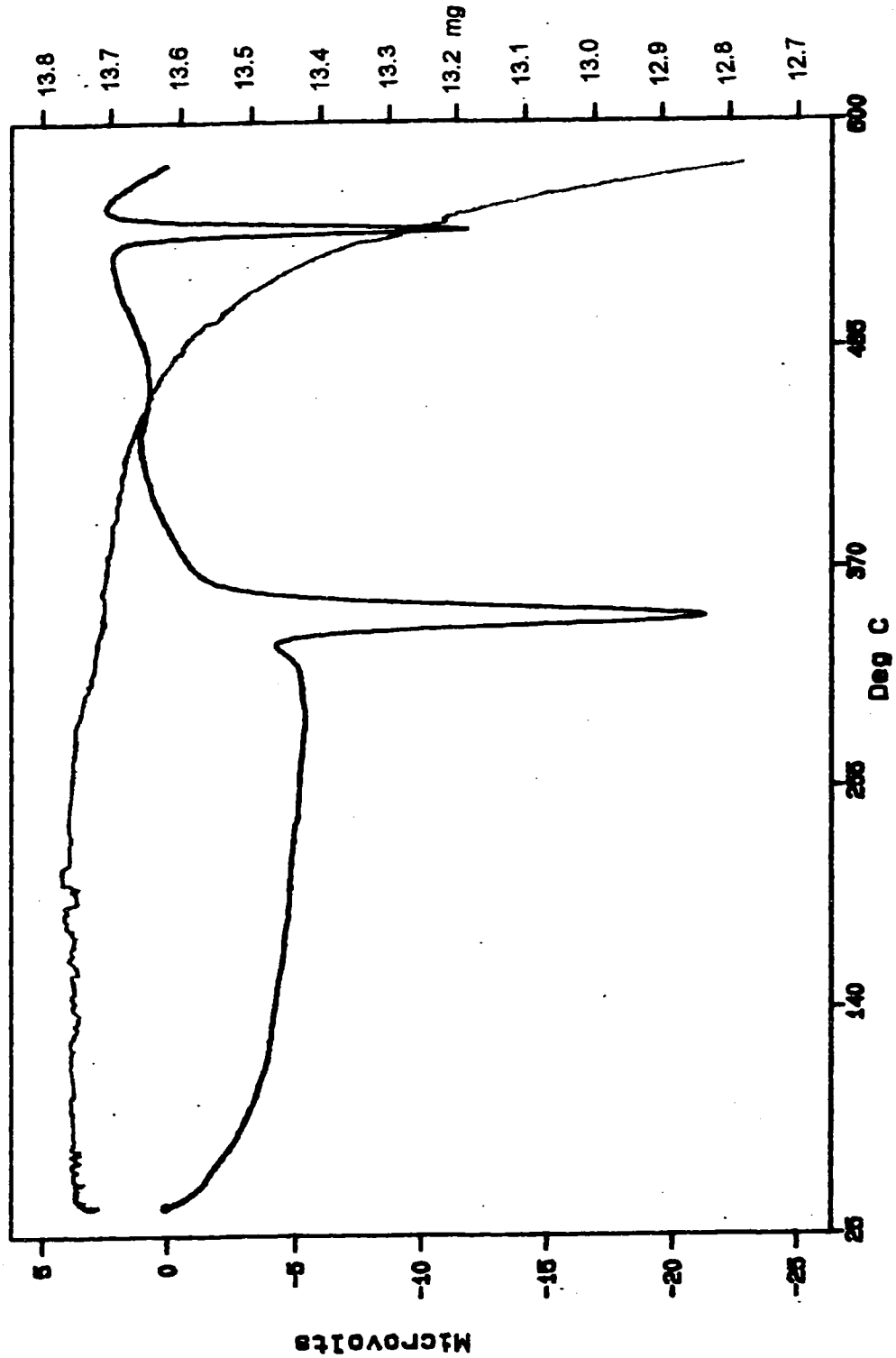

Figure 21: DTA / TGA Curves of $SrSn_2F_6.H_2O$ (repeat)

molecule is very tightly held in the solid and is removed only either by prolonged heating at 250 °C under inert atmosphere overnight or by heating at higher temperature, which results in the decomposition of the material. Since decomposition occurs above 400 to 500 °C, SnF_2 vaporizes (melting point = 215 °C) which explains the large weight loss observed. The slight weight loss of 0.4% observed in the range 273 - 336°C indicates that there may be more that one kind of water molecules in the solid. This does not seem to correspond to adsorbed water which would be lost at much lower temperature, probably below 100 °C.

The DTA curve (figures 21 and 22) shows no peak up to 300 °C. The 0.4% weight loss occuring in the range 273 - 335 °C is probably too spread over the temperature scale and involves too little energy to give a DTA peak, however, it probably corresponds to the baseline curvature just before the peak at 335 °C.

Above 300°C, three main thermal events are noticeable:

- an endothermic peak at 335°C, ΔH = 10.44 cal/g = 4.8 kcal/mol
- a baseline change in the range 425 - 475 °C
- an endothermic peak at 541°C, ΔH = 3.77 cal/g = 1.7 kcal/mol

The latent heat for the two peaks was calculated from the signal intensity and using the latent heat of melting of an indium sample for calibration. The peak position was taken at the intersection between the tangent at the inflection point and the interpolated baseline, according to

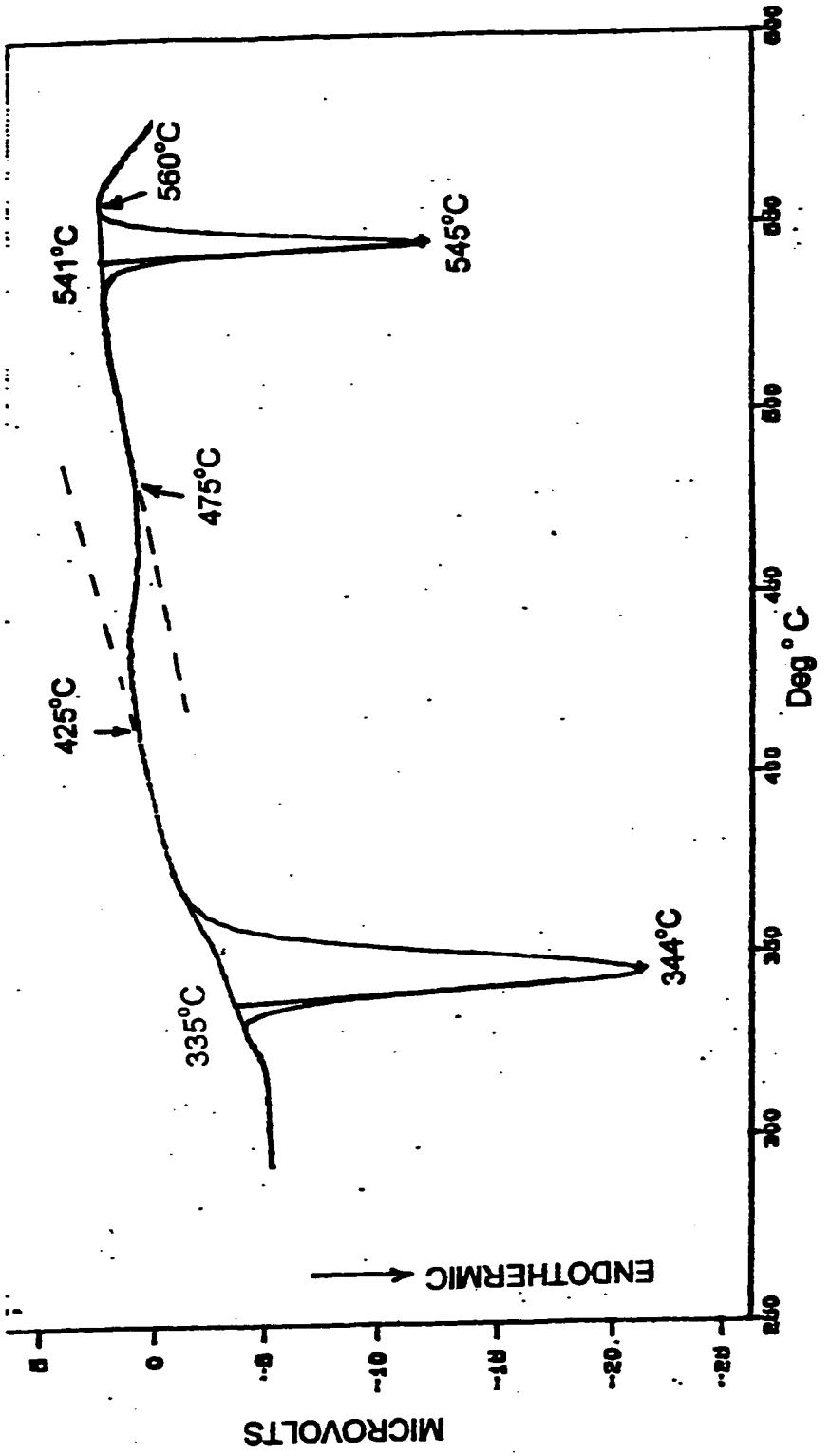

Figure 22: DTA Curve of $SrSn_2F_6.H_2O$

international procedures; the maximum of the peak corresponds to the end of the thermal event.

The first peak corresponds to the end of the slight weight loss of 0.4% and is probably due to a major reorganization of the solid (e.g. structural reorganisation due to water loss). However, it does not correspond to a decomposition, since a decomposition would most likely release the ca. 90% of water remaining in the solid (2.5% of the sample mass). However, the energy involved is too high for a solid state transition.

The base line change in the range 425 - 475°C corresponds to the region where the weight loss is accelerating rapidly; this looks like the type of signal observed at a glass transition (glass ---> ceramic), except that it is exothermic for glass transitions whereas it is endothermic for $SrSn_2F_6.H_2O$. Further investigation by X-ray diffraction versus temperature would be required to explain this phenomenon.

The peak at 541°C corresponds to the end of the dehydration. From the DTA and TGA curves, it can be concluded that $SrSn_2F_6.H_2O$ looses 10% of its water in the range 273 - 335°C, then it looses the rest progressively up to 545°C (end of second peak) and the anhydrous product starts to decompose at around 555 - 560°C. The decomposition results in an evaporation of SnF_2. The curvature of the DTA curve starting at ca. 560°C represents this decomposition. The thermal behavior of $SrSn_2F_6.H_2O$ is summarized in figure 23.

$SrSn_2F_6.H_2O$

↓ 273 - 335°C, Δ m = -0.4%

$SrSn_2F_6.0.9H_2O$

↓ 335 - 345°C, Δ H = 4.8 kcal / mol

$[SrSn_2F_6.0.9H_2O]'$

↓ 367 - 425°C, Δ m = -0.2%

$SrSn_2F_6.0.85H_2O$

↓ 425 - 475°C, baseline change, Δ m = -0.4%

$SrSn_2F_6.0.75H_2O$

↓ 475 - 545°C, Δ m = -2.94%

541 - 545°C, Δ H = 1.8 kcal / mol

$SrSn_2F_6$

Decomposition starting at 560°C

Figure 23: Thermal behavior of $SrSn_2F_6.H_2O$

The thermal behaviour and characteristics of $Sr_2Sn_2NO_3F_7.2H_2O$ were also examined. Due to the presence of the nitrate group in this compound, good thermal stability was never expected [53]. The TGA curve is shown on figure 24.

The sample was placed in the holder and slowly heated. No changes on the TGA curve were observed until the sample reached ca.204°C. At that point an explosive decomposition takes place, resulting in a massive weight loss. The following equation represents the decomposition:

$$Sr_2Sn_2NO_3F_7.2H_2O \text{ ---> } 2SrF_2 + 2SnO_2 + \text{gases} \qquad (5)$$

The theoretical weight loss calculated from equation (5) is 14%. This does not exactly represent the measured weight loss during the decomposition of the sample, since the violent explosive decomposition ejected a part of the sample from the sample holder. The recorded loss was 39% of the sample weight.

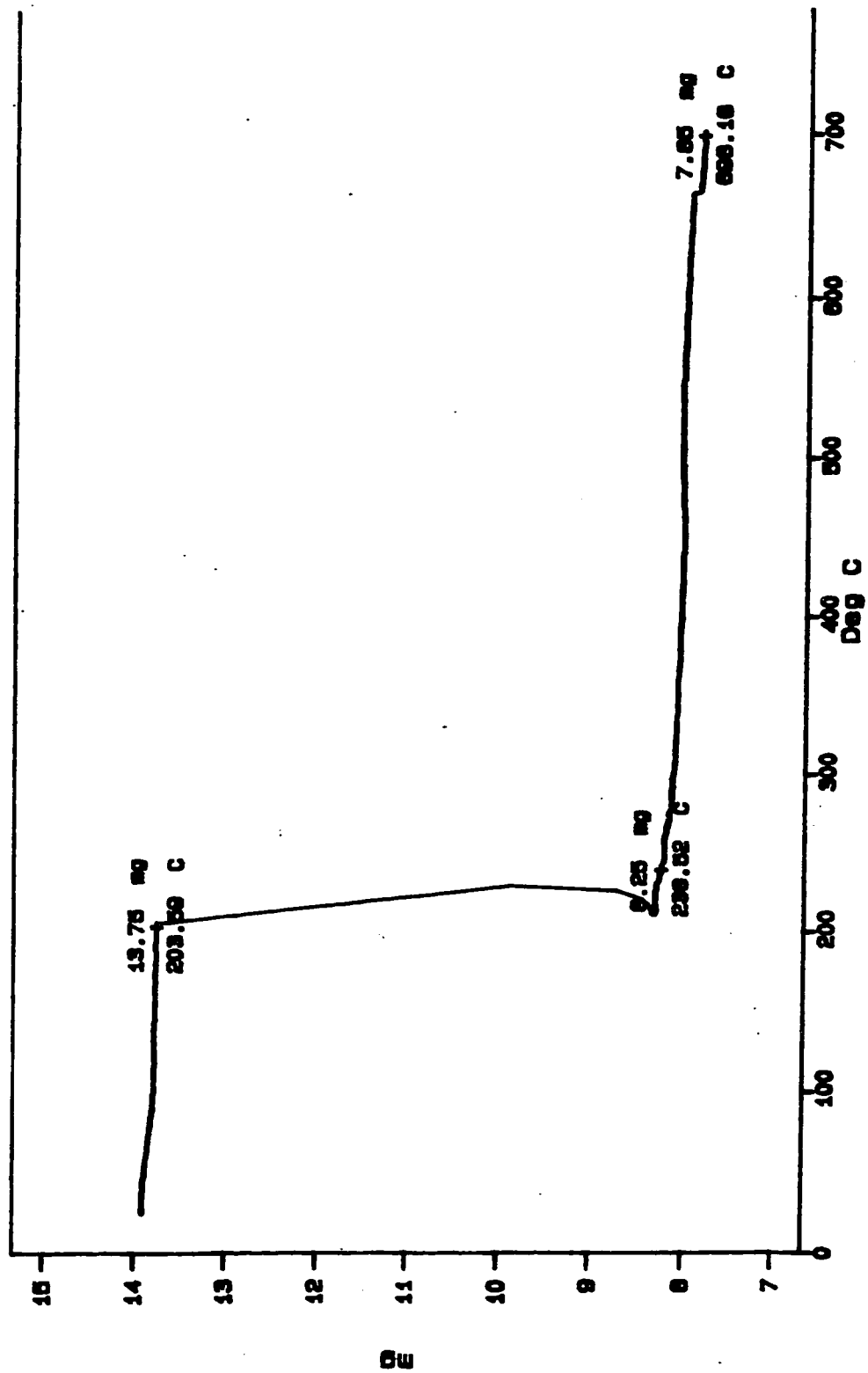

Figure 24: Decomposition of $Sr_2Sn_2NO_3F_7.2H_2O$ upon heating

3.6. X - RAY POWDER DIFFRACTION

X-ray powder diffraction (XRD) is the most widely used technique throughout this research work. It serves as a very powerful tool for identification of crystalline phases, be it pure or in a mixture, and the determination of the unit cell parameters when the peak indexation is known.

All products of reactions between aqueous solutions of strontium nitrate and stannous fluoride were first examined by XRD in order to identify what product is being formed under specific reaction conditions. By varying one or more reaction parameters, it was established what conditions are critical for the preparation of a given product.

The influence of specific reaction parameters is described in the following sections.

3.6.1. INFLUENCE OF THE MOLAR RATIO AND THE ORDER OF ADDITION

Molar ratio X, defined as $X = [Sr(NO_3)_2] / [SnF_2]$, was varied from 0.1 to 11 for both orders of addition.

In the first set of experiments, the solution of strontium nitrate was added to the solution of tin fluoride (Sr-->Sn) at a constant rate of 5ml/min. In the second set of experiments, the order of addition was reversed, i.e. the solution of tin fluoride was added to the solution of strontium nitrate (Sn-->Sr).

All experiments were performed at room temperature, in glass beakers, at a medium rate of stirring. Both t (SnF2) and t (product) were kept at zero. All precipitates were filtered out by suction and washed with 2 x 20 ml of water and dried at room temperature.

The results of the X-ray diffraction analysis, presented on figure 25, show the following:

- For the order of addition: Sr-->Sn, the X-ray powder pattern of $SrSn_2F_6.H_2O$ was obtained for the values of the molar ratio X = 0.10 to 1.00. For X = 2.00 to 11.0, the X-ray powder pattern of $Sr_2Sn_2NO_3F_7.2H_2O$ was identified.
- For the order of addition: Sn-->Sr, the X-ray powder pattern of $SrSn_2F_6.H_2O$ was obtained for the values of the molar ratio X = 0.10 to 0.40. For X = 0.45 to 0.80, a mixture of $SrSn_2F_6.H_2O$ and $Sr_2Sn_2NO_3F_7.2H_2O$ was identified with the amount of the first compound decreasing and that for the second one increasing as X increases. For X = 0.85 to 11.00, the X-ray powder pattern of pure $Sr_2Sn_2NO_3F_7.2H_2O$ was identified.

The results indicate that the solid obtained depends on the ions in excess at the reaction site in the solution:

1) When Sn^{2+} and F^- are in excess, $SrSn_2F_6.H_2O$ is obtained and the result does not depend on the molar ratio.

2) When Sr^{2+} and NO_3^- are in excess, the result depends on the molar ratio X.

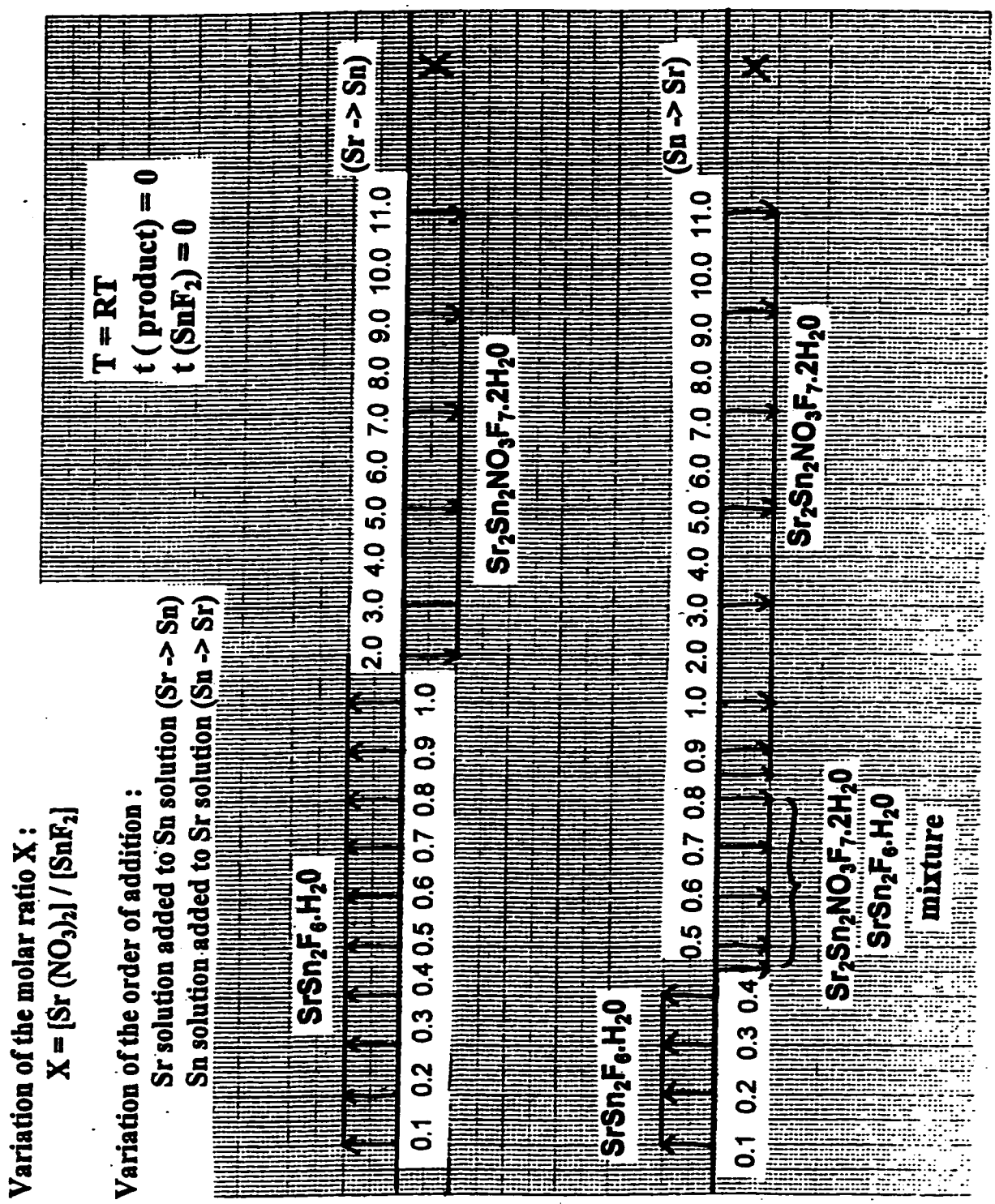

Figure 25: Infuence of the Variation of the Molar Ratio X and of the Order of Addition on the Formation of Products in the Strontium Nitrate - Stannous Fluoride System

This case is similar to the coprecipitation of SiO_2 and Al_2O_3. If these compounds are obtained separately, they have different rate of precipitation ($k_1 \neq k_2$). If the precursor of the first compound A is in excess, A is formed pure and the result does not depend on the ratio AB_1. However, if precursor of the second compound B is in excess, the materials obtained depend on the molar ratio AB_2 [57].

A new finding not reported by Donaldson and Senior, is the dependance on the molar ratio when Sn-->Sr, especially the fact that $SrSn_2F_6.H_2O$ can be obtained under this condition and is pure provided $X \leqq 0.4$.

From figure 25 is apparent that there are two regions that needed further investigation - the first one being between X = 1.00 and 2.00 (Sr-->Sn) where the formation of $SrSn_2F_6.H_2O$ changes into the formation of $Sr_2Sn_2NO_3F_7.2H_2O$ and the second at X = 0.40 to 0.85 (Sn-->Sr) where the mixture of $SrSn_2F_6.H_2O$ and $Sr_2Sn_2NO_3F_7.2H_2O$ is produced.

The values of X, that underwent further investigation were selected as 0.50 (ratio of Sr^{2+} to Sn^{2+} is 1:2) and 2.00 (ratio of Sr^{2+} to Sn^{2+} is 2:1). These X values were studied as a function of various reaction parameters for both orders of addition. The results are presented in the following sections and the summary is illustrated on figure 26.

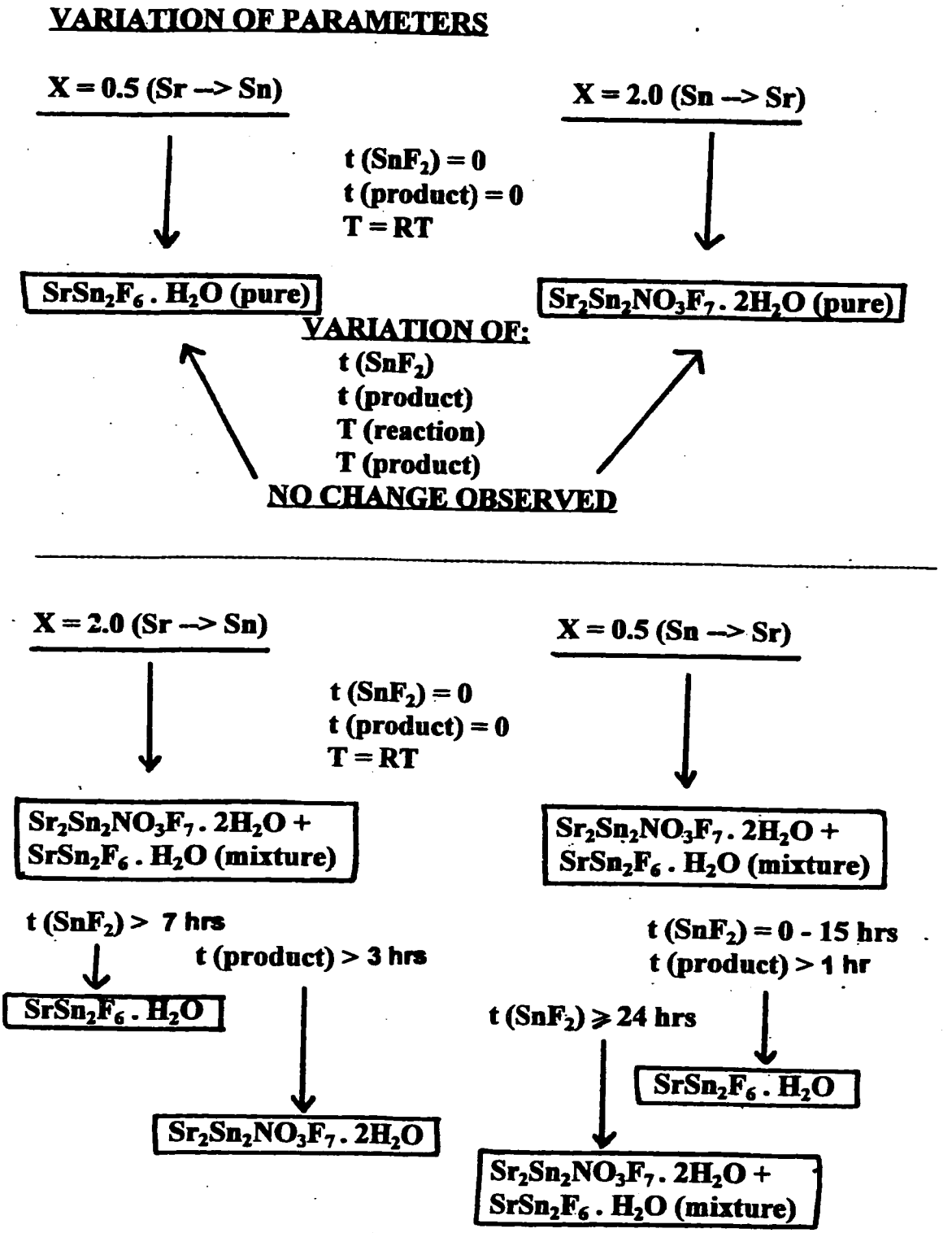

Figure 26: Influence of Variation of Reaction Parameters on the Formation of Products in the Strontium Nitrate - Stannous Fluoride System

3.6.2. INFLUENCE OF TIME

There are three time-related parameters that were considered to be important and have a potential influence on the outcome of the precipitation reaction: t (SnF_2), t (product) and t (suspension).

- t (SnF2) [time between the end of dissolution of SnF_2 and the beginning of the reaction] : the values selected were 0, 7, 15, 24 and 30 hours. No change was detected neither for X = 0.50 (Sr-->Sn), where pure $SrSn_2F_6.H_2O$ was identified by X-ray diffraction, nor for X = 2.00 (Sn-->Sr), where pure $Sr_2Sn_2NO_3F_7.2H_2O$ was obtained. However, for X = 2.00 (Sr-->Sn), and for X = 0.50 (Sn-->Sr) where mixture of both principal products was identified for t (SnF_2) = 0, the results are different. For X = 2.00 (Sr-->Sn), $SrSn_2F_6.H_2O$ was identified if t (SnF_2) $\geqq$7 hours. For X = 0.50 (Sn-->Sr), $SrSn_2F_6.H_2O$ was identified if t (SnF_2)=7 and 15 hours. If t (SnF_2) $\geqq$24 hours, mixture of both main reaction products was obtained.
- t (product) [time between the end of reaction and the filtration of the product] : the values selected were 0, 1, 3, 5, 7, 10, 15, 22, 30, 48 and 168 hours. No change was detected neither for X = 0.5 (Sr-->Sn), where pure $SrSn_2F_6.H_2O$ was identified by X-ray diffraction, nor for X = 2.0 (Sn-->Sr), where pure $Sr_2Sn_2NO_3F_7.2H_2O$ was obtained. However, for X = 2.0 (Sr-->Sn) and for X = 0.5 (Sn-->Sr), where mixture of both principal products was identified for t (product) = 0, the results are the following. For X = 2.0 (Sr-->Sn), $Sr_2Sn_2NO_3F_7.2H_2O$ was identified if t (product) $\geqq$ 3

hours. For X = 0.5 (Sn-->Sr), $SrSn_2F_6.H_2O$ was identified if t (product) ≧ 1 hour.

- t (suspension) [suspension of dry products in H_2O for long period of time] : the value selected was 168 hours (7 days). 1.5g of pure $SrSn_2F_6.H_2O$ was suspended in 50 ml of water for 7 days, then filtered, dried and identified by X-ray diffraction. The same experiment was repeated with $Sr_2Sn_2NO_3F_7.2H_2O$. No changes in the product composition were observed.

From the above described experiments is apparent that the products of reaction in the regions of X = 2.0 (Sr-->Sn) and X = 0.5 (Sn-->Sr) are strongly dependant on the time-related paramenters t (SnF_2) and t (product). Such a dependence has also been observed in the reaction of lead(II) nitrate and tin(II) fluoride in aqueous solutions [35].

3.6.3. INFLUENCE OF TEMPERATURE

There are two temperature-related parameters that were considered to be important and have a potential influence on the outcome of the precipitation reaction: T (reaction) and T (product).

- T (reaction) [temperature of the reaction] values were selected as 40, 65 and 90°C. For X = 0.5 (Sr-->Sn), $SrSn_2F_6.H_2O$ was identified at all three cases. It is the same compound that was isolated after precipitation at ambient temperature. The second set of experiments was performed at X =

2.0 (Sn-->Sr). $Sr_2Sn_2NO_3F_7.2H_2O$ was identified in all three cases. Once again, it is the same reaction product that was identified after precipitation at ambient temperature.

- T (product) [temperature of heating of the products after precipitation] the following values were selected: 60 and 80°C. For X = 0.5 (Sr-->Sn), $SrSn_2F_6.H_2O$ was identified in both cases. It is the same compound that was isolated after precipitation at ambient temperature. For X = 2.0 (Sn-->Sr), $Sr_2Sn_2NO_3F_7.2H_2O$ was identified in both cases. Once again, it is the same reaction product that was identified after precipitation at ambient temperature.

Variation in the temperature of reaction or in the temperature of heating of the products after precipitation does not seem to have any effect on the products of the reaction for X = 0.5 (Sr-->Sn) and X = 2.0 (Sn-->Sr). This contrasts with the reaction of $Pb(NO_3)_2$ and SnF_2 in water, where a strong temperature dependence is observed [35].

3.6.4. INFLUENCE OF MIXING SPEED

The rate of stirring was varied from low to high for two values of the molar ratio: X = 0.5 (Sr-->Sn) and X = 2.0 (Sn-->Sr) in order to see if it influences the formation of either compound. All other reaction parameters were kept the same as in the section 3.6.1. For X = 0.5 (Sr-->Sn), the

diffraction pattern of $SrSn_2F_6.H_2O$ was identifed for all three samples prepared at low, medium or high rate of stirring. Similar results were obtained for X = 2.0 (Sn-->Sr) where the diffraction pattern of $Sr_2Sn_2NO_3F_7.2H_2O$ was identified for all three cases. The rate of stirring does not seem to affect the formation of $SrSn_2F_6.H_2O$ or $Sr_2Sn_2NO_3F_7.2H_2O$ under the reaction parameters described above. This contrasts very strongly with the case of the reaction of lead(II) nitrate and tin(II) fluoride in water [34].

3.6.5. INFLUENCE OF THE VOLUME OF WATER USED FOR WASHING

The amount of water used for washing of the precipitates was investigated for X = 0.5 (Sr-->Sn), region where pure $SrSn_2F_6.H_2O$ is formed and X = 2.0 (Sn-->Sr), region where pure $Sr_2Sn_2NO_3F_7.2H_2O$ is obtained. The volume of water used for washing does not seem to have any effect on the reaction products formed in the above described regions. This behaviour is unlike that observed in the reaction of calcium nitrate and tin(II) fluoride where washing water leaches SnF_2 from the $CaSn_2F_6$ phase formed at low X = $Ca(NO_3)_2.4H_20$ / SnF_2 ratios, thereby transforming it into the microcrystalline fluorite type $Ca_{1-x}Sn_xF_2$ solid solution [11,36-37].

3.6.6. INVESTIGATION OF THE EFFECT OF RECRYSTALLIZATION FROM NITRIC ACID

3.6.6.1. RECRYSTALLIZATION OF $SrSn_2F_6.H_2O$ AND $Sr_2Sn_2NO_3F_7.2H_2O$ FROM 1N NITRIC ACID AFTER DRYING

Both dried compounds were recrystallized from 1N nitric acid. Amount of acid as well as the heating time were varied. A summary of the results is depicted on figure 27.

In the first part of this experiment, pure dry $SrSn_2F_6.H_2O$ (formed by precipitation at X = 0.5 (Sr-->Sn), filtered, washed twice with 20 ml of water) was suspended in 25 ml H_2O and heated to 90°C.

a) 1N nitric acid was added dropwise untill a complete dissolution of the product was achieved. This required about 20 ml of 1N nitric acid. The solution was allowed to cool down (an ice bath was used in order to facilitate the precipitation), the precipitate was collected by suction, washed with 20 ml of water, allowed to dry and studied by the means of X-ray diffraction. The precipitate was identified as $SrSn_2F_6.H_2O$.

b) A set of samples prepared at identical conditions was recrystallized but less nitric acid was used. In order to achieve complete dissolution, the heating time was extended. Samples were isolated the same way as described in part a). It was determined that the precipitates are either $SrSn_2F_6.H_2O$ or a mixture of $SrSn_2F_6.H_2O$ and $Sr_2Sn_2NO_3F_7.2H_2O$ (figure 27).

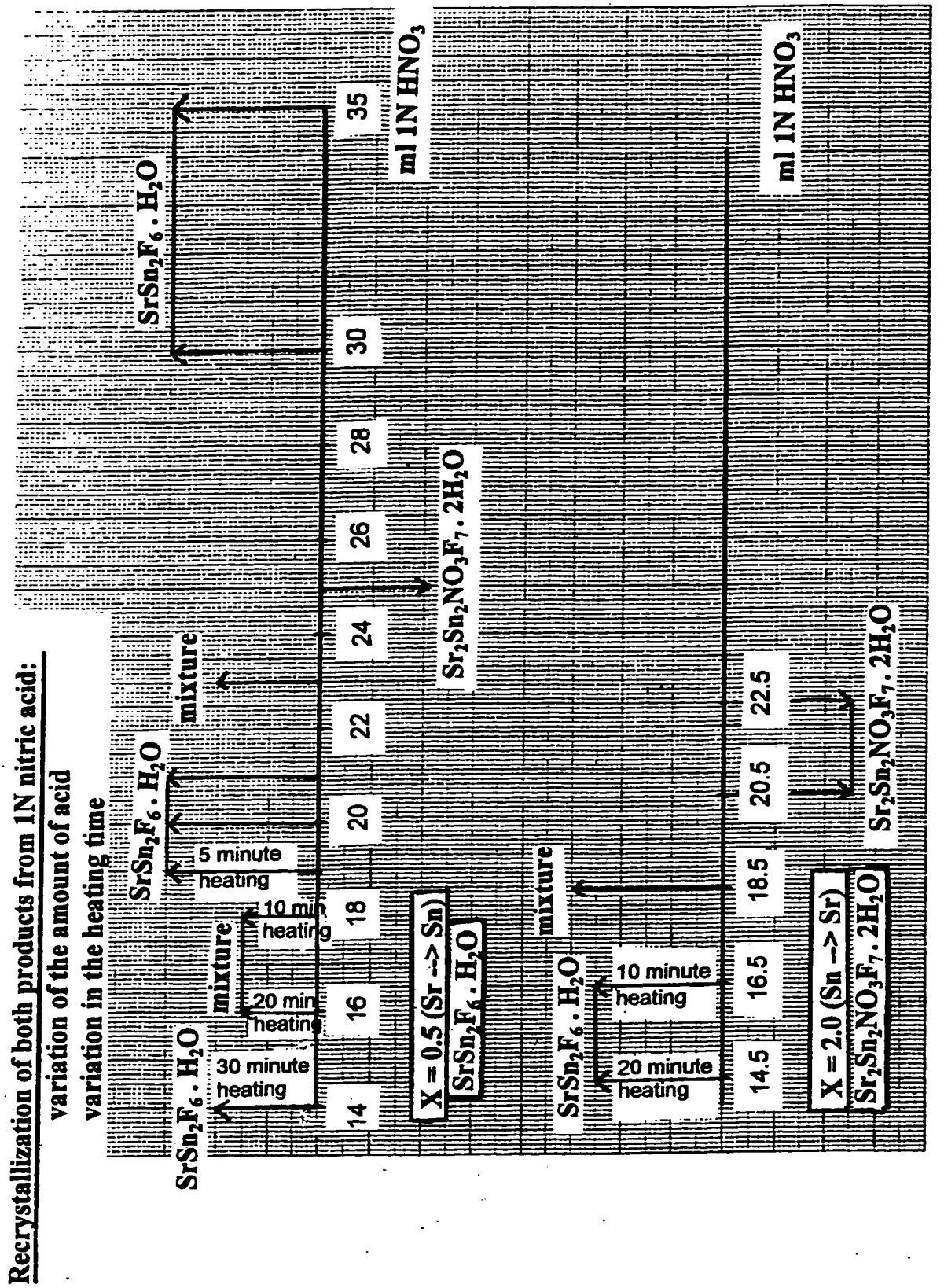

Figure 27: Results of Recrystallization of Dried $SrSn_2F_6.H_2O$ and Dried $Sr_2Sn_2NO_3F_7.2H_2O$ from 1N Nitric Acid.

c) Another set of samples was recrystallized by using more nitric acid than the minimum (20 ml) needed to dissolve the sample suspended in 25ml H_20 at 90°C. The samples were immediately removed from the heating plate and isolated the same way as described in part a). The results of analysis show that a mixture of $SrSn_2F_6.H_2O$ and $Sr_2Sn_2NO_3F_7.2H_2O$, then pure $Sr_2Sn_2NO_3F_7.2H_2O$ and then pure $SrSn_2F_6.H_2O$ are formed as the volume of nitric acid is being increased (figure 27). It is important to mention that the % recovery of the product sharply declined as we approach high volume of acid added (16% of the initial sample weight if 30ml of nitric acid was used, 4% of the initial sample weight if 35ml of nitric acid was used).

In the second part of this experiment, pure dry $Sr_2Sn_2NO_3F_7.2H_2O$ (formed by precipitation at X = 2.0 (Sn-->Sr), filtered, washed twice with 20 ml of water) was suspended in 50 ml H_2O and heated to 90°C.

a) 1N nitric acid was added dropwise untill a complete dissolution of the product was achieved. 18.5 ml of 1 N nitric acid was needed. The solution was allowed to cool down (an ice bath was used in order to facilitate the precipitation), the precipitate was collected by suction, washed with 20 ml of water, allowed to dry and analyzed by the means of X-ray diffraction. The precipitate was found to be a mixture of $SrSn_2F_6.H_2O$ and $Sr_2Sn_2NO_3F_7.2H_2O$.

b) A set of samples prepared at identical conditions was recrystallized but less nitric acid was used. In order to achieve complete dissolution, the heating time was extended. Samples were isolated the same way as described in part a). Precipitates were identified as $SrSn_2F_6.H_2O$ (figure 27).

c) Another set of samples was recrystallized by using more nitric acid than the minimum needed to dissolve the sample suspended in 25ml H_20 at 90°C. The samples were immediately removed from the heating plate and isolated the same way as described in part a). The results of analysis show $Sr_2Sn_2NO_3F_7.2H_2O$ is formed as the volume of nitric acid is increased (figure 27). The % recovery of the product was about 31% of the original sample weight for 20.5ml of nitric acid used and about 25% for 22.5ml of nitric acid used.

The use of an ice bath for facilitation of precipitation seems to play an important role. Problems with precipitation were noticed in the initial part of the study, where recrystallization of both pure compounds, that were analyzed by X-ray diffraction prior to the suspension in water and subsequent recrystallization with minimum amount of nitric acid used at 90°C, resulted in precipitation problems. It was not possible to initiate the formation of crystals, even with the use of an ice bath. Both samples were therefore evaporated to dryness at room temperature and when the X-ray diffraction pattern was analyzed it was identical to that of microcrystalline SnO_2. This is not surprising since it has been shown in our laboratory that Sn(II) oxidizes rapidly to tin(IV) in aqueous solutions exposed to air if the solution is acidic and if the temperature is high [54].

These results obtained here are different from those obtained on recrystallization of dried $PbSnF_4$ from nitric acid. Only o-$PbSnF_4$ dissolves in significant amount of nitric acid solution, and recrystallization gives several

phases, which show extreme cases of preferred orientation due to the layered shape of the crystallites [55,56].

3.6.6.2. RECRYSTALLIZATION OF $SrSn_2F_6.H_2O$ AND $Sr_2Sn_2NO_3F_7.2H_2O$ FROM MOTHER SOLUTION AND VARIATION OF t (product+HNO_3)

In the first part of this experiment, the precipitate of $SrSn_2F_6.H_2O$, formed at X = 0.50 (Sr-->Sn) was left in the mother solution, heated to 90°C and dissolved in the minimum amount of nitric acid necessary. The t (product+ HNO_3) times were selected as 0, 23, 95 and 166 hours. Then the product was filtered out by suction, washed twice with 20 ml of water, dried and identified by X-ray diffraction. The product obtained was identified as $SrSn_2F_6.H_2O$ in all cases (figure 28).

The same layout of the experiment was repeated for the precipitate of $Sr_2Sn_2NO_3F_7.2H_2O$, formed at X = 2.00 (Sn-->Sr). The product obtained was identified by X-ray diffraction as $Sr_2Sn_2NO_3F_7.2H_2O$ regardless of the time the sample was immersed in nitric acid (figure 28).

During the X-ray diffraction analysis was noticed that several recrystallized samples have certain peaks enhanced whereas other peaks seem to be rather weak. In a few cases, the enhancement of peaks in one direction was so strong that it was not possible to find any suitable match for these samples in the JCPD database. This is texture effect and is due to the preferred

Recrystallization of both products in the mother solution from 1N nitric acid as t (product+ HNO3) is varied

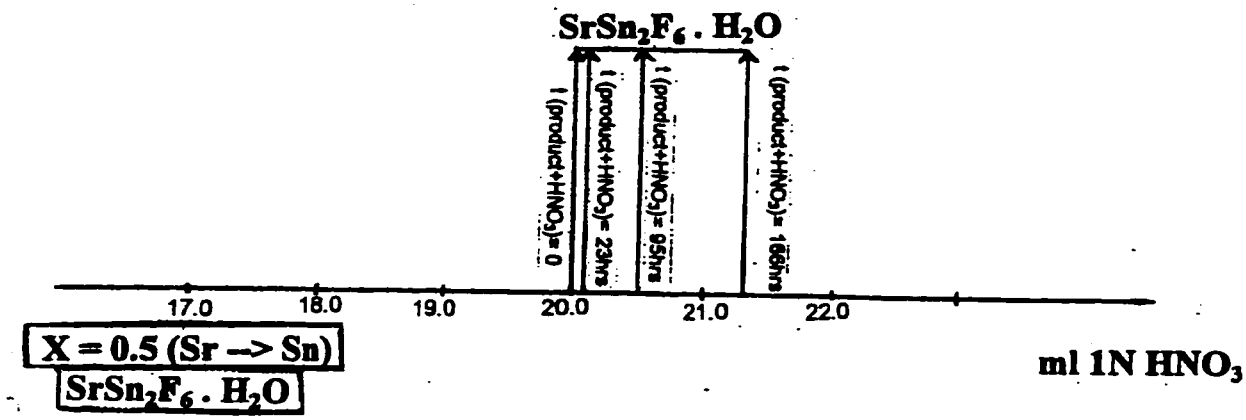

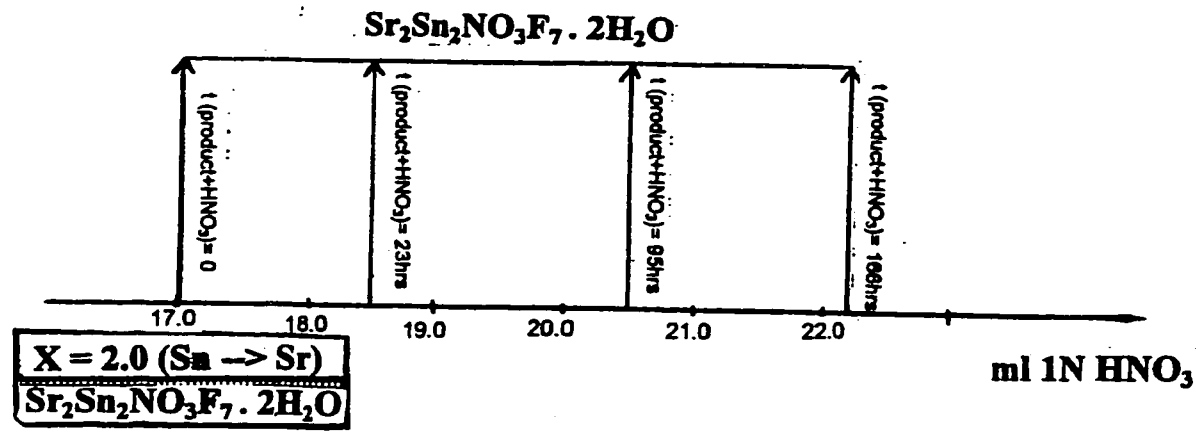

Figure 28: Results of Recrystallization of $SrSn_2F_6.H_2O$ and $Sr_2Sn_2NO_3F_7.2H_2O$ in the Mother Solution from 1N Nitric Acid as t (product+HNO_3) is Varied

orientation of crystallites in one direction. This phenomenon is frequent in divalent compounds because of the anisotropy of bonding generated by the lone pair of electrons. It is further discussed in section 3.6.7.

These results are similar to those observed when α-$PbSnF_4$ is recrystallized in its mother solution by adding nitric acid at high temperature, then allowed to cool. This produces very large and extremely thin sheets which stack parallel to one another, perpendicularly to the *c* axis, causing a very acute case of preferred orientation (only the (00l) peaks are observed) making it impossible to identify the non-ground material by computer search match [13, 14].

3.6.6.3. IMPREGNATION OF $SrSn_2F_6.H_2O$ AND $Sr_2Sn_2NO_3F_7.2H_2O$ WITH CONCENTRATED NITRIC ACID

A sample of $SrSn_2F_6.H_2O$ (about 1g) was placed on a watch glass and concentrated nitric acid was added slowly, dropwise. Just enough acid was used to achieve sample impregnation. This reaction was quite violent, evolution of brownish gas was observed. The sample was allowed to dry and then it was analyzed by X-ray diffraction.

The same experiment was repeated with $Sr_2Sn_2NO_3F_7.2H_2O$. In this case, no evalution of fumes was observed, the sample became slightly yellowish. Once again, the sample was allowed to dry and then it was analyzed by X-ray diffraction.

The results of the search match identified $Sr(NO_3)_2$ as the principal component in both materials. Also, broad peaks of low intensity characteristic of microcrystalline SnO_2 are evident in the X-ray diffraction pattern of both samples. It is evident that concentrated nitric acid causes rapid decomposition of pure $SrSn_2F_6.H_2O$ and $Sr_2Sn_2NO_3F_7.2H_2O$. Tin(II) was oxidized to tin(IV) by the nitrate ion, whereby nitrogen(V) was reduced to nitrogen(IV) as evidenced by brown vapor of NO_2 being evolved. The same was observed by Dénès when the white paste obtained by evaporation of an aqueous solution of magnesium nitrate and tin(II) fluoride was being cut to small pieces by a spatula which triggered an explosion [53].

3.6.7. INVESTIGATION OF PREFERRED ORIENTATION

In order to identify some of the highly oriented materials, it was necessary to remove the preferred orientation of the crystallites. It was demonstrated that manual grinding using a mortar and a pestle (for over 15 minutes) was not able to remove the preferred orientation.

Mechanical grinding by ball milling (use of an amalgamator) had to be employed in order to achieve a significant reduction of orientation.

Short time milling (several seconds) reduces the degree of orientation of the particles as well as the crystallinity. This is reflected by the broadening of the lines.

If the milling is continued for longer periods of time (several minutes), the lines become very broad and low in intensity. The materials loose their crystallinity and they become microcrystalline or amorphous.

The influence of ball milling on highly oriented $SrSn_2F_6.H_2O$ and $Sr_2Sn_2NO_3F_7.2H_2O$ and the comparison of non-oriented compounds is illustrated on figures 29, 30, 31 and 32.

Ball milling of our materials gives results strongly different from those observed for $PbSnF_4$. For $PbSnF_4$, there is also a drastic decrease of preferred orientation and decreased particle size just after 10 to 20 seconds of ball milling. However, further milling results in phase transitions where every sign of Pb / Sn order disappears (i.e. all superstructure reflections and line splittings disappear) and microcrystalline γ- $PbSnF_4$, which has the fluorite type structure, is obtained [21,38]. This high temperature phase could not be stabilized to ambient temperature by other means. Phase transitions in PbF_2 are also known to occur when ball milled [28].

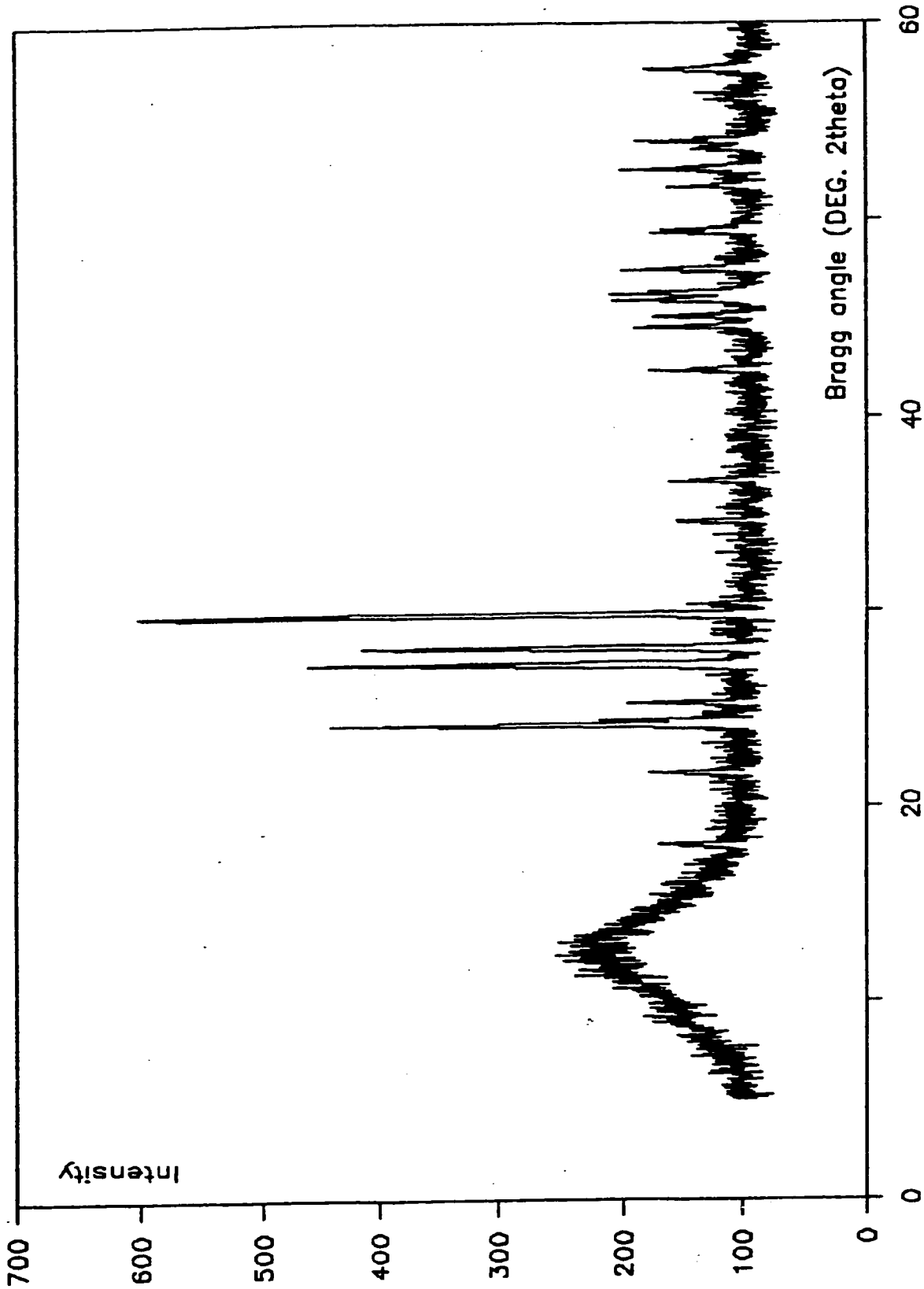

Figure 29: X-ray Diffraction Pattern of Non-oriented $SrSn_2F_6.H_2O$

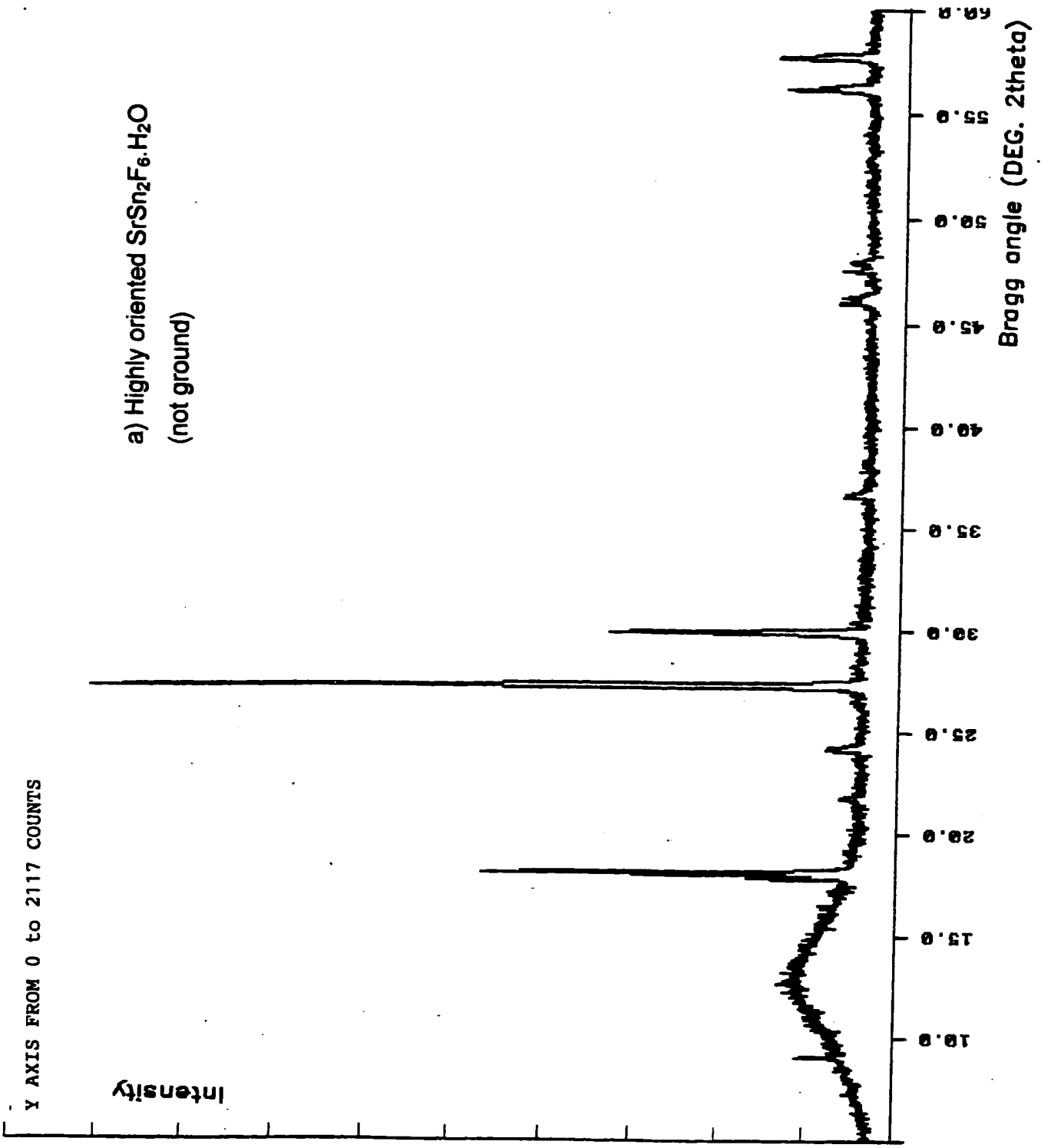

Figure 30: X-ray Diffraction Pattern of Highly Oriented $SrSn_2F_6.H_2O$ (a) and the Reduction of Crystallinity by Ball Milling (b)

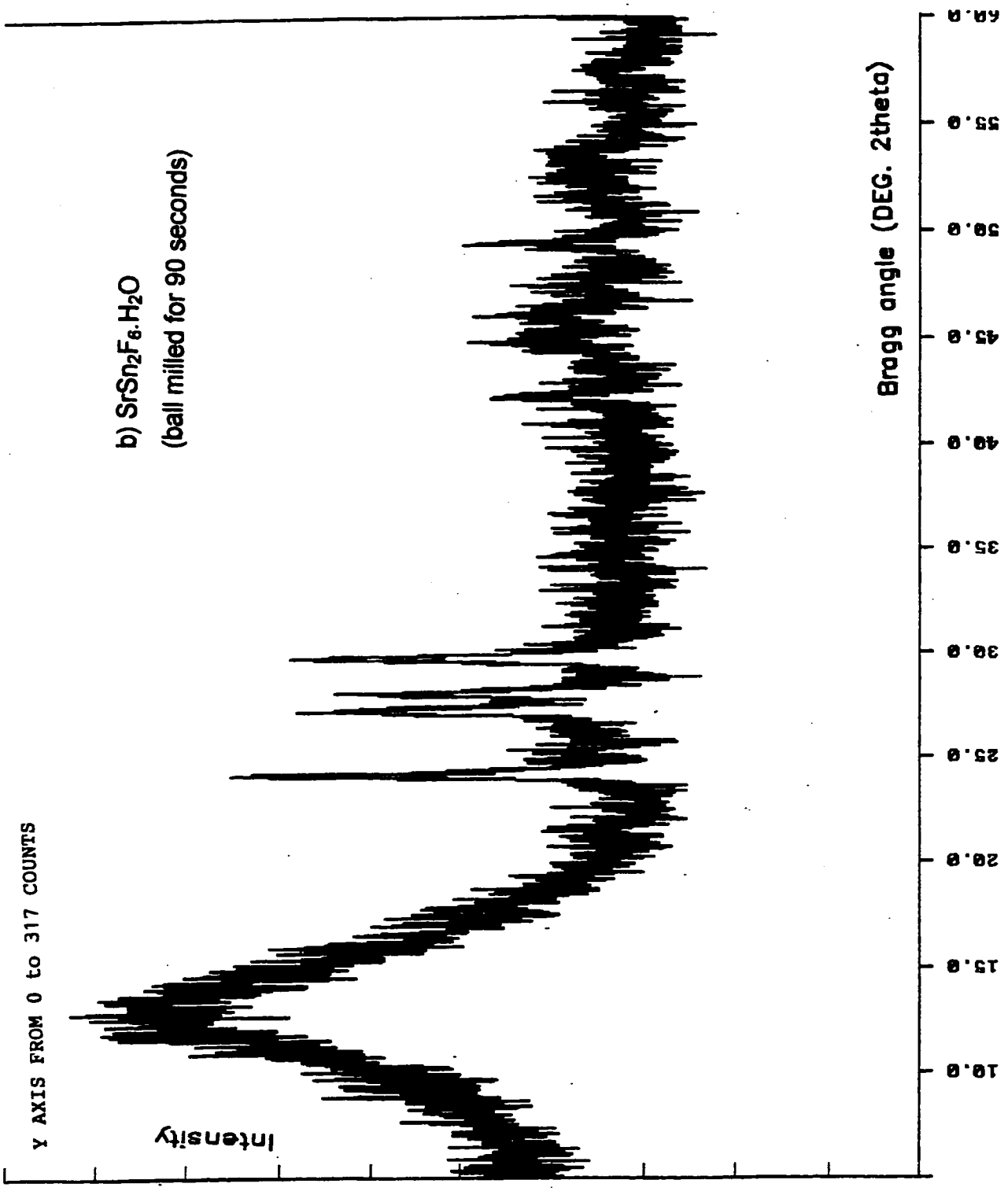

Figure 30: X-ray Diffraction Pattern of Highly Oriented $SrSn_2F_6.H_2O$ (a) and the Reduction of Crystallinity by Ball Milling (b)

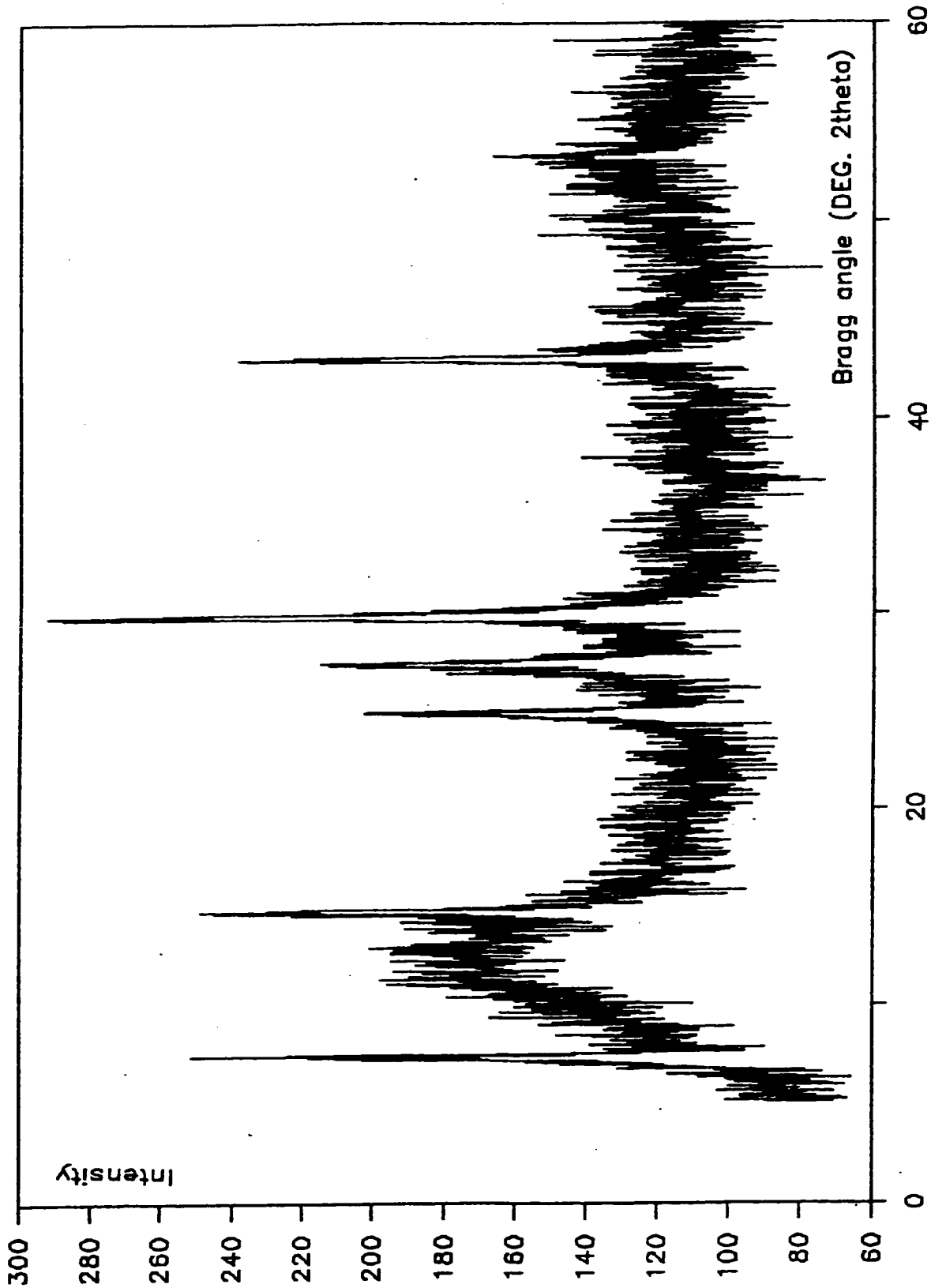

Figure 31: X-ray Diffraction Pattern of Non-oriented $Sr_2Sn_2NO_3F_7.2H_2O$

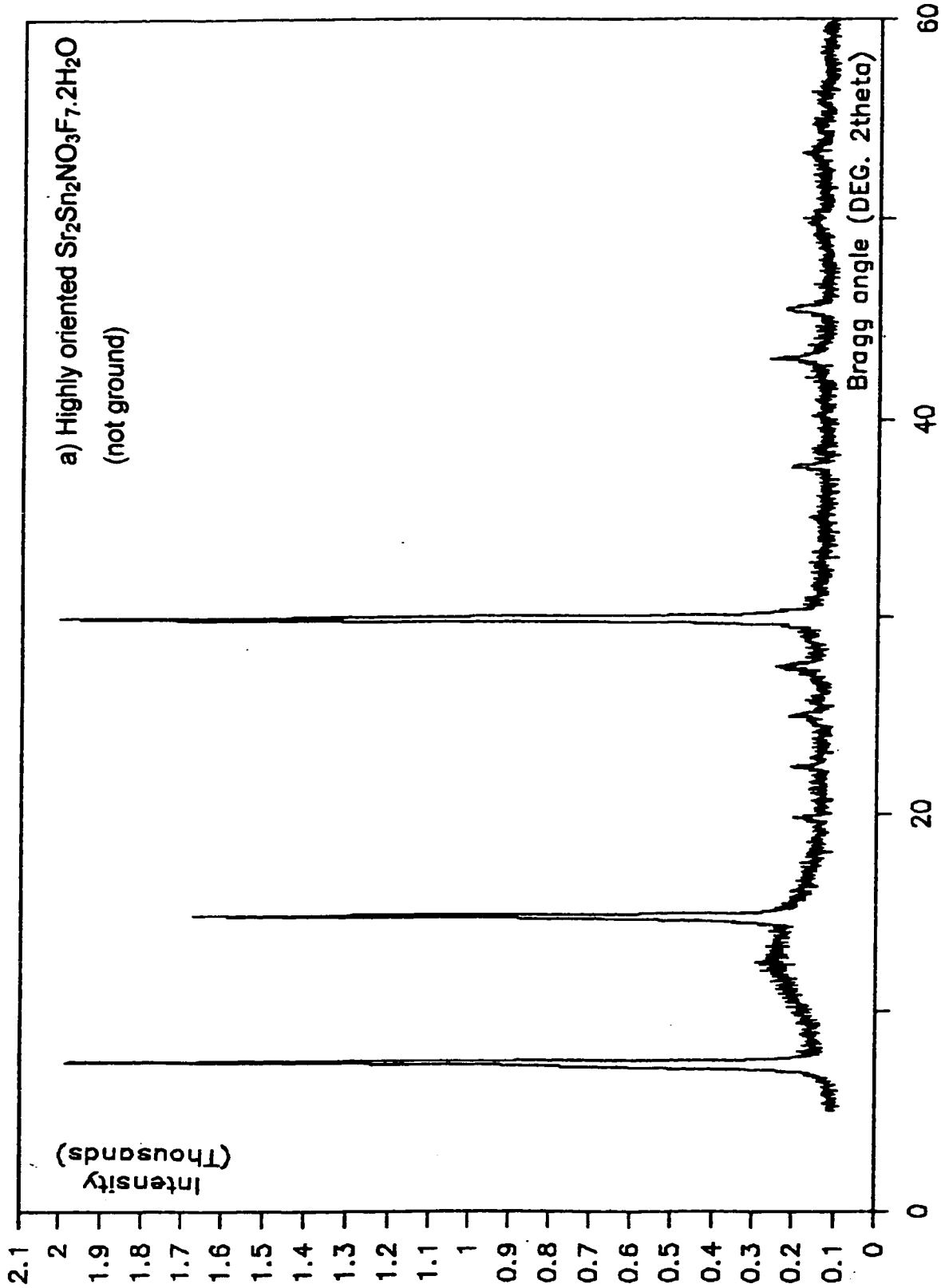

Figure 32: X-ray Diffraction Pattern of Highly Oriented $Sr_2Sn_2NO_3F_7.2H_2O$ (a) and the Reduction of Crystallinity by Ball Milling (b, c, d)

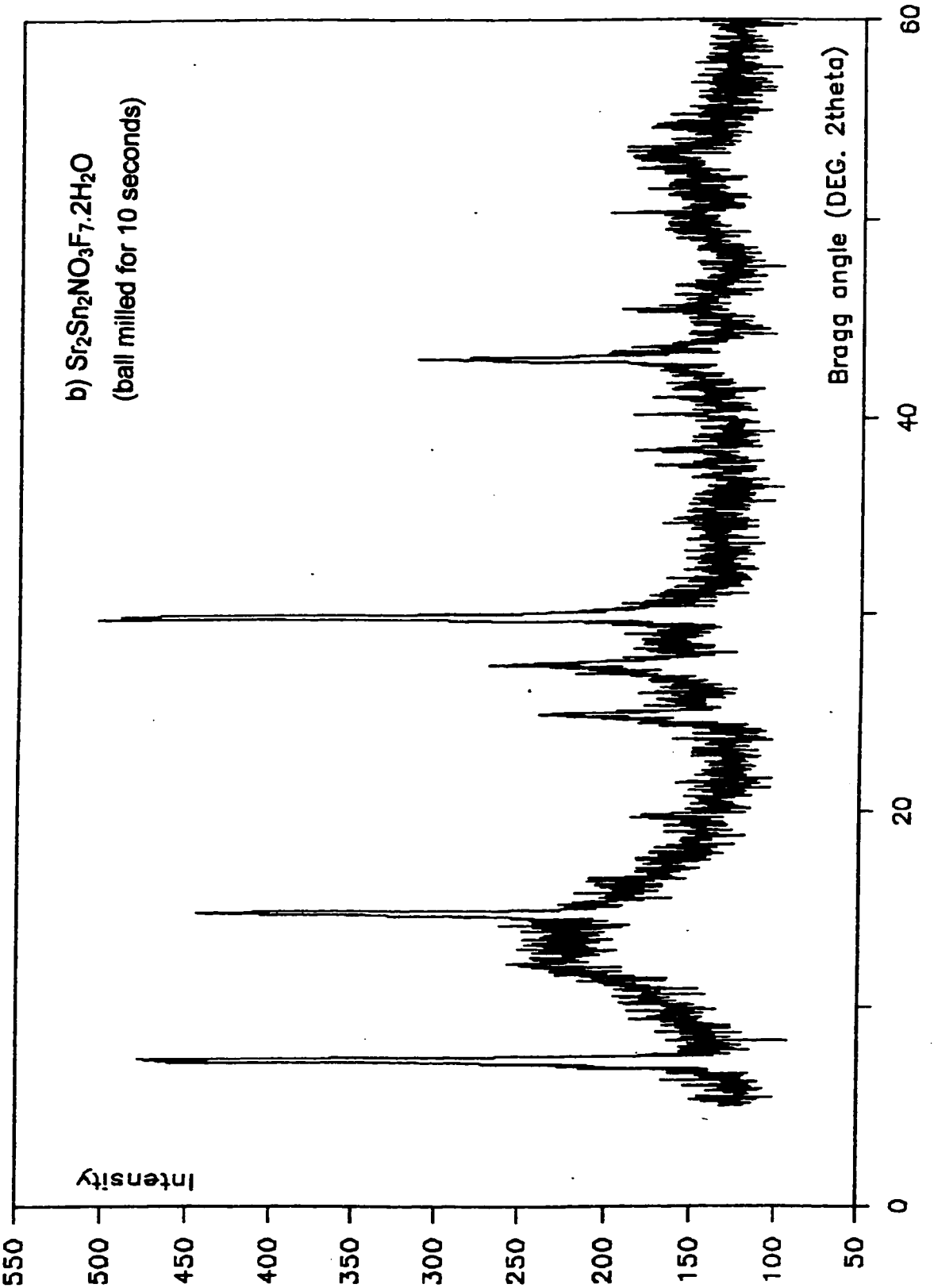

Figure 32: X-ray Diffraction Pattern of Highly Oriented $Sr_2Sn_2NO_3F_7.2H_2O$ (a) and the Reduction of Crystallinity by Ball Milling (b, c, d)

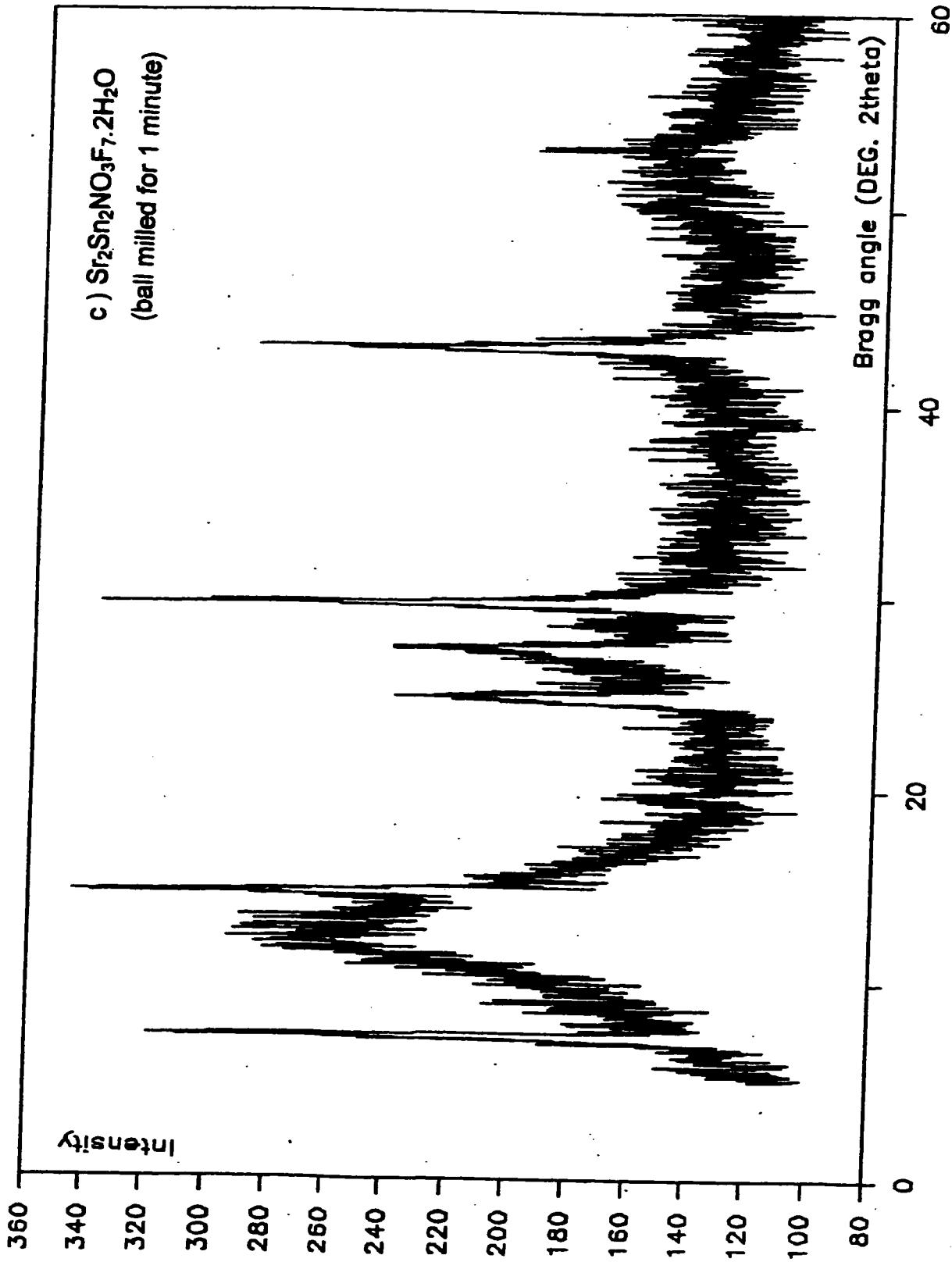

Figure 32: X-ray Diffraction Pattern of Highly Oriented $Sr_2Sn_2NO_3F_7.2H_2O$ (a) and the Reduction of Crystallinity by Ball Milling (b, c, d)

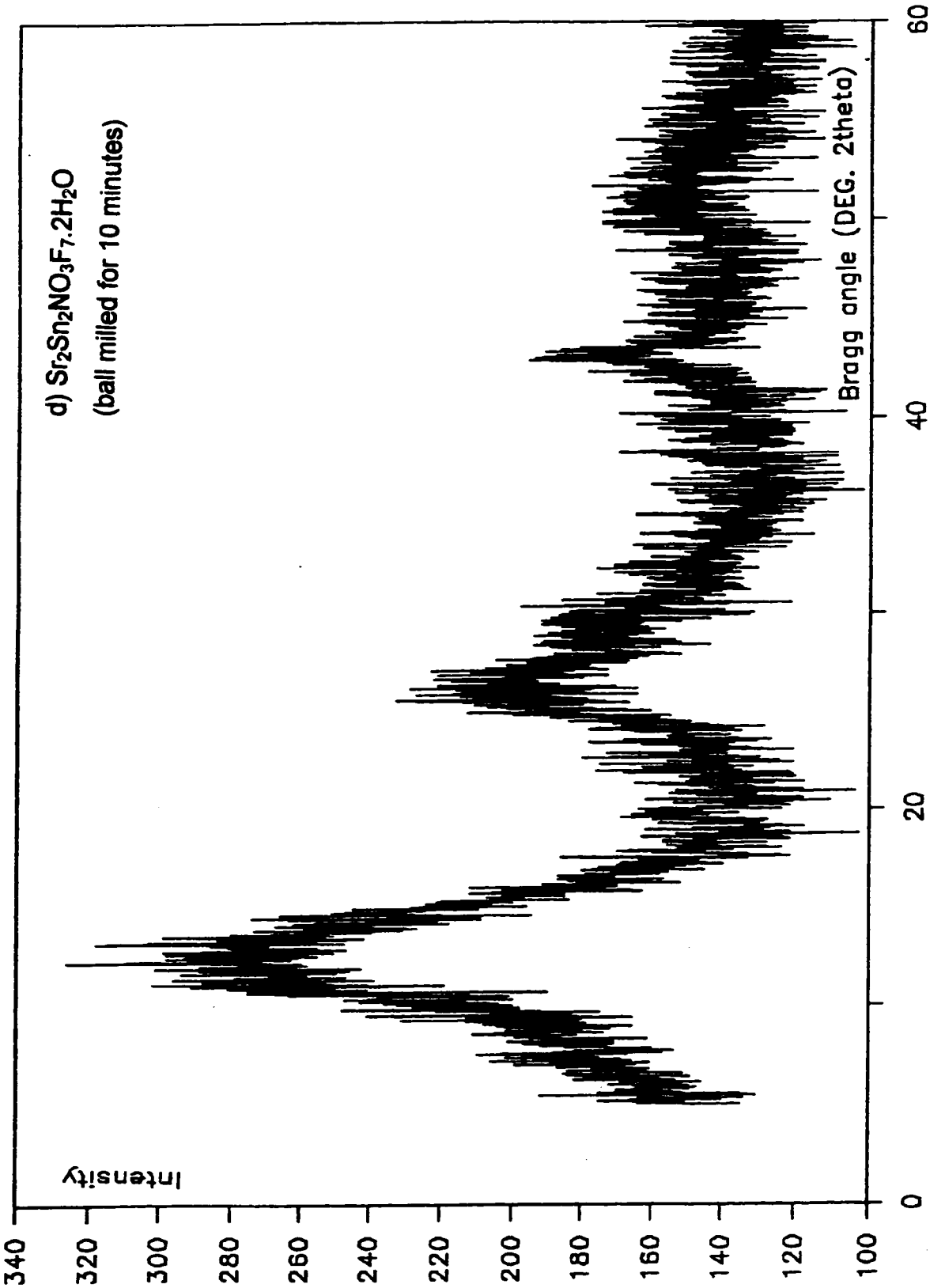

Figure 32: X-ray Diffraction Pattern of Highly Oriented $Sr_2Sn_2NO_3F_7.2H_2O$ (a) and the Reduction of Crystallinity by Ball Milling (b, c, d)

Chapter 4.0. RESULTS AND DISCUSSION (2)

Chemical Analyses and Physical Characterization of the Materials Formed in the Strontium Chloride - Stannous Fluoride System

4.1. X-RAY POWDER DIFFRACTION

In the same manner as described in the previous chapter, all products of reactions between aqueous solutions of strontium chloride and stannous fluoride were first examined by XRD in order to identify what product is being formed under specific reaction conditions. The influence of various parameters is described in the following sections.

4.1.1. INFLUENCE OF THE MOLAR RATIO AND THE ORDER OF ADDITION

The molar ratio X, defined as X = $[SrCl_2]$ / $[SnF_2]$, was varied from 0.05 to 10.0 for both orders of addition (i.e. for Sr-->Sn and for Sn-->Sr).

In the first set of experiments, the solution of strontium chloride was added to the solution of tin fluoride (Sr-->Sn) at a constant rate of 5ml/min. In the second set of experiments, the order of addition was reversed, i.e. solution of tin fluoride was added to the solution of strontium chloride (Sn-->Sr). All experiments were performed at room temperature, in glass beakers,

at a medium stirring rate. Both t (SnF2) and t (product) were kept at zero. All precipitates were filtered out by suction and washed with 2 x 20 ml of water and dried at room temperature.

The results of the X-ray diffraction analysis, presented on figure 33, show the following:

- For the order of addition: Sr-->Sn, the X-ray powder pattern of pure $SrSn_2F_6.H_2O$ was obtained for the values of the molar ratio X = 0.10 to 0.20 (region 1). For X = 0.30 to 0.80, the X-ray powder pattern of $SrSn_2F_6.H_2O$ and an unknown compound or a mixture of unknown compounds was observed (region 2). For X = 0.90 to 10.0, no suitable search match was obtained. An unknown compound or a mixture of unknown compounds is formed in this region 3 (figure 33).
- For the order of addition: Sn-->Sr, the X-ray powder pattern of $SrSn_2F_6.H_2O$ was obtained for the values of the molar ratio X = 0.05 to 0.15 (region 1). For X = 0.20, a mixture of $SrSn_2F_6.H_2O$ and an unknown compound or a mixture of unknown compounds was identified (region 2). For X = 0.30 to 10.0, no suitable search match was obtained. An unknown compound or a mixture of unknown compounds is formed in this region 3 (figure 33).

It is apparent , that $SrSn_2F_6.H_2O$ is obtained pure only at a very low values of X (Sn^{2+} in excess, region 1). As soon as X increases, products from region 2, that contain $SrSn_2F_6.H_2O$ and unknown compounds, are obtained. In region 3, unknown compounds only are formed. From the X-ray diffraction

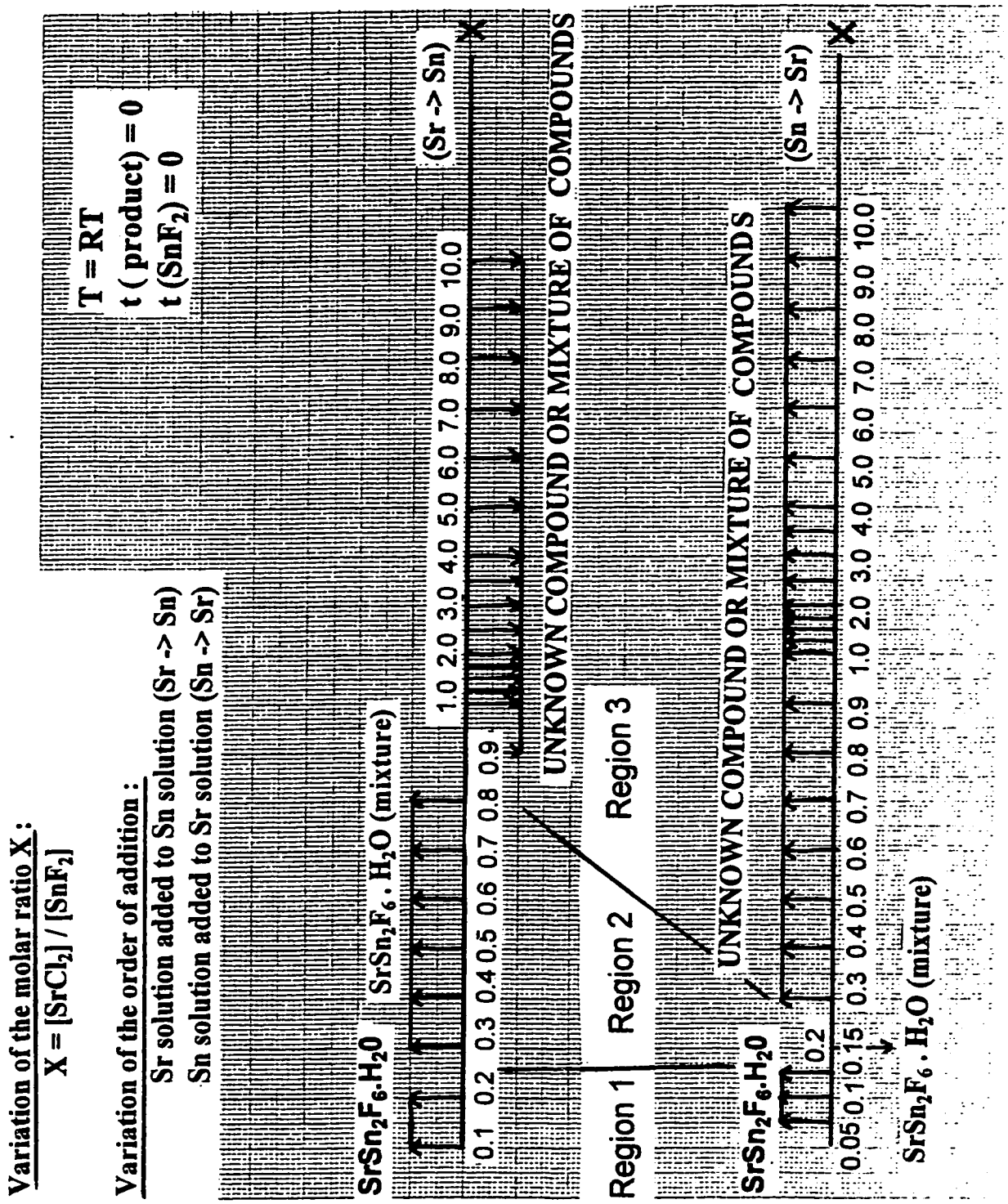

Figure 33: Infuence of the Variation of the Molar Ratio X and of the Order of Addition on the Formation of Products in the Strontium Chloride - Stannous Fluoride System

pattern is obvious, that these materials are either microcrystalline or amorphous. It is also important to mention that the intensities of peaks and also their positions change throughout this region. There is no clear trend in this region and the XRD results are not always reproducible. Examples of X-ray diffraction patterns of materials obtained in region 3 are presented on figure 34. This seems to suggest that there are unknown parameters we are not aware of, that are not properly controlled despite our efforts to keep all the other parameters constant in every preparation. It makes the interpretation of the results impossible without further research. Therefore, a further investigation of this region in the future is needed.

These results present some similarity with the $BaCl_2$ / SnF_2 system, where for both orders of addition $BaSn_2F_6$ is obtained at very low $BaCl_2$ / SnF_2 ratio, a mixture of $BaSn_2F_6$ and new phases at higher ratios, and a pure new phase or a mixture of new phases at even higher $BaCl_2$ / SnF_2 ratios [11,41,45]. However, the analogy stops there. In the $BaCl_2$ / SnF_2 system, the new phases are well crystalline, trends versus the $BaCl_2$ / SnF_2 ratio are clear, and the syntheses are well reproducible. In addition, at very high $BaCl_2$ / SnF_2 ratio (X>5.0) a

$Ba_{1-x}Sn_xCl_{1+y}F_{1-y}$ solid solution is obtained with x and y close to 0.1, which has a BaClF structure with total Ba/Sn disorder and shows some substitution of F by Cl on the F planes (disordered) whereas the Cl planes remain fully populated by Cl. No such $Sr_{1-x}Sn_xCl_{1+y}F_{1-y}$ solid solution was observed in the $SrCl_2$ / SnF_2 system.

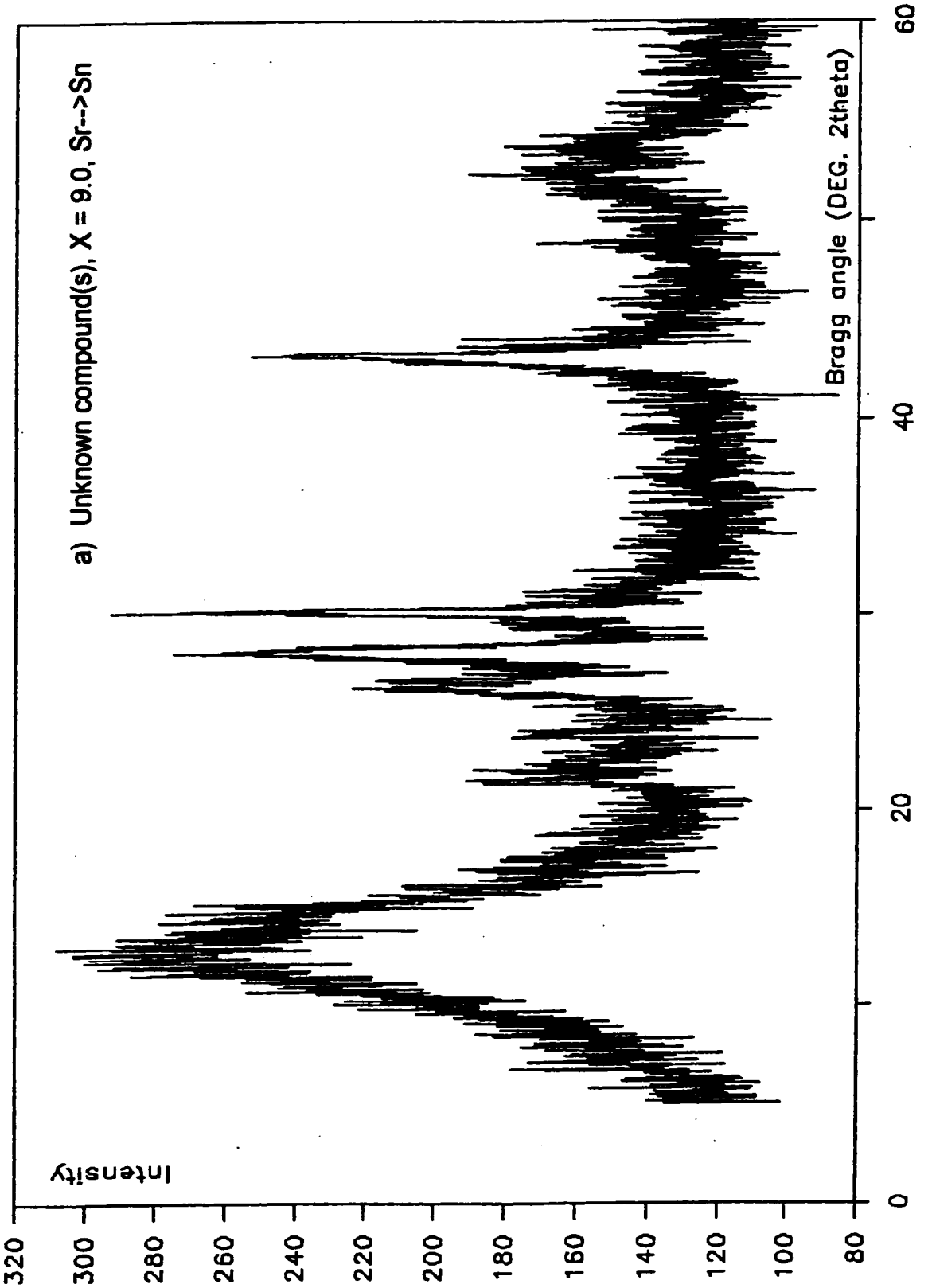

Figure 34: X-ray Diffraction Patterns of Unknown Compounds Formed in Region 3 (Strontium Chloride - Stannous Fluoride System) (a, b)

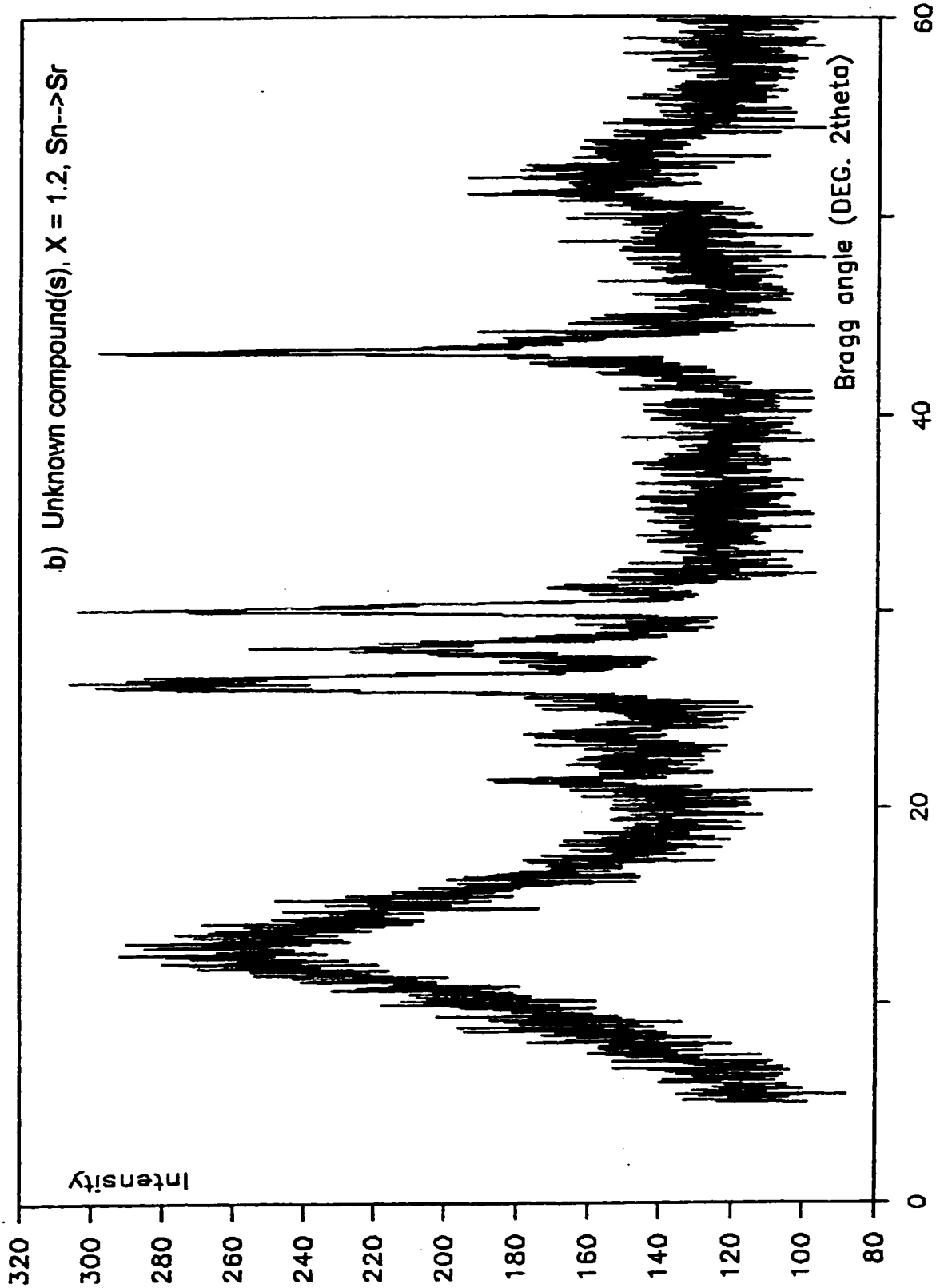

Figure 34: X-ray Diffraction Patterns of Unknown Compounds Formed in Region 3 (Strontium Chloride - Stannous Fluoride System) (a, b)

The region of X = 1.0, where the concentration of Sn is equal to the concentration of Sr, was further investigated by changing several reaction parameters. The results are described in the sections below and summarized in figure 35.

4.1.2. INFLUENCE OF MIXING SPEED

At X = 1.0 the mixing speed was varied as low, medium and high for both orders of addition. It was noticed that at low mixing speed for the order of addition Sr-->Sn as well as Sn-->Sr, product from region 2 was identified ($SrSn_2F_6.H_2O$ and unknown compound or a mixture of compounds). In all other cases, unknown compound or a mixture of compounds were obtained (region 3 of fig. 33).

4.1.3. INFLUENCE OF TIME AND TEMPERATURE

For X = 1.0 (Sr-->Sn, Sn-->Sr), t (product) values were selected as 0, 1, 7, 24, 48 and 120 hours. Also, for 1.0 (Sr-->Sn), T(product) was selected as 90°C. In either case, no change in the product of reaction was observed, product(s) from region 3 was (were) obtained.

4.1.4. INFLUENCE OF THE VOLUME OF WATER USED FOR WASHING

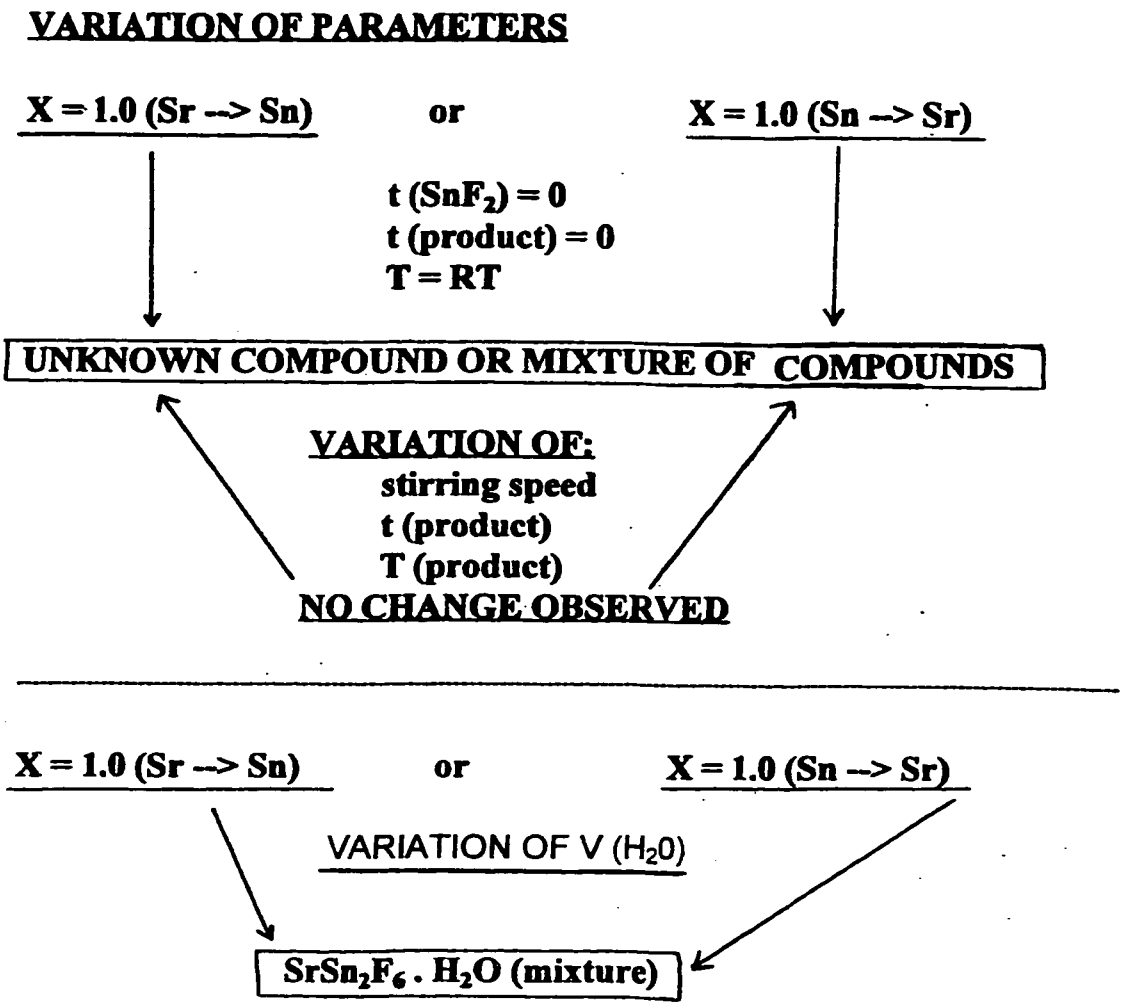

NOTE: The larger the volume of water used for washing the purer the compound.

Figure 35: Influence of the Variation of Reaction Parameters on the Formation of Products in the Strontium Chloride - Stannous Fluoride System

For X = 1.0 (Sn-->Sr and Sr-->Sn), the volume of water used for washing was varied as 5, 10, 20, 2 x 20, 100, 150, 200 and 300 ml. It was found that at very low values of V (H_20), $SrSn_2F_6.H_2O$ and unknown compound or a mixture of compounds is obtained. However, the pattern becomes more similar to pure $SrSn_2F_6.H_2O$ as the volume of water used for washing increases. This can be explained by two different scenarios: either the unknown compound or a mixture of compounds is water soluble and is dissolved as larger volume of water is used for washing or it is transformed into $SrSn_2F_6.H_2O$ when exposed to water by loosing some material that probably contains chlorides.The latter scenario would be similar to the decomposition of $CaSn_2F_6$ by washing water, where SnF_2 is removed and the final solid is a $Ca_{1-x}Sn_xF_2$ microcrystalline solid solution. This was observed in the reaction of calcium nitrate and tin(II) fluoride where washing water leaches SnF_2 from the $CaSn_2F_6$ phase formed at low X = $Ca(NO_3)_2.4H_20$ / SnF_2 ratios, thereby transforming it into the microcrystalline fluorite type $Ca_{1-x}Sn_xF_2$ solid solution [11, 36-37].

This will need further investigation. It will be important to verify, if samples that do not contain lines for $SrSn_2F_6.H_2O$ (mixture of unknown materials obtained in region 3) give $SrSn_2F_6.H_2O$ X-ray diffraction pattern after washing. This will mean that the precipitate is decomposed by water. The volume of water used for washing will then become a critical reaction parameter.

Chapter 5. CONCLUSION

The work described in this thesis is concerned with the preparation and characterization of stannous fluoride materials containing strontium.

Two different systems were investigated : the strontium nitrate/stannous fluoride system and the strontium chloride/stannous fluoride system.

It was established that the reactions in both systems are strongly sensitive to some of the conditions of preparation. Certain reaction parameters, such as molar ratio and the order of addition of reagents play a very important role in the synthesis.

Strontium nitrate and stannous fluoride system:

The reaction of aqueous solutions of strontium nitrate and stannous fluoride results in the formation of a precipitate which is $SrSn_2F_6.H_2O$, or $Sr_2Sn_2NO_3F_7.2H_2O$, or a mixture of both, depending on the conditions. The conditions of preparation of both materials have been defined. The nature of the products was investigated by various analytical techniques, such as atomic absorption spectrophotometry, fluoride ion electrode analysis, infrared spectroscopy, X-ray diffraction, thermal analyses and Mössbauer spectroscopy. The presence of water in $SrSn_2F_6.H_2O$ was detected by infrared spectroscopy as well as thermal analyses. The poor stability of

anhydrous $SrSn_2F_6$ was also demonstrated since it decomposes as soon as the water of hydration is lost. Mössbauer spectroscopy shows that in both compounds, Sn(II) possesses a stereoactive lone pair of electrons, which has a considerable non "s" density. This results in high anisotropy in bonding and makes textured samples. Recrystallization of $SrSn_2F_6.H_2O$ and $Sr_2Sn_2NO_3F_7.2H_2O$ from nitric acid yielded highly oriented samples.

Following are some suggestions for future work.

A diffraction study after heating at selected temperatures would help to understand the behavior versus temperature. Diffraction versus temperature would be even better, if we had a furnace for diffraction.

The Mössbauer spectrum recorded versus temperature might reveal possible changes in the lattice strength and phase transitions.

For neutron diffraction of $SrSn_2F_6.D_2O$ and $Sr_2Sn_2NO_3F_7.2D_2O$, one would have to prepare both compounds in D_2O, wash them with D_2O, dry in vacuum and handle them in closed atmosphere to prevent D_2O <--> H_2O exchange. Deuterated compounds will have to be used because the incoherent scattering by ^1H would give a very high background count. From neutron diffraction, one might be able to elucidate the crystal structures, and obtain the coordination of Sr and Sn, the packing of ions and perhaps its correlation to the mobility of fluoride ion, if these are proven to be mobile in these compounds.

Scanning electron microscopy on highly oriented samples and their comparison with the samples that do not exhibit preferred orientation would provide information about the shape of the crystallites.

Also, it would be interesting to perform conductivity measurements on both compounds and compare the results with the data obtained in other systems.

Strontium chloride and stannous fluoride system:

The reaction of aqueous solutions of strontium chloride and stannous fluoride results in the formation of a precipitate which is $SrSn_2F_6.H_2O$ or a mixture of unknown compounds, depending on the conditions. The study in this system is by no means complete. The unknown compound or mixture of compounds has to be identified. The investigation of the influence of the volume of water used for washing of the precipitate must be completed. After that, other reaction parameters (e.g. time and temperature related) must be investigated.

Once the unknown compounds are fully characterized and their preparation described in detail, one can perform some of the experiments described under suggestions for future work in strontium nitrate and stannous fluoride system.

It is important to mention that each $M(NO_3)_2$ / SnF_2 and MCl_2 / SnF_2 system is unique, even when M is large enough to give the fluorite type

structure MF_2, i.e. to have an eight -fold coordination (M = Cd, Ca, Sr, Pb, Ba...classified here by increasing M^{2+} ionic radius). This is probably due to their relative size compared to Sn(II), and also to their higher polarizability for Cd^{2+} and Pb^{2+} since these ions do not have a noble gas configuration. This is particularly obvious for Pb^{2+} which has Pb/Sn/F and Pb/Sn/NO_3/F systems much richer than the others, and may therefore exhibit unique phase transitions not found in the other systems.

Chapter 6. REFERENCES

[1] G.Dénès, J.Pannetier and J.Lucas, C. R. Acad. Sc. Paris. t.280 (1975) série C 831-834

[2] T.Birchall, G.Dénès, K.Ruebenbauer and J.Pannetier, Hyperfine Interact. 29, 1331-1334 (1984)

[3] G.Dénès, Y.H.Yu, T.Tyliszczak and A.P.Hitchcock, J.Solid State Chem. 91, 1-15 (1991)

[4] Y.Ito, T.Mukoyama, H.Funatomi, S.Yoshikado and T.Tanaka, Solid State Ionics 67, 301-305 (1994)

[5] R.Kanno, K.Ohno, H.Izumi, Y.Kawamoto, T.Kamiyama, H.Asano and F.Izumi, Solid State Ionics 70/71, 253-258 (1994)

[6] G.Dénès, M.C.Madamba and J.M.Parris, Solid State Ionics, Mat. Res. Soc. Symp. Proc., Vol. 369, 463-468 (1995)

[7] G.Dénès; Journal of Solid State Chemistry 74, 343-352 (1988)

[8] G.Dénès, Y.H.Yu, T.Tyliszczak and A.P.Hitchcock, J.Solid State Chem. 104, 239-252 (1993)

[9] C.Lucat, A.Rhandour, L.Cot and J.M.Réau, Solid State Comm. 32, 167-169 (1979)

[10] M.Durand, J.Pannetier and G.Dénès, J. Physique (Paris) 41, 831-836 (1980)

[11] G.Dénès, A.Muntasar and Z.Zhu, Hyperfine Interact. C 1, 468-471 (1996)

[12] G.Pérez, W.Granier and S.Vilminot, C.R. Acad. Sc. Paris t. 290, 337-339 (1980)

[13] T.Birchall, G.Dénès, K.Ruebenbauer and J.Pannetier, J. Chem. Soc. (A), Dalton Tr., 2296-2299 (1981)

[14] R.Calandrino, A.Collin, G.Dénès, M.C.Madamba and J.M. Parris, Mat. Res. Soc. Symp. Proc., Vol. 453, 585-590 (1997)

[15] J.M. Réau, C.Lucat, J.Portier, P.Hagenmuller, L.Cot and S.Vilminot, Mat. Res. Bull. 13, 877-882 (1978)

[16] J.Pannetier, G.Dénès and J.Lucas; Mat. Res. Bull. Vol. 14 , 627-631 (1979)

[17] G.Pérez, S.Vilminot, W.Granier, L.Cot, C.Lucat, J.M.Réau, J.Portier and P.Hagenmuller, Mat. Res. Bull. Vol. 15 , 587-593 (1980)

[18] G.Dénès, M.C.Madamba and G.Milova, Mat. Res. Soc. Symp. Proc. Vol. 398, 525-530 (1996)

[19] G.Dénès and M.C.Madamba, Mater. Chem 3, 227-245 (1996)

[20] G.Dénès and M.C.Madamba, Mat. Res. Soc. Symp. Proc., in press (1998)

[21] G.Dénès, D. Le Roux and M.C.Madamba, Mat. Res. Soc. Symp. Proc., in press (1998)

[22] R.Kanno, S.Nakamura, K.Ohno and Y.Kawamoto, Mat. Res. Bull. 26, 1111-1117 (1991)

[23] G.Villeneuve, P.Echegut, C.Lucat, J.M.Réau and P.Hagenmuller, Phys. Stat. Sol. (b) 97, 205-300 (1980)

[24] S.Vilminot, G.Pérez, W.Granier and L.Cot, Solid State Ionics 2, 91-94 (1981)

[25] G.Dénès, T.Birchall, M.Sayer and M.F.Bell, Solid State Ionics 13, 213-219 (1984)

[26] M.Durand - Le Floch, J.Pannetier and G.Dénès, Phys. Rev. B 33, 632-634 (1986)

[27] G.Dénès, Mat. Res. Soc. Symp. Proc., Vol. 369, 295-300 (1995)

[28] G.Dénès, G.Milova, M.C.Madamba and M.Perfiliev; Solid State Ionics, 86-88, 77-82 (1996)

[29] G.Milova, G.Dénès, M.C.Madamba and M.Perfiliev, Mat. Res. Soc. Symp. Proc., Vol. 411, 151-156 (1996)

[30] A.Wakagi and J.Kuwano, J. Mater. Chem. 4, 973-975 (1994)

[31] A.Wakagi, J.Kuwano, M.Kato and H.Hanamoto, Solid State Ionics 70/71, 601-605 (1994)

[32] J.D.Donaldson and B.J.Senior, J. Chem. Soc. (A), 1821-1825 (1967)

[33] G.Dénès, unpublished results

[34] G.Dénès and M.C.Madamba, unpublished results

[35] J.M.Parris; M.Sc. thesis, Concordia University (1988)

[36] Z.Zhu, M.Sc. thesis, Concordia University (1990)

[37] M.F.Bell, G.Dénès and Z.Zhu, Mat. Res. Soc. Symp. Proc., in press (1998)

[38] G.Dénès and M.C.Madamba, Mater. Struct. 3, 227-245 (1996)

[39] G.Dénès and J.E.Greedan, unpublished results

[40] G.Dénès; Proc. 2nd Nassau Mössbauer Conference, ed.: C.J.Wynter and E.E.Alp, W.C. Brown Publishers,109-135 (1994)

[41] A.Muntasar, D.Le Roux and G.Dénès, J. Radioanal. Nucl. Chem., Articles 190, 431-437 (1995)

[42] G.Dénès and A.Muntasar, Proceedings of the International Conference on the Applications of the Mössbauer Effect ICAME-95, SIF, Bologna, ed: I.Ortalli, Vol. 50, 83-86 (1996)

[43] A.Muntasar and G.Dénès, Proceedings of the International Conference on the Applications of the Mössbauer Effect ICAME-95, SIF, Bologna, ed: I.Ortalli, Vol. 50, 127-130 (1996)

[44] G.Dénès, J.Bratigny, D.Le Roux and A.Muntasar, Mat. Res. Soc. Symp. Proc. 453, 177-182 (1997)

[45] G.Dénès and A.Muntasar, Mater. Struct. 3, 246-260 (1996)

[46] N.N.Greenwood, T.C.Gibb; Mössbauer spectroscopy, Chapman and Hall, London (1971)

[47] R.W.G.Wyckoff; Crystal Structures, vol.1, ed.2, Interscience, New York, p.294 (1963)

[48] A.R.West; Solid State Chemistry and its Applications, J.Wiley & Sons Ltd., New York (1984)

[49] D.C.Harris; Quantitative Chemical Analysis, W.H.Freeman and Company, New York (1987)

[50] R.J.Fessenden & J.S.Fessenden; Organic Chemistry, Brooks/Cole Publishing Company, Monterey, California (1986)

[51] M.E.Brown; Introduction to Thermal Analysis - Techniques and Applications, Chapman and Hall, New York (1988)

[52] G.Dénès, J. Solid State Chem. 77, 54-59 (1988)

[53] G.Dénès; Chemical & Engineering News, American Chemical Society, p.2 (April 1988)

[54] G.Dénès and G.Lazanas, Hyperfine Interactions , 90, 435-439 (1994)

[55] G.Dénès, D.Dubé, M.Le Rouzès and M.C.Madamba, unpublished results (1996)

[56] M.Le Rouzès, Chemistry 419 Research Report, Concordia University (1997)

[57] J. Chaussidon, J Fripiat, A.Jelli; Chimie-Physique des Phénomènes de Surface, Masson et cie, Editeurs, Paris p.368-369, (1971)